Technical Memorandum

Wakulla Spring MFL: Hydrodynamic Model for Thermal Refuge Evaluation

Prepared for:
Northwest Florida Water Management District
81 Water Management Drive
Havana, FL 32333-4712

Prepared by:
Janicki Environmental, Inc.
1155 Eden Isle Drive NE
St. Petersburg, FL 33704

March 2021

Table of Contents

List of Figures

List of Tables

Acronyms and Abbreviations

cfs - cubic feet per second

CH3D - Curvilinear Hydrodynamics in 3-Dimensions

COMPS - Coastal Ocean Monitoring and Prediction System (University of South Florida)

ECOMSED - Estuarine Coastal and Ocean Model with Sediment Dynamics

EFDC - Environmental Fluid Dynamics Code

EPA - U.S. Environmental Protection Agency

FGS – Florida Geological Survey

FVCOM - Unstructured Grid Finite Volume Coastal Ocean Model

GOTM - General Ocean Turbulent Model

IFAS FAWN - Institute of Food and Agricultural Sciences Florida Automated Weather Network

MAE - Mean Absolute Error

ME - Mean Error

MFLs - Minimum Flows and Levels

NAVD88 - North American Vertical Datum of 1988

NWFWMD - Northwest Florida Water Management District

NWS - National Oceanic and Atmospheric Administration National Weather Service

POM - Princeton Ocean Model

REFDIF - Phase-resolving parabolic refraction-diffraction model for ocean surface wave propagation

RMSE - Root Mean Square Error

STWAVE - Steady-State Spectral Wave Model (developed by U.S. Army Corps of Engineers)

SWAN - Simulating Waves Nearshore (wave model developed at Delft University of Technology)

UF - University of Florida

USF - University of South Florida

USGS - United States Geological Survey

1 Introduction and Objectives

The Northwest Florida Water Management District (NWFWMD or District) is developing minimum flows and levels (MFLs) for Wakulla Spring and Sally Ward Spring in accordance with Section 373.042(1), Florida Statutes. The MFLs will address protection of water resources and ecology affected by reduced spring flows. The MFL technical assessment for Wakulla Spring and Sally Ward Spring will quantify the limit of reductions in spring discharge commensurate with prevention of significant harm to the water resources or the ecology of the area. One such water resource is the availability of warm water refuge for Florida manatees *(Trichechus manatus latirostris)* in Wakulla Spring during winter months.

Previous MFLs for springs have used two separate criteria for the protection of manatee warm water refuge (Rouhani et al. 2007, SRWMD 2013, SWFWMD 2004, SWFWMD 2008, SWFWMD 2012a, SWFWMD 2012b, SWFWMD 2017). Most often, these include a chronic stress criterion that water temperatures of suitable depth for manatees (> 3.8 ft) must not fall below 20°C for more than three consecutive days, and an acute stress criterion that water temperatures do not fall below 15°C for more than four consecutive hours. These temperature criteria were selected for the current MFL evaluation based upon their documentation in the literature and for consistency among MFL evaluations throughout Florida. For the evaluation described here, these criteria, temperature limits of 20°C and 15°C, are used.

Manatee use of Wakulla Spring has been a relatively recent and limited occurrence (Figure 1). Prior to the winter of 2002-2003, manatee use of Wakulla Spring as a winter warm water refuge either did not occur or was not recorded. Numbers increased until the winter of 2012-2013. Since that time the number of individuals observed using the warm water refuge during the winter months has declined somewhat. Manatees have been observed primarily utilizing the spring pool (approximately 1.1 acres) on the coldest days of the year, although manatees have been observed by District staff more than 0.59 miles downstream near the Wakulla Boat Tram during freezing temperatures. Water in excess of 20°C has also been documented to extend past the Boat Tram during freezing air temperature events (Figures 2 and 3).

Sally Ward Spring and its associated spring run (Figure 3), which flows into the Wakulla River near the Wakulla Spring vent, is not a documented warm water refuge for manatee. The Sally Ward Spring run does provide data needed as model boundary conditions for inflows and associated water temperature.

Assuming each manatee requires a surface area of 28.5 ft^2 (Rouhani et al. 2007), the spring pool alone could provide thermal refuge for 1,685 manatees. The maximum usage of manatees documented using the warm water refuge during winter months (n = 46) accounts for a 2.7% usage of the spring pool, with considerably more habitat available downstream. Additional habitat is available when considering the volume of water present in the spring pool as a result of the deep water column. Wakulla Spring provides a considerable amount of spring water at a relatively constant and stable temperature.

Spring vent water temperatures regularly fall below the chronic temperature criterion of 20°C for considerably longer than three consecutive days (Figure 4). One of the coldest water events at the vent on record is 19.36°C, which occurred on March 7, 2013 during a period of increased manatee overwintering (Figures 1 and 4). During this time, the vent temperature dropped below 19.5°C for more than three days in a row, and below 20°C for 10 days. The chronic thermal refuge criterion for manatees is regularly violated under natural conditions at Wakulla Spring. Violation of the acute temperature criterion (below 15°C for more than four consecutive hours) has never been documented near Wakulla Spring for any period of time.

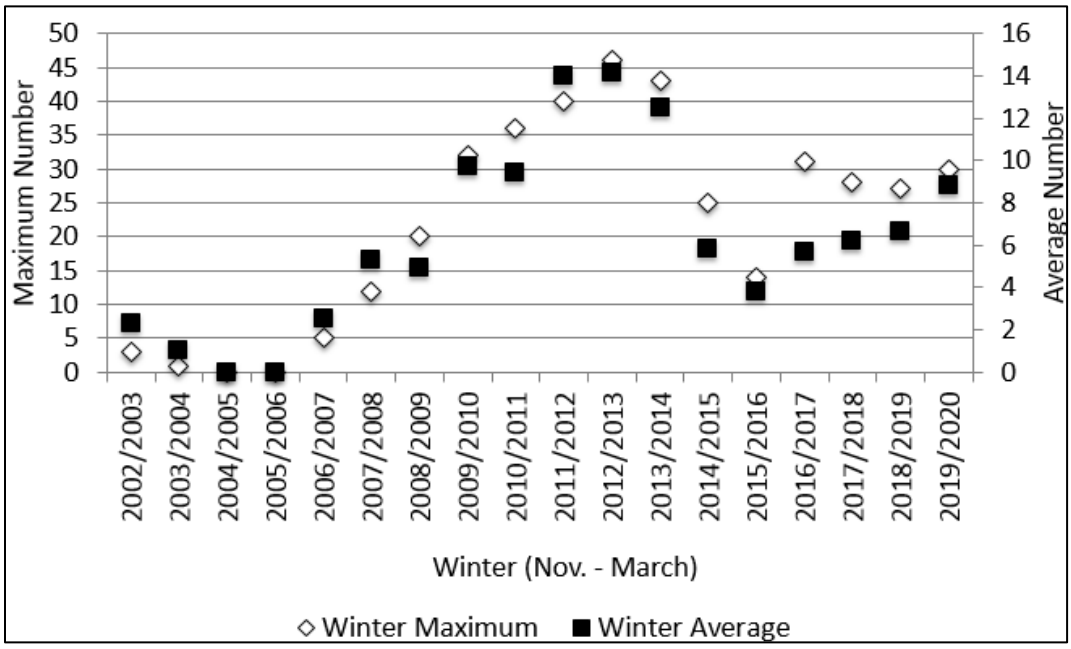

Figure 1. Maximum number of manatees reported by Wakulla Spring boat tour staff during winter months. Daily manatee count data from the Edward Ball Wakulla Springs State Park staff prior to 2008 are not available.

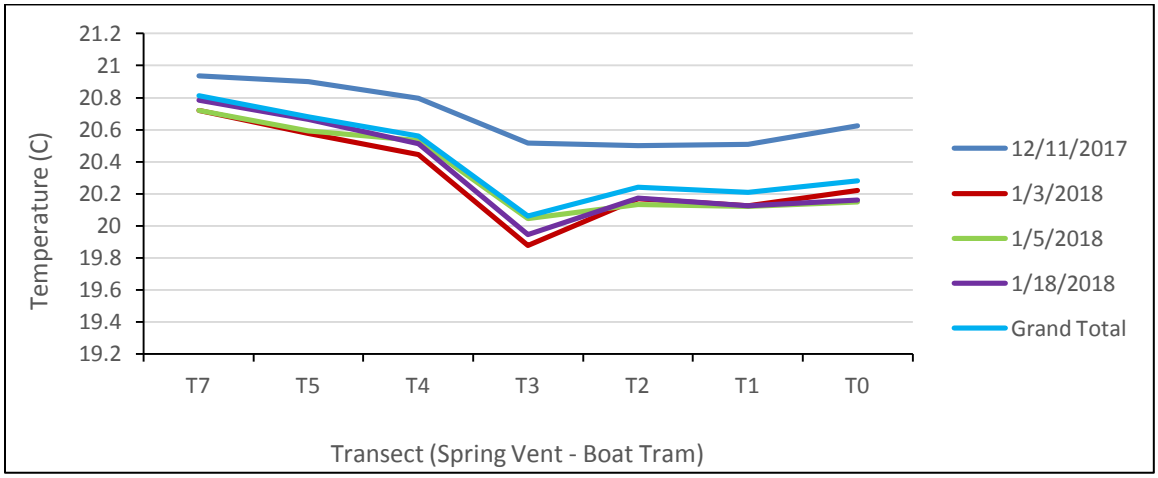

Figure 2. Average Wakulla River water temperature from the Spring Vent (T7) to Boat Tram (T0), which is located 0.59 miles downstream, during recent winter dates.

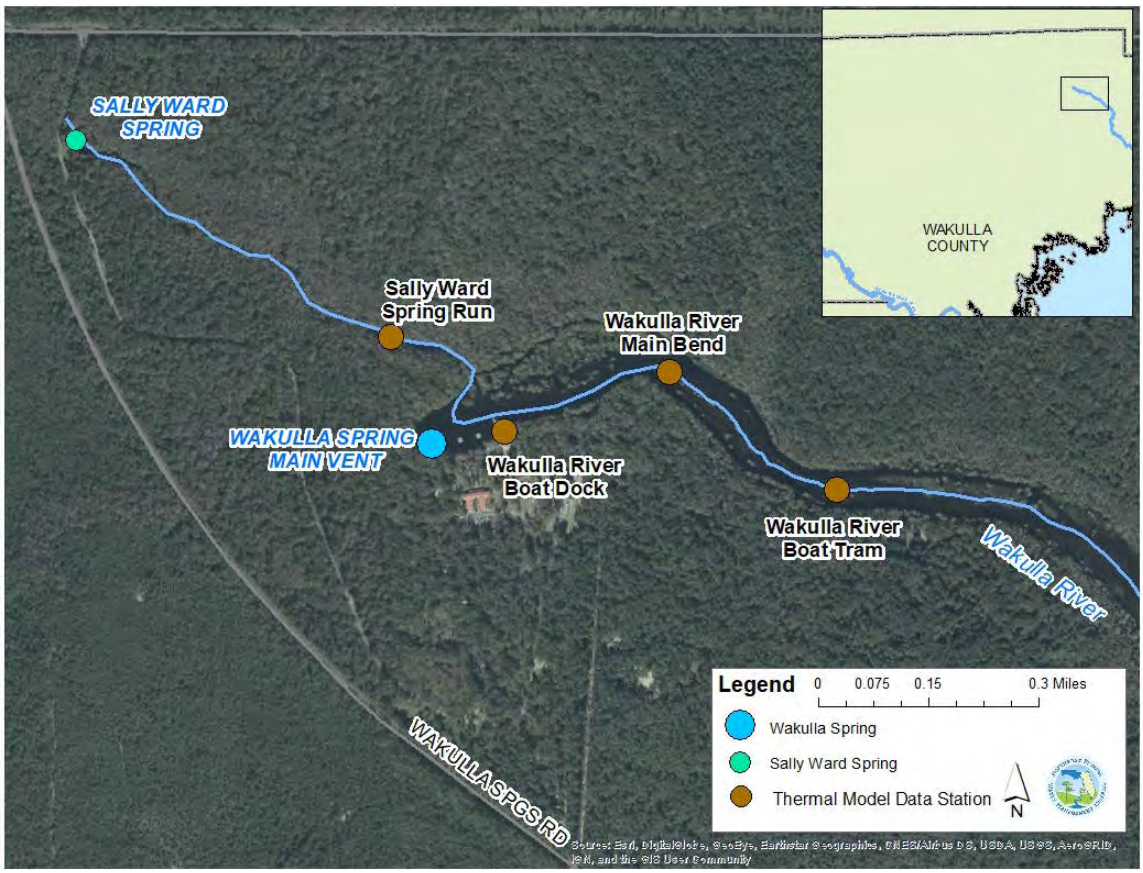

Figure 3. Wakulla Spring system: the EFDC model domain extends from the Spring Vent to the Boat Tram.

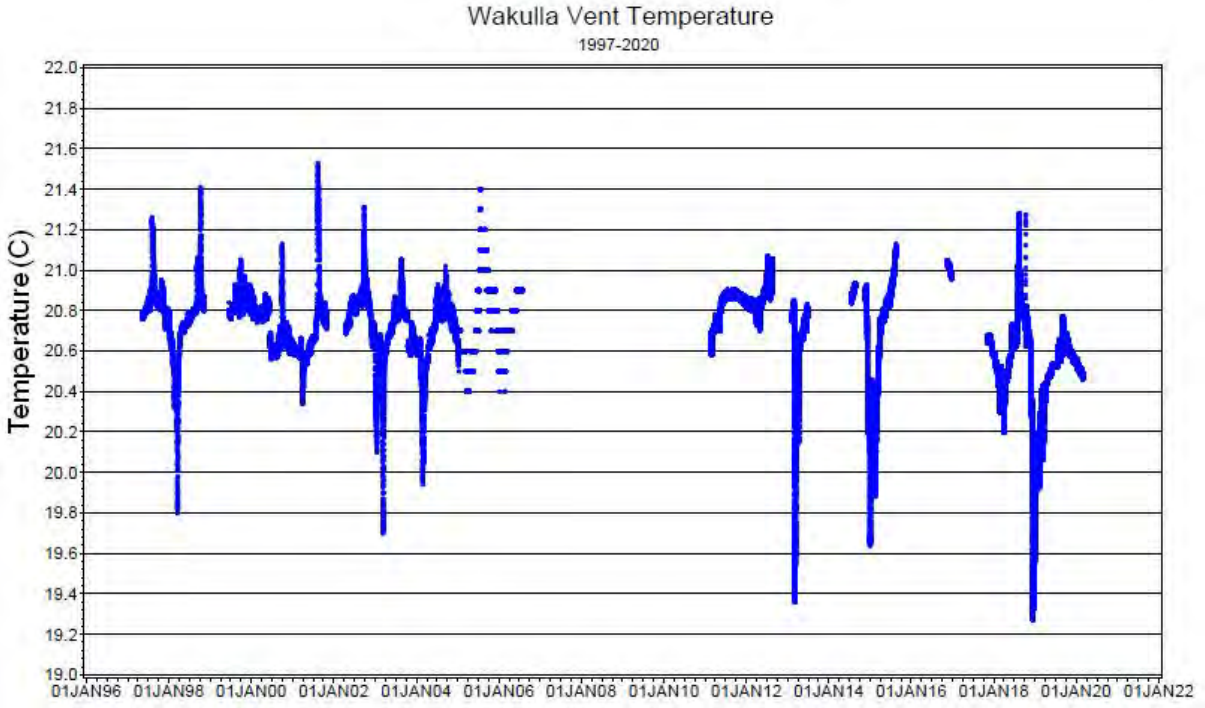

Figure 4. Wakulla Spring Vent water temperature for the available period of record, May 9, 1997, to February 28, 2020.

The objective of this work effort is to evaluate the expected results of potential flow reductions from the spring with respect to available manatee warm water refuge habitat in Wakulla Spring and the immediate downstream area during the winter months. The chain of logic concerning the spring temperature response to cold weather events is that the relatively constant spring temperatures would be affected by the cold air temperatures such that a reduction in spring flow could result in a reduction in water temperatures downstream of the vent, as the water cooled due to interaction with the cold air. However, the observed interactions among vent water temperatures, vent flows, and air temperatures provide a more complicated response to cold weather events for the Wakulla Spring system.

Winter cold weather events are often the result of frontal system passage, with associated rainfall, and increased infiltration to the groundwater system. It is hypothesized that increased inflows of surface water to the groundwater system through karst features such as sinkholes, swallets, and karst windows affect the temperature of the resultant groundwater (spring) discharge from the vent. In some instances, surface water flowing into the Floridan aquifer from multiple sinking streams has been shown to be rapidly transported in the aquifer system to Wakulla Spring (FGS 2012). The temperature of this water entering the groundwater system is related to air temperature during and following the rainfall events. The more rapid the movement of groundwater through the aquifer system to the Wakulla vent, the less chance for the temperature of the groundwater to equilibrate**.**

The winter of 2011-2012 provides an example of a period when there were several excursions of air temperatures below freezing without large changes in vent flows or vent water temperatures (Figures 5-7). While air temperatures varied between less than 0°C and almost 30°C (Figure 5), vent discharges varied between 470 cfs and more than 800 cfs (Figure 6) with no especially large sudden temperature excursions, as vent water temperatures varied by only 0.1°C (Figure 7) and never dropped below 20.8°C.

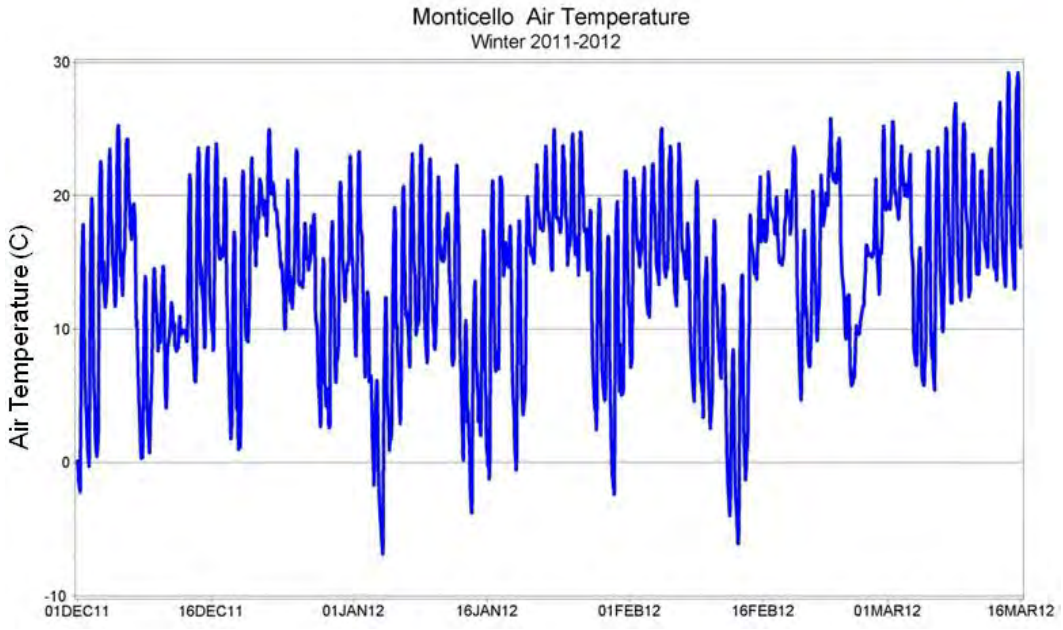

Figure 5. Air temperature at IFAS Monticello site, winter 2011-2012 (Dec. 1, 2011 - Mar. 15, 2012).

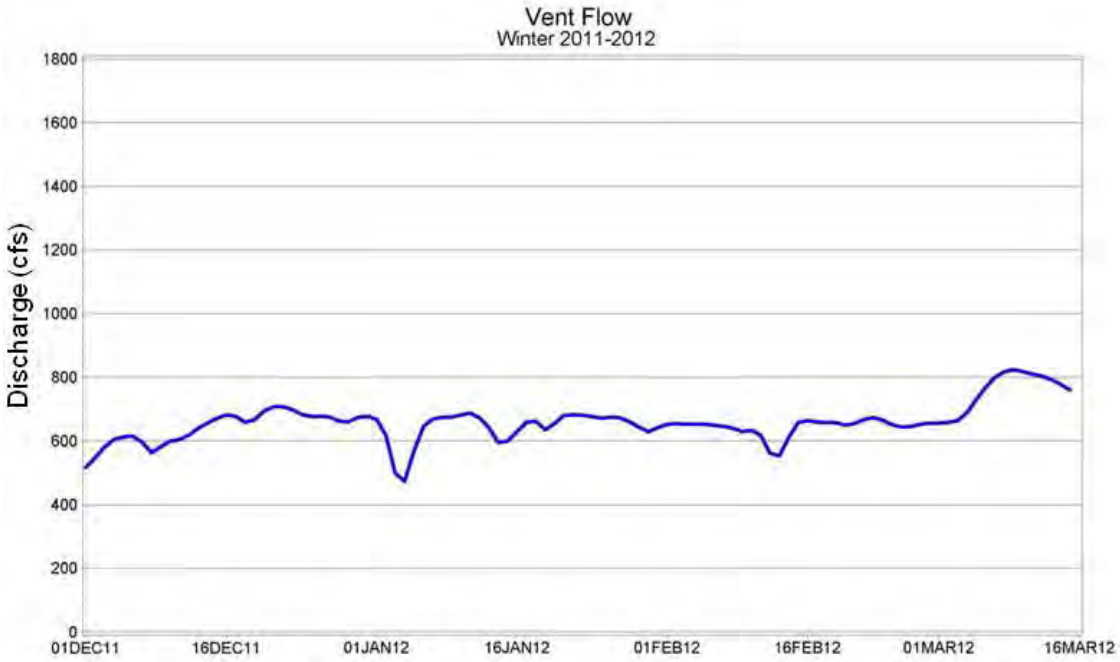

Figure 6. Discharge from Wakulla Spring vent, winter 2011-2012 (Dec. 1, 2011 - Mar. 15, 2012).

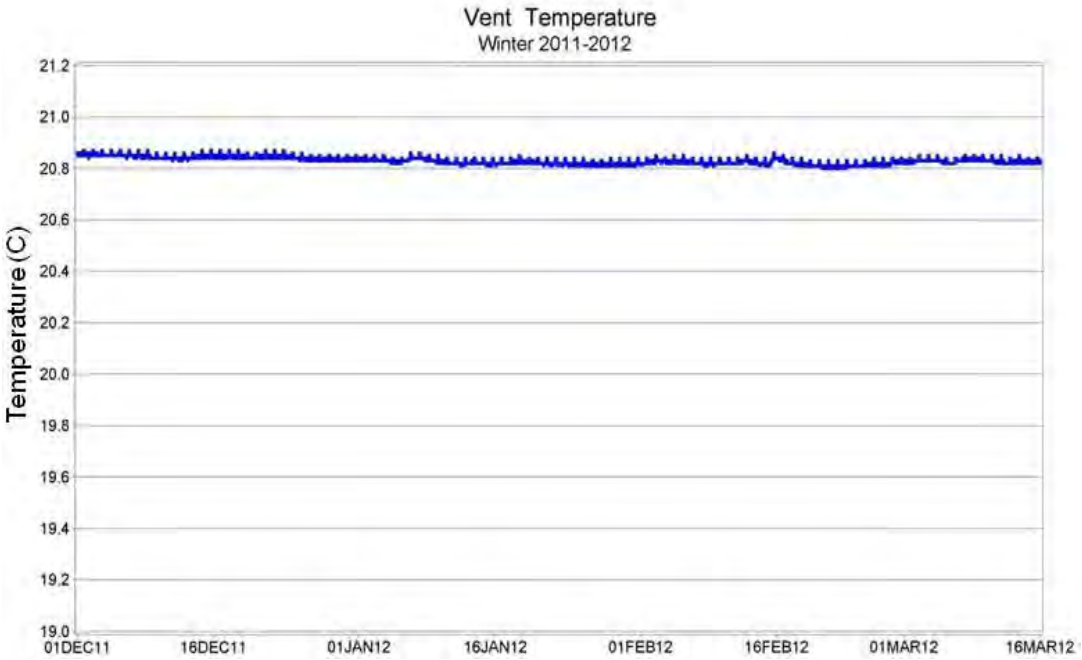

Figure 7. Water temperature in Wakulla Spring vent, winter 2011-2012 (Dec. 1, 2011 - Mar. 15, 2012).

A different combination of vent discharges, air temperature, and resulting vent temperatures was observed in the winter of 2018-2019, however. The December air temperatures dropped to near or below 0°C during the first half of the month (Figure 8), and vent discharges showed two rapid increases to more than 1200 cfs during the first three weeks of December (Figure 9) before returning to 800 cfs or less by early February. This increase in vent discharge is likely associated

with heavy precipitation during the cold fronts. The response in vent temperatures (Figure 10) shows a sharp decline by mid-December of a full 1°C, to below 20°C, and vent water temperatures remained below 20°C until early January.

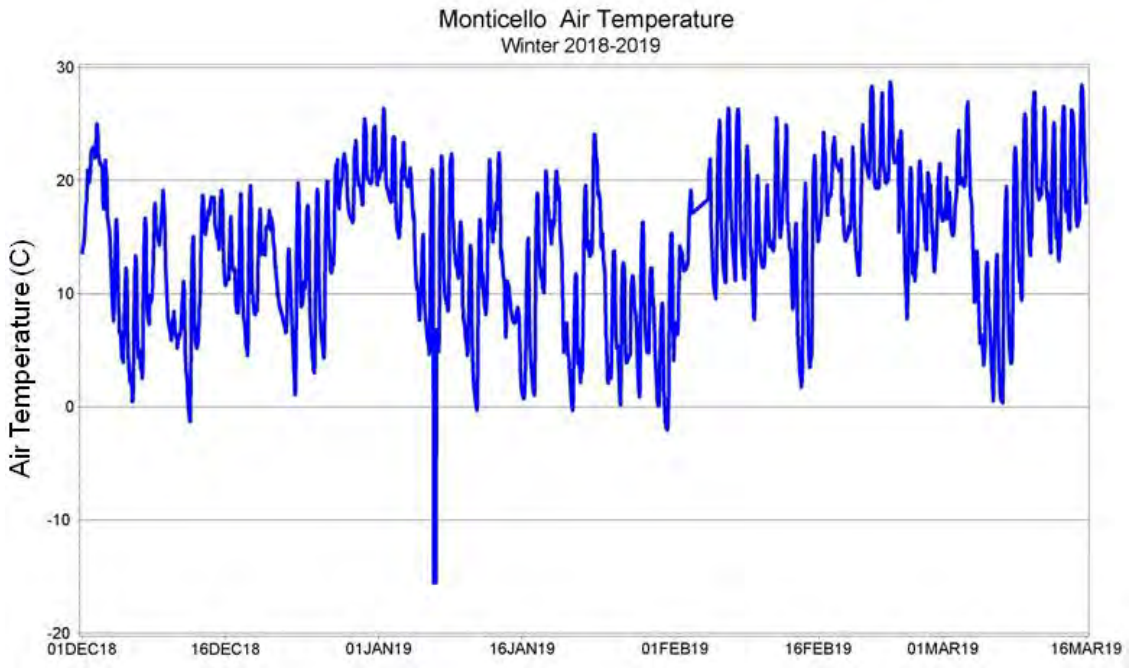

Figure 8. Air temperature at IFAS Monticello site, winter 2018-2019 (Dec. 1, 2018 - Mar. 15, 2019).

Figure 9. Discharge from Wakulla Spring vent, winter 2018-2019 (Dec. 1, 2018 - Mar. 15, 2019).

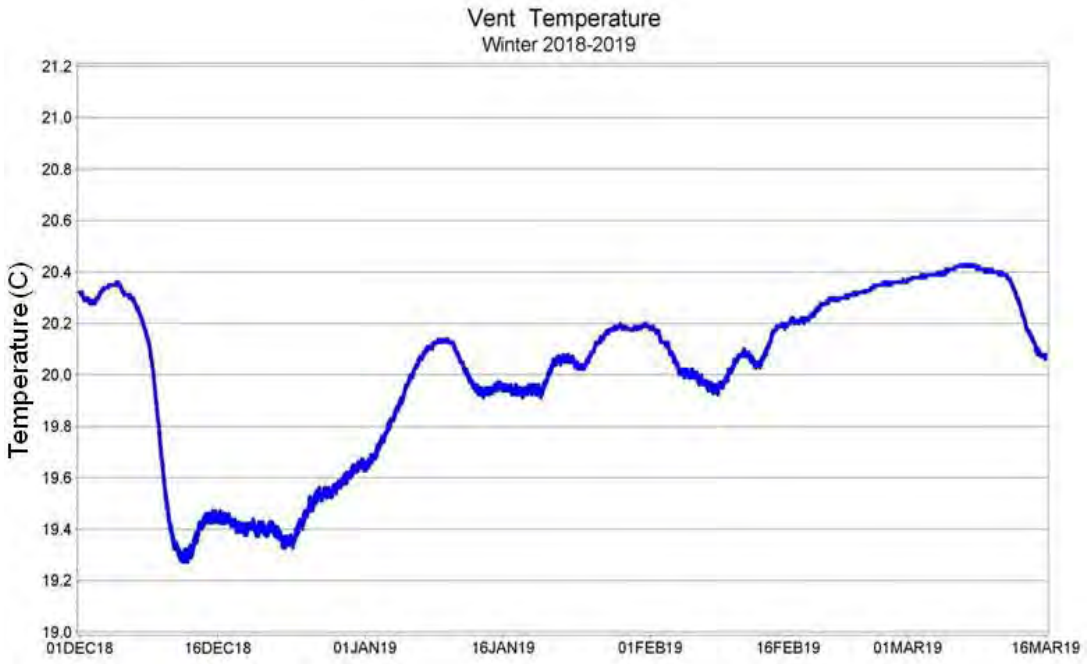

Figure 10. Water temperature in Wakulla Spring vent, winter 2018-2019 (Dec. 1, 2018 - Mar. 15, 2019).

Given the observed responses in Wakulla Spring vent temperatures during cold events, it is apparent that there is not a straightforward relationship between air temperature and available warm water refuge habitat. The responses in available warm water refuge habitat to potential spring flow reductions is dependent on not only the air temperature during the cold event, but also on the vent discharges and vent water temperatures during the cold event. It is conceivable that during a period of low (< 20°C) vent water temperatures, a potential spring flow reduction could result in more, rather than less, available manatee warm water refuge habitat, as the volume of cold water entering the spring pool and river system via the vent would be reduced.

To evaluate the expected changes in the surface area or volume of suitable warm water refuge habitat associated with changes in spring discharge and accompanying vent water temperatures, a hydrodynamic model has been developed to provide longitudinal (along the axis of the river) and cross-river temperature responses and associated temperature envelope surface area and volume changes expected from reduced flows from Wakulla Spring during cold weather events.

The following sections of this document provide the rationale for selection of the thermal model used, a description of model development and calibration including description of the data available for this effort, the selection of winter periods for MFL evaluation including data description, and the results of a flow reduction scenario, with graphical and tabular presentation of results.

2 Hydrodynamic Model Selection

Our experience with the Environmental Fluid Dynamics Code (EFDC) modeling suite and the use of this suite to evaluate MFLs for the St. Marks River Rise (Janicki Environmental, 2018) and in other Florida west coast regions (Suwannee River Water Management District, Southwest Florida Water Management District) is a strong recommendation for this model. This section provides brief summaries of several hydrodynamic models and compares them to provide support for the selection of the EFDC model for this effort.

The primary hydrodynamic models considered for this application included the following:

- Princeton Ocean Model (POM),
- Estuarine Coastal and Ocean Model with Sediment Dynamics (ECOMSED) ,
- Curvilinear Hydrodynamics in 3-Dimensions (CH3D),
- EFDC, and
- Unstructured Grid Finite Volume Coastal Ocean Model (FVCOM).

Hydrodynamic models utilizing all of these packages have been applied to estuarine systems, including both rivers and embayments. The EFDC model is part of the EPA's development of models for use in establishing Numeric Nutrient Criteria, in addition to having already been applied to numerous river estuaries in Florida.

Princeton Ocean Model (POM):
http://www.ccpo.odu.edu/POMWEB/
POM is a three-dimensional (3-D) time-dependent hydrodynamic model with the following principal attributes:

- solution of full momentum, continuity, temperature, salinity and density equations,
- sigma coordinate representation of vertical component,
- curvilinear orthogonal coordinate system in the horizontal,
- imbedded second-order turbulence closure scheme to represent turbulence mixing,
- 2-D/3-D mode-splitting solution scheme where the full external solution is in two dimensions and an internal mode to solve for the vertical variations,
- full simulation of the density (baroclinic) terms in 3-D (salinity and temperature),
- full simulation of heat exchange and internal response (temperature), and
- open and available source code.

POM has been utilized in numerous applications throughout the US and has been the base code for numerous modifications that have become widely used public domain hydrodynamic models. While the base POM model is still fully supported and maintained, numerous versions have been created and renamed. These models have been built upon the POM framework and subsequent

additional attributes, linkages, and capabilities added to improve their applicability and performance in coastal systems.

Estuarine Coastal and Ocean Model with Sediment Dynamics (ECOMSED):
https://www.hdrinc.com/services/environmental-sciences/water-quality-hydrodynamic-modeling-software
ECOMSED is a 3-D hydrodynamic model with the following principal attributes:

- solution of full momentum, continuity, temperature, salinity and density equations,
- sigma coordinate representation of vertical component,
- curvilinear orthogonal coordinate system in the horizontal,
- imbedded second-order turbulence closure scheme to represent turbulence mixing,
- 2-D/3-D mode-splitting solution scheme where the full external solution is in two dimensions and an internal mode to solve for the vertical variations,
- full simulation of the density (baroclinic) terms in 3-D (salinity and temperature),
- full simulation of heat exchange and internal response (temperature), and
- open and available source code.

The development of ECOMSED has its origins in the mid 1980s with the creation of the POM and its version for shallow water environments – rivers, bays, estuaries and the coastal ocean and reservoirs and lakes - named ECOM. In the mid 1990s, concepts for cohesive sediment re-suspension, settling and consolidation were incorporated within the ECOM modeling framework. During the last several years, ECOMSED was enhanced to include generalized open boundary conditions, tracers, better bottom shear stresses through a sub-model for bottom boundary layer physics, surface wave models, non-cohesive sediment transport, and dissolved and sediment-bound tracer capabilities.

ECOMSED has a number of specific attributes that are useful for estuarine river modeling, including:

- thin wall barrier to represent narrow barriers such as causeways without impacting grid resolution,
- simulation of connecting structures such as culverts,
- spatially varying meteorological forcing (i.e., wind fields),
- wave model sub-component linkage (SWAN or Donnelin Model),
- efficient parallelization on standard personal computing environment, and
- fully tested sub-grid linkage to water quality model (allowing simulation of water quality conditions within only a portion of the hydrodynamic domain).

Environmental Fluid Dynamics Code (EFDC):
https://www.epa.gov/ceam/environmental-fluid-dynamics-code-efdc
EFDC is a 3-D time-dependent hydrodynamic model with the following principal attributes:

- solution of full momentum, continuity, temperature, salinity and density equations,
- option for either sigma coordinate representation of vertical component or generalized vertical coordinate option (a laterally constrained localized [LCL] sigma transform, which can be mixed with standard sigma vertical grids on a sub-domain basis in a single model),
- curvilinear orthogonal coordinate system in the horizontal,
- embedded second-order turbulence closure scheme to represent turbulence mixing,
- 2-D/3-D mode-splitting solution scheme where the full external solution is in two dimensions and an internal mode to solve for the vertical variations,
- full simulation of the density (baroclinic) terms in 3-D (salinity and temperature),
- full simulation of heat exchange and internal response (temperature), and
- open and available source code.

While the EFDC model is not as directly tied to the POM model development as ECOMSED, it is nearly identical in its overall representation of the model domain and its solution schemes and techniques. EFDC has integrated links for simulation of sediment transport, a fully integrated water quality component, and numerous biological component linkages.

EFDC has a number of specific attributes that are useful for the application for estuarine river modeling, including:

- thin wall barrier to represent narrow barriers such as causeways without impacting grid resolution,
- simulation of connecting structures such as culverts,
- spatially varying meteorological forcing (i.e., wind fields),
- wave model sub-component linkage (SWAN or STWAVE), and
- efficient parallelization on standard personal computing environment.

Curvilinear Hydrodynamic Model in 3-Dimensions (CH3D):
http://ch3d.coastal.ufl.edu/
CH3D is a 3-D hydrodynamic model with the following principal attributes:

- solution of full momentum, continuity, temperature, salinity and density equations,
- sigma coordinate representation of vertical component,
- curvilinear non-orthogonal coordinate system in the horizontal,
- imbedded second-order turbulence closure scheme to represent turbulence mixing,
- 2-D/3-D mode-splitting solution scheme where the full external solution is in two dimensions and an internal mode to solve for the vertical variations,
- full simulation of the density (baroclinic) terms in 3-D (salinity and temperature),
- full simulation of heat exchange and internal response (temperature), and
- open and available source code.

While the CH3D model is not as directly tied to the POM model development as ECOMSED, it is nearly identical in its overall representation of the model domain and its solution schemes and techniques. The one key difference is that CH3D is a non-orthogonal grid model which allows some additional flexibility in terms of representation of shorelines and geometry. CH3D also has integrated links for simulation of sediment transport, a fully integrated water quality component, and numerous biological component linkages, although some of these attributes are not directly available as open source code versions.

CH3D has a number of specific attributes that are useful for estuarine river modeling, including:

- thin wall barrier to represent narrow barriers such as causeways without impacting grid resolution,
- spatially varying meteorological forcing (i.e., wind fields),
- wave model sub-component linkage (SWAN or REFDIF), and
- efficient parallelization on standard personal computing environment.

Unstructured Grid Finite Volume Coastal Ocean Model (FVCOM):
http://fvcom.smast.umassd.edu/fvcom/
FVCOM is a 3-D hydrodynamic model with the following principal attributes:

- sigma coordinate representation of vertical component,
- 2-D/3-D mode-splitting solution scheme where the full external solution is in two dimensions and an internal mode to solve for the vertical variations,
- unstructured grid, finite volume,
- solution of full momentum, continuity, temperature, salinity and density equations,
- utilizes General Ocean Turbulent Model (GOTM) developed by Burchard's research group in Germany (Burchard, 2002) to provide optional vertical turbulent closure schemes,
- full simulation of the density (baroclinic) terms in 3-D (salinity and temperature),
- full simulation of heat exchange and internal response (temperature), and
- open and available source code.

While the other models presented are structured grid finite difference models, the FVCOM is the only unstructured grid model considered for this project. The key aspect of unstructured grid modeling is the flexibility and resolution obtainable with the grid representation of the overall system. FVCOM has integrated links for sediment transport, water quality, biological modeling, and waves. One limitation on the FVCOM model is that its use is limited to "…use in non-commercial academic research and education", making it unsuitable for use in this effort.

The major advantage of the FVCOM model as compared to the other structured grid models is the degree to which the geometric conditions in the system can be simulated, and the flexibility in the application of finer grids within targeted areas of the system.

Selected Hydrodynamic Model

Table 1 shows key attributes needed for the hydrodynamic modeling of Wakulla Spring temperatures from the vent through the near downstream river run, the area most likely to provide manatee thermal refuge during cold weather events. For each attribute, the model is identified to either have or not have sufficient capability in that area. Overall, the models' capabilities are similar and the determination of the model to be utilized reflects minor advantages. It is important to recall that use of the model in development of several other MFLs along Florida's west coast, including that for the St. Marks River Rise, and familiarity of the project team with the model being utilized, are strong recommendations for use of the EFDC model.

Table 1. Hydrodynamic model key attributes for comparison.

Attribute	POM	ECOMSED	EFDC	CH3D	FVCOM
Full 3-D Momentum, Continuity, Density, Temperature, Salinity	√	√	√	√	√
Full Turbulence	√	√	√	√	√
Flexible Grid	√	√	√	√	√
Representation of Structures		√	√		
Spatially Variant Wind Field	√	√	√	√	√
Wave Sub-Model		√	√	√	√
Open/available Source Code	√	√	√		√
Efficient Parallelization		√	√	√	√
Water Quality Linkage		√	√	√	√

Examination of the attributes shown in Table 1 indicates that both ECOMSED and EFDC have very similar capabilities for this project. Given the appropriateness of the EFDC model, the use of this model in several other west Florida tidal rivers, and our familiarity with it, the EFDC model was selected for this calibration effort.

3 Model Development and Calibration

This section provides the description of the model development and calibration effort, including description of the data used for both model input and calibration comparisons. The period of interest for calibration is the most recent winter period 2019-2020, during which multiple events occurred with air temperatures below 0°C. The rationale for selecting this period is based on both the data availability for this period and the occurrence of Hurricane Michael in fall 2018 which resulted in scouring and deposition, discussed further in Section 3.3. Winter 2019-2020 represents the period after the system has had a chance to adjust to the impacts of Hurricane Michael.

3.1 Boundary Condition and Calibration Data

The data types needed for model development and calibration include the following data used for model boundary conditions, as well as those used for calibration (comparison of model output to observed data). These data are provided graphically for the locations noted for water temperature, flows, and water surface elevations (see Figure 3 for map display of locations), and at the frequencies listed parenthetically in the data listing:

- Water Temperatures
  - Main Vent: Used as input data for model upstream boundary conditions (15-minute)
  - Sally Ward Run: Used as input data for model upstream boundary conditions, collected just upstream of mouth of Sally Ward run (15-minute)
  - Boat Dock: Used as calibration data (15-minute)
  - Main Bend: Used as calibration data (15-minute)
  - Profiles: Used as calibration data (Jan. 22 and Feb. 28, 2020)
  - Boat Tram: Used as downstream boundary condition (15-minute)
- Flows
  - Main Vent: Used as input data for model upstream boundary conditions (15-minute)
  - Sally Ward Run: Used as input data for model upstream boundary conditions (5-minute)
- Water Surface Elevations
  - Boat Dock: Used as calibration data (15-minute)
  - Boat Tram: Used as downstream boundary condition (15-minute)
- Meteorological Boundary Condition Data
  - Air Temperature: Tallahassee Airport, NWS (hourly)
  - Atmospheric Pressure: Tallahassee Airport, NWS (hourly)
  - Relative Humidity: Tallahassee Airport, NWS (hourly)
  - Rainfall: Tallahassee Airport, NWS (hourly)
  - Cloud Cover: Tallahassee Airport, NWS (hourly)
  - Evapotranspiration: Monticello, UF IFAS FAWN (daily)
  - Solar Radiation: Monticello, UF IFAS FAWN(hourly)
  - Wind Speed and Direction: Shell Point, USF COMPS (6-minute)
- Initial Conditions
  - Water Temperature
  - Water Surface Elevation
- Bathymetry

The winter 2019-2020 period used for calibration was simulated for the 91-day period Dec. 1, 2019 - Feb. 28, 2020. Time series plots of the temperature input boundary condition data and temperature calibration data are provided below in Figures 11-15, with the locations of the profile data collected during Jan. and Feb. 2020 provided in Figure 16.

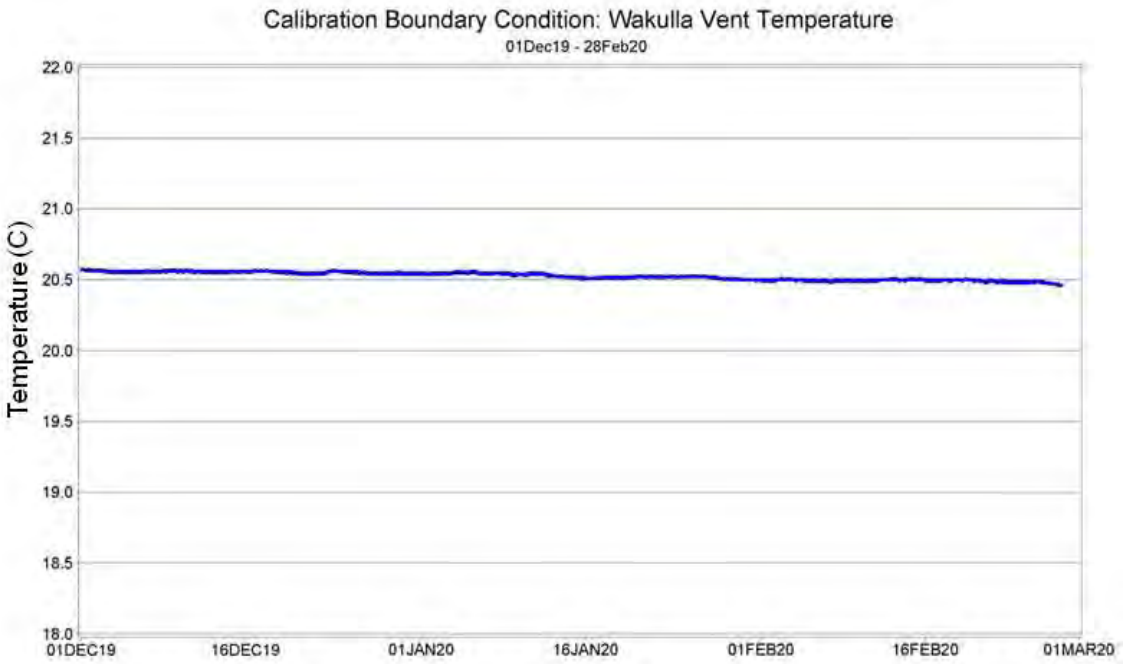

Figure 11. Wakulla Spring Vent water temperature for calibration period, December 1, 2019 to February 28, 2020, used for boundary condition.

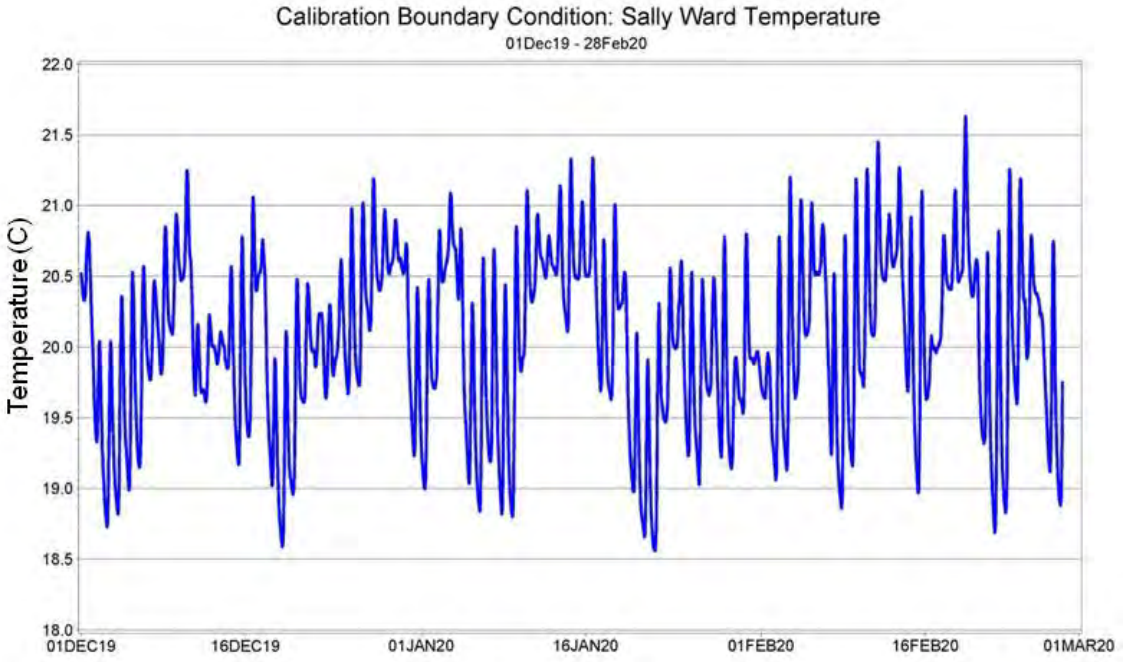

Figure 12. Sally Ward Run water temperature for calibration period, December 1, 2019 to February 28, 2020, used for boundary condition.

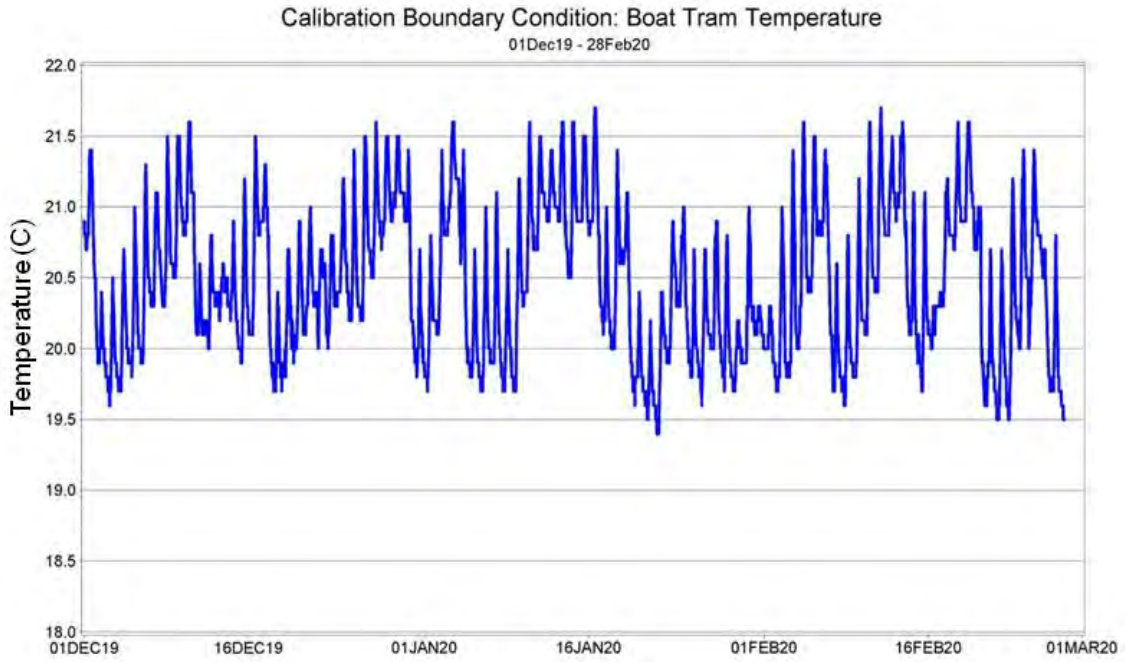

Figure 13. Water temperature at the Boat Tram for calibration period, December 1, 2019 to February 28, 2020, used for boundary condition.

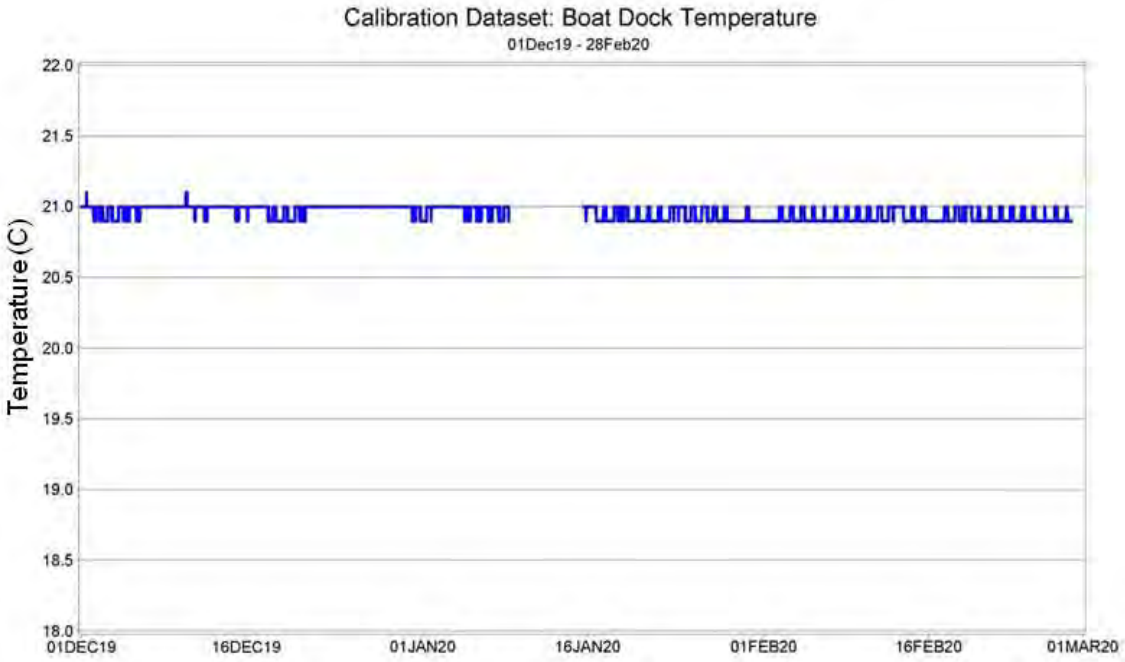

Figure 14. Water temperature at the Boat Dock for calibration period, December 1, 2019 to February 28, 2020, used for calibration. Water temperature data are collected at a resolution of 0.1°C.

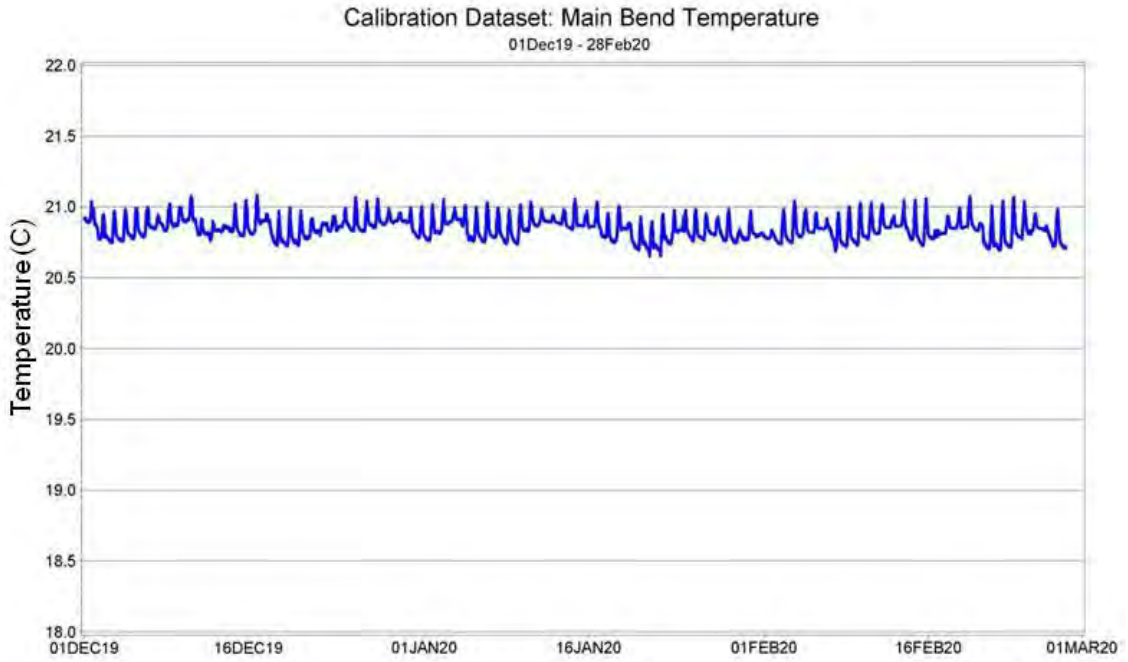

Figure15. Water temperature at the Main Bend for calibration period, December 1, 2019 to February 28, 2020, used for calibration.

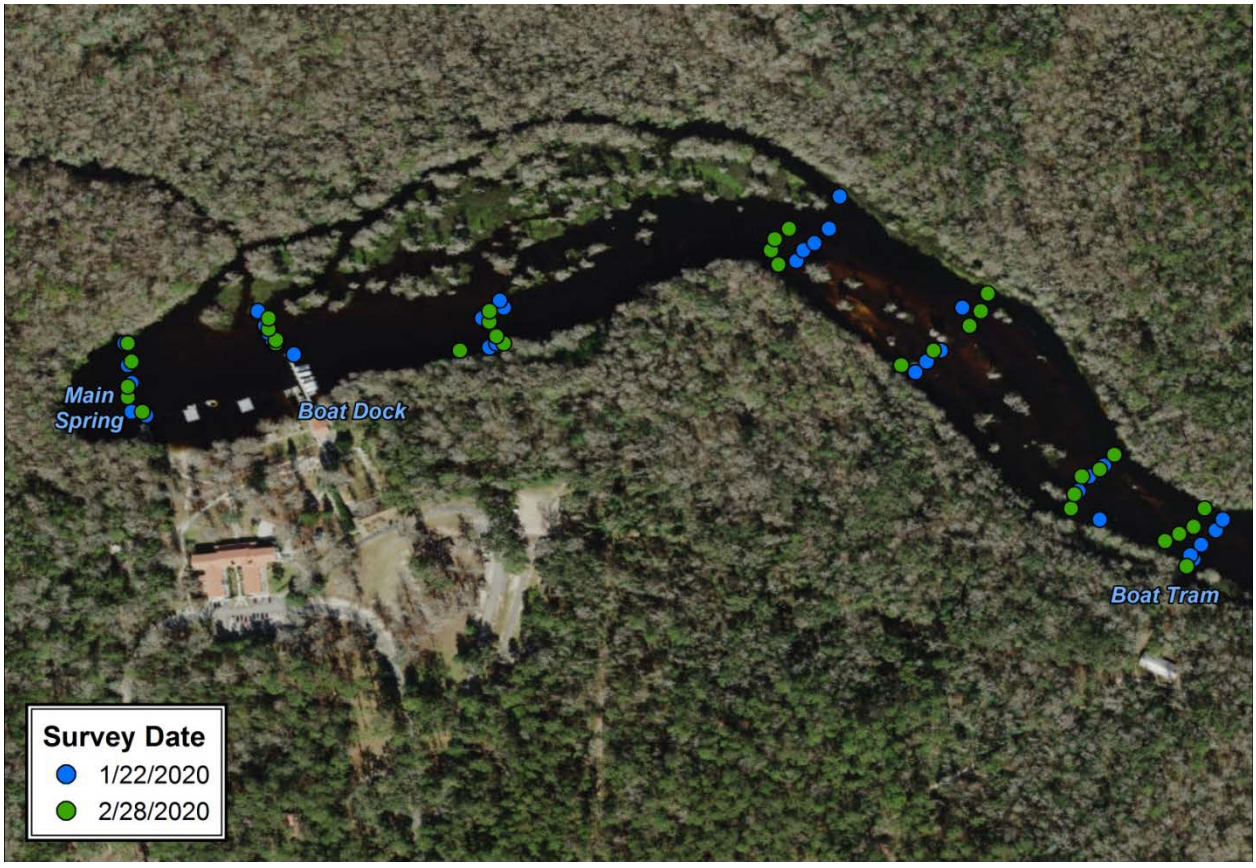

Figure 16. Locations of water temperature profile data used for calibration.

Of note is the very low variability in temperatures from the Main Vent (Figure 11), at the nearby Boat Dock location (Figure 14), and at the Main Bend (Figure 15), the slightly greater temperature variability at the Boat Tram location (Figure 13), and the greater variability in temperatures from Sally Ward (Figure 12). The range in temperatures is very small at all sites, however, with maximum range of just over 3°C at the Sally Ward location. Similar patterns occur during all winter periods for which simultaneous water temperature data are available at the five locations, as shown in Figures 17-20 for the winter periods (December 1 - March 15) of 2016-2017, 2017-2018, 2018-2019, and 2019-2020.

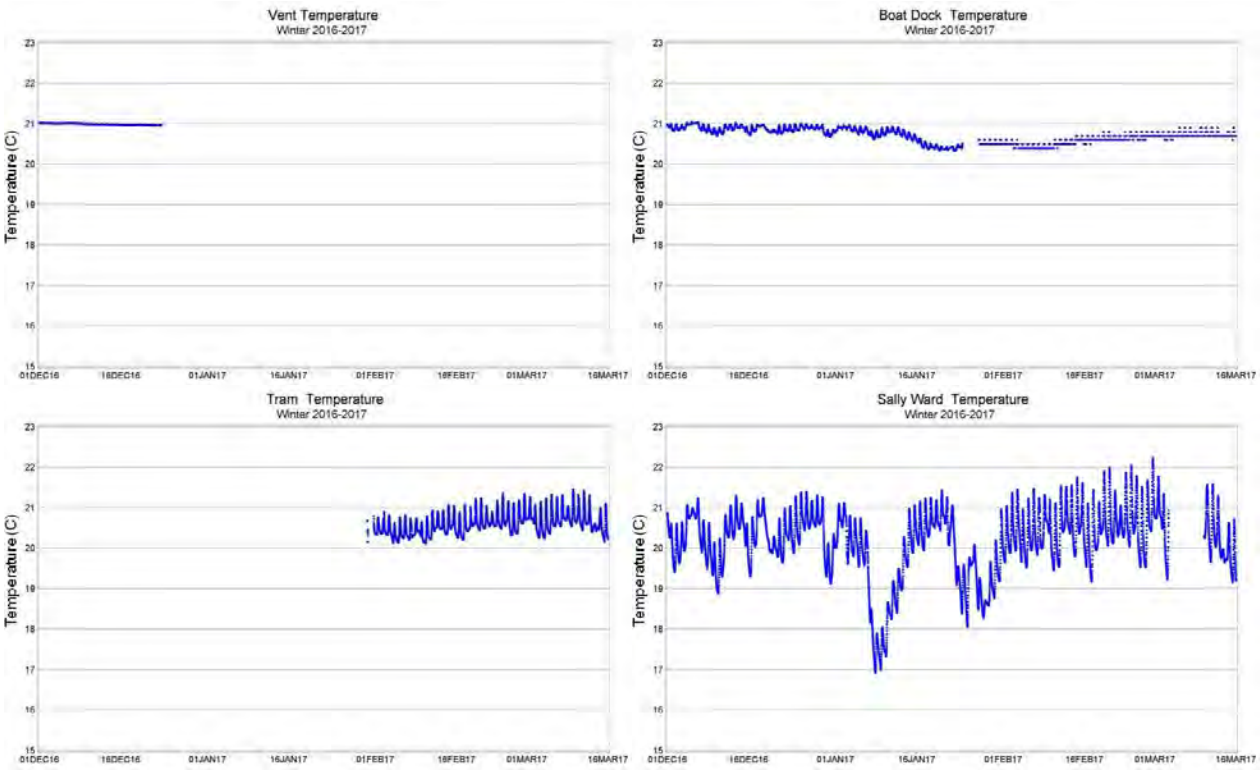

Figure 17. Water temperatures during winter 2016-2017 (December 1, 2016 - March 15, 2017): Wakulla Spring Vent (upper left), Boat Dock (upper right), Boat Tram (lower left), and Sally Ward Run (lower right). Vertical scale is 15-23°C.

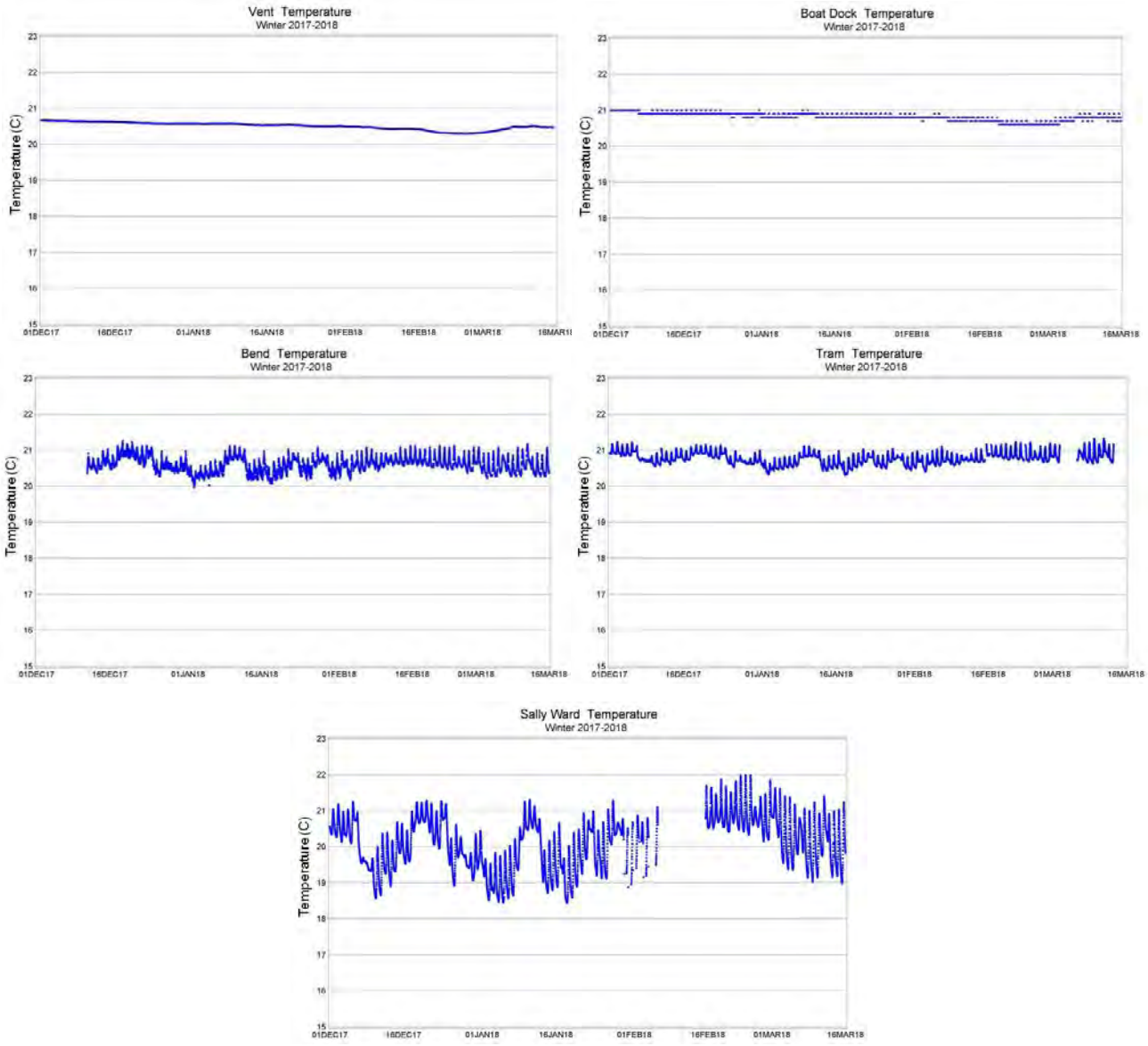

Figure 18. Water temperatures during winter 2017-2018 (December 1, 2017 - March 15, 2018): Wakulla Spring Vent (upper left), Boat Dock (upper right), River Bend (middle left), Boat Tram (middle right), and Sally Ward Run (bottom). Vertical scale is 15-23°C.

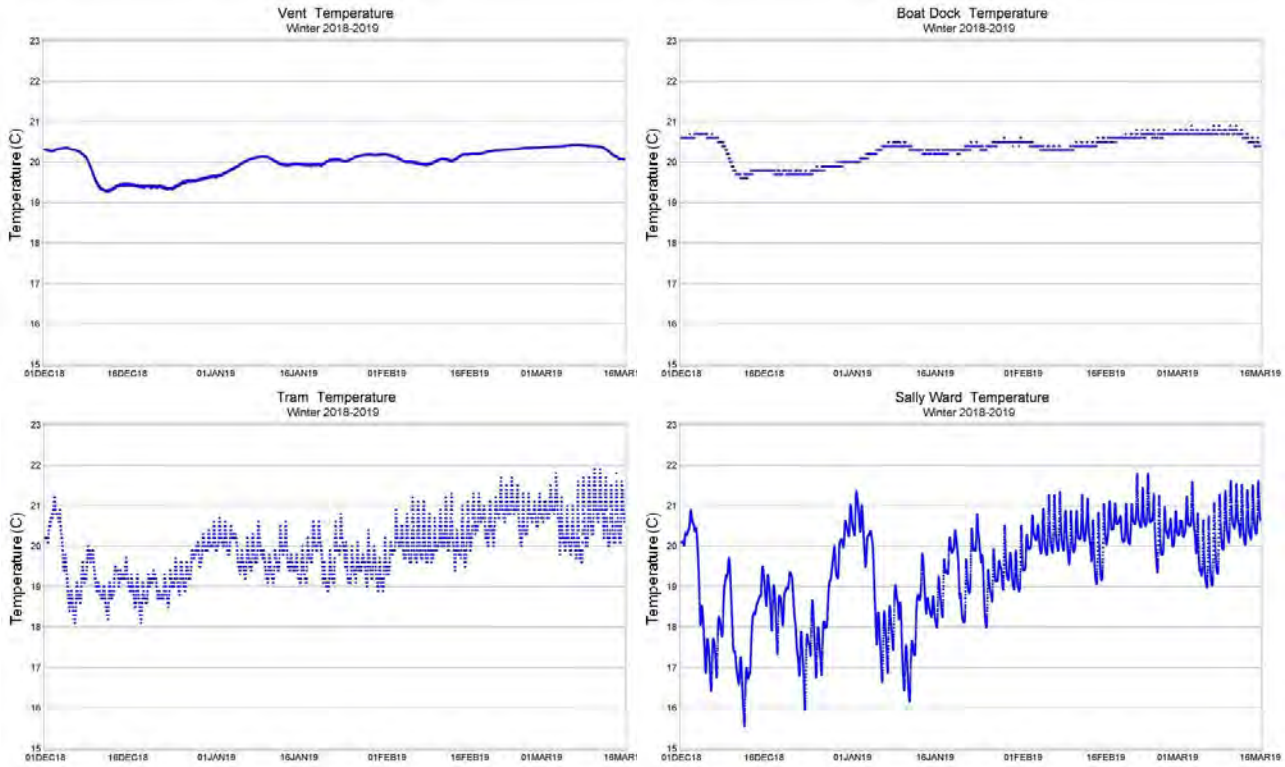

Figure 19. Water temperatures during winter 2018-2019 (December 1, 2018 - March 15, 2019): Wakulla Spring Vent (upper left), Boat Dock (upper right), Boat Tram (lower left), and Sally Ward Run (lower right). Vertical scale is 15-23°C.

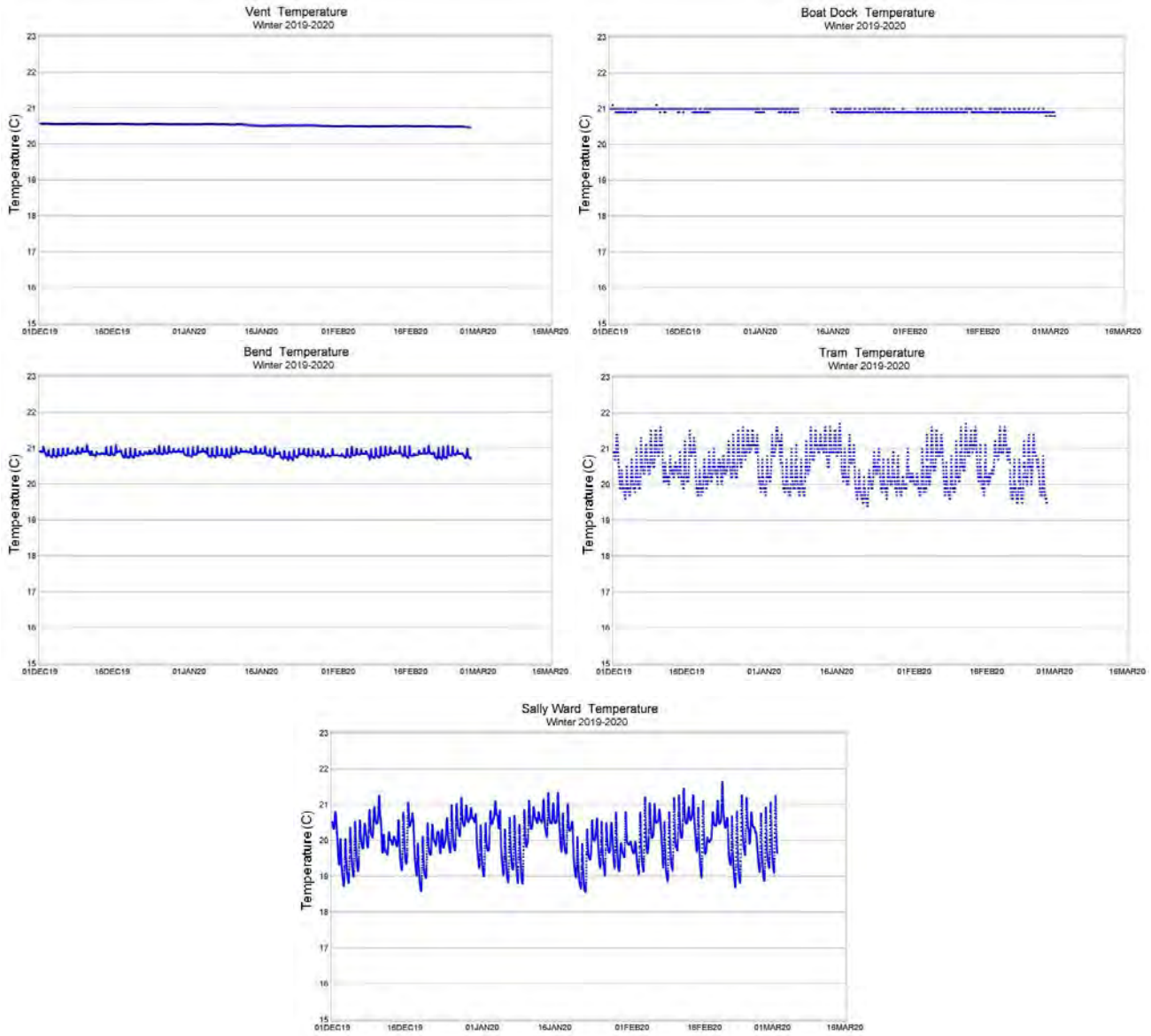

Figure 20. Water temperatures during winter 2019-2020 (December 1, 2019 - March 1, 2020): Wakulla Spring Vent (upper left), Boat Dock (upper right), River Bend (middle left), Boat Tram (middle right), and Sally Ward Run (bottom). Vertical scale is 15-23°C.

Flow data from the Main Vent and from Sally Ward were used as inputs for boundary conditions as well, for the December 2019 - February 2020 period (Figures 21 and 22). Sally Ward Run discharges comprise a very minor contribution to the Wakulla River and spring run, typically being less than five percent of the amount of discharge from the Main Vent. The missing flows for the Sally Ward input were interpolated between the preceding and following flows for the period 10Feb20 23:20 - 28Feb20 12:10.

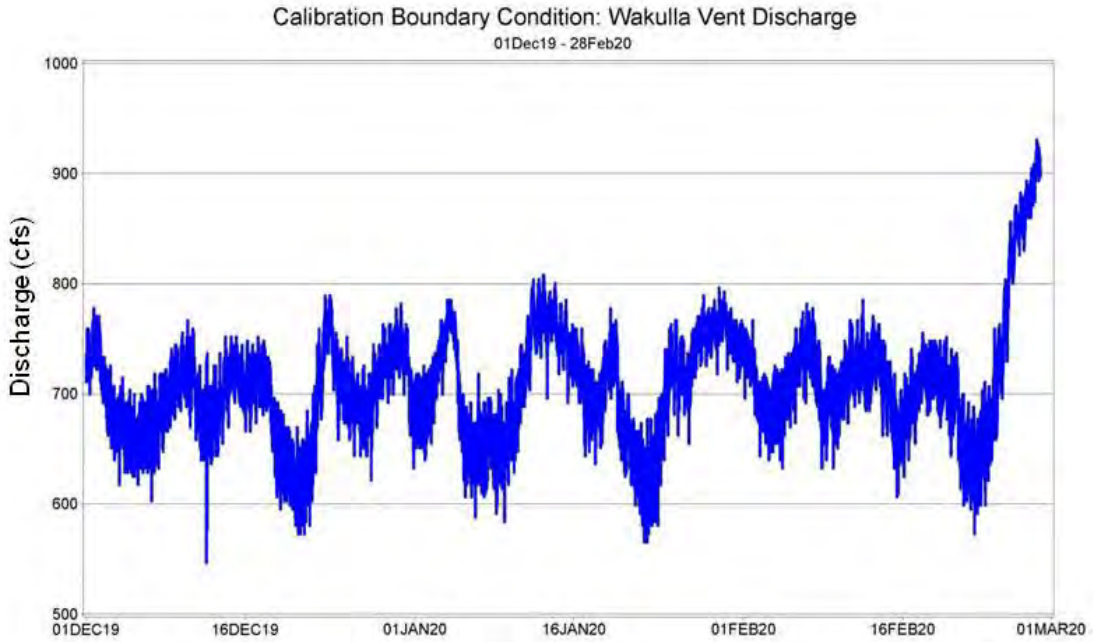

Figure 21. Discharge from Wakulla Main Vent during calibration period, December 1, 2019, to February 28, 2020, used for boundary condition.

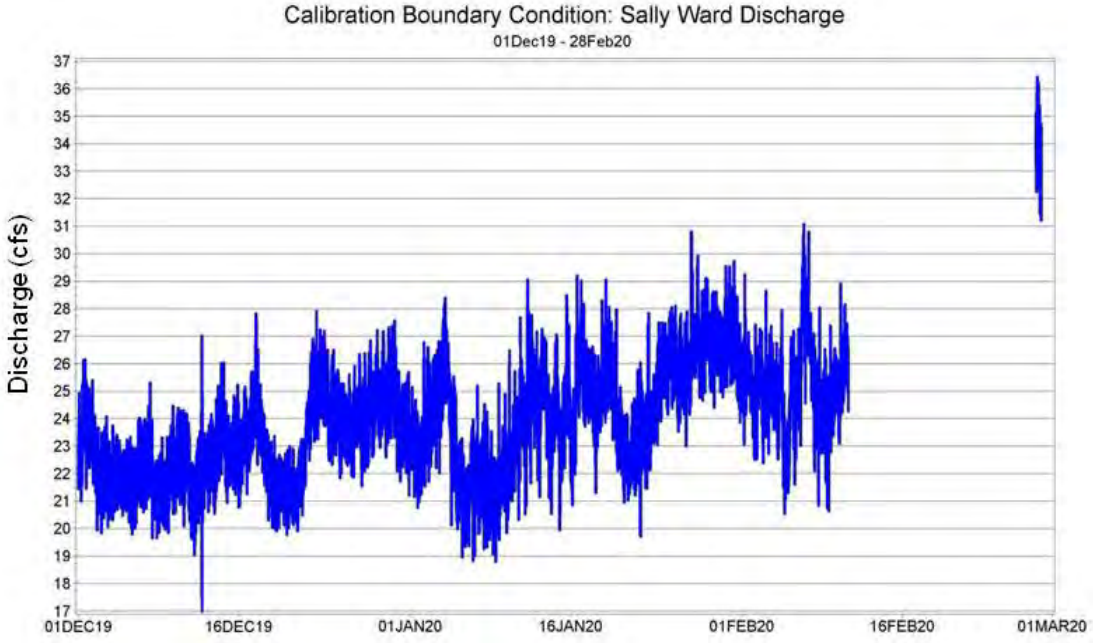

Figure 22. Discharge from Sally Ward Run during calibration period, December 1, 2019, to February 28, 2020, used for boundary condition.

Water surface elevations at the Boat Tram were used as a downstream boundary condition, and water surface elevations at the Boat Dock were used as calibration data. Observed water surface elevations at the Boat Tram ended during 22Jan20. A relationship was developed between water surface elevations at the Boat Tram and at the Boat Dock using data for the period 01Nov19 - 22Jan20, and this relationship was used to estimate Boat Tram water surface elevations for the period following the end of observations during 22Jan20 through 28Feb20. This relationship was very strong, with an R^2 of 0.96, and was as follows:

Boat Tram elevation = 1.07334*Boat Dock elev - 0.80002.

The resultant 15-minute Boat Tram water surface elevations for the period 01Dec19 - 28Feb20 are displayed in Figure 23, with the 15-minute Boat Dock water surface elevations, used for model calibration, shown in Figure 24.

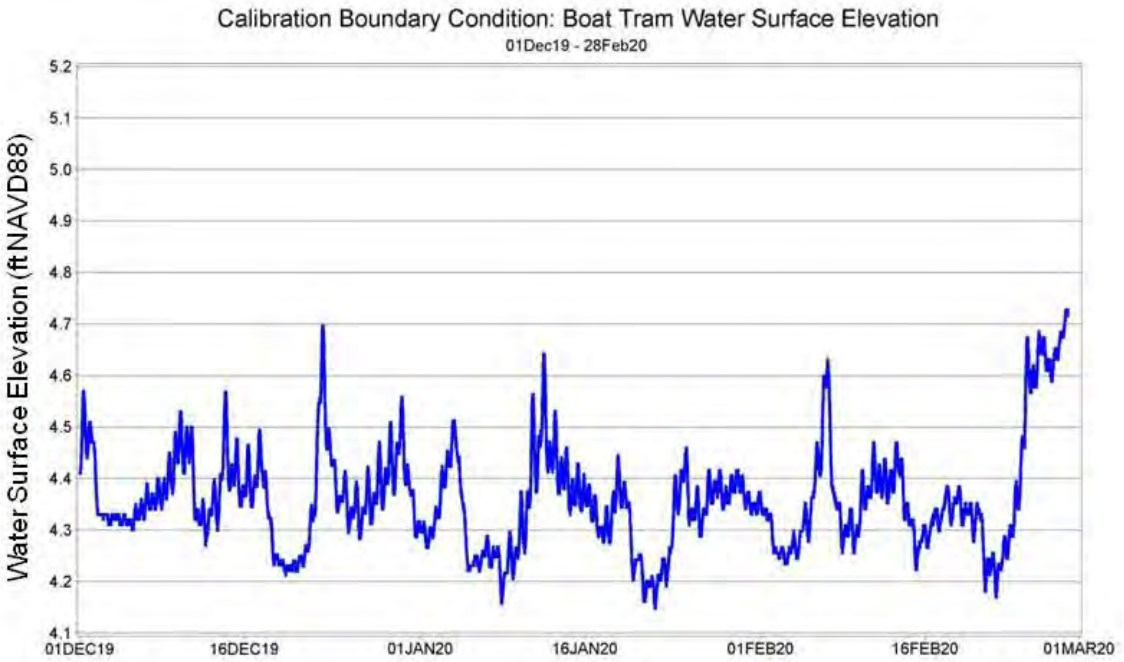

Figure 23. Water surface elevations at Boat Tram during calibration period, December 1, 2019, to February 28, 2020, used for boundary condition.

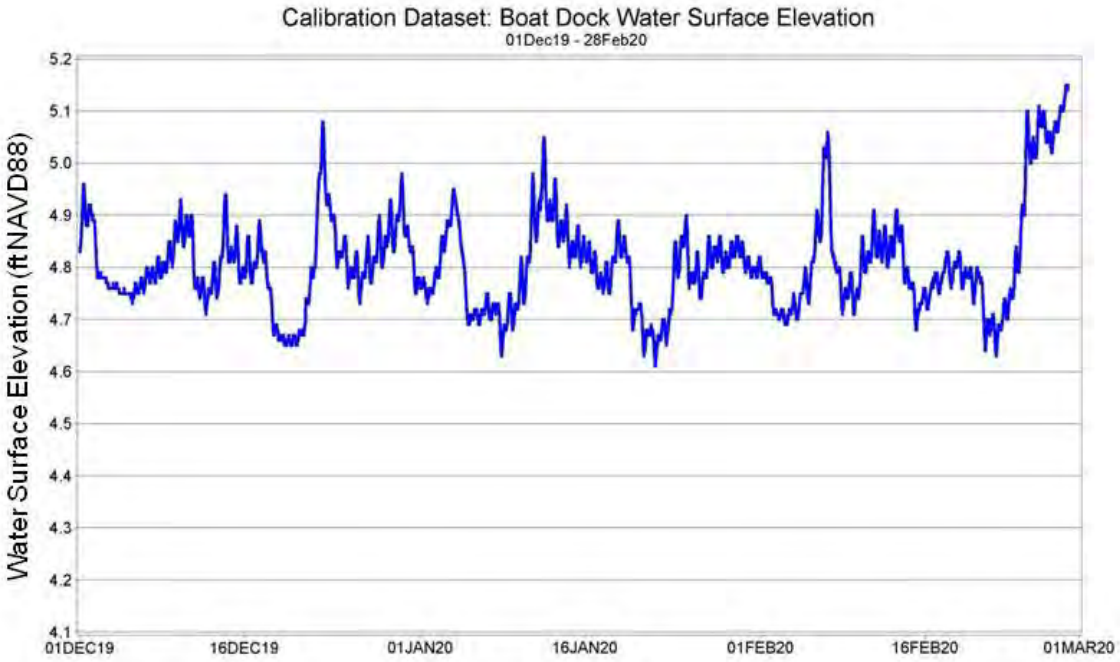

Figure 24. Water surface elevations at Boat Dock during calibration period, December 1, 2019, to February 28, 2020, used for calibration.

Time series plots of hourly meteorological data are provided in Figures 25-31, with the NWS site at Tallahassee Regional Airport providing relative humidity, atmospheric pressure, air temperature, cloud cover, and rainfall. Hourly solar radiation data were obtained for the IFAS FAWN Monticello site, along with daily evapotranspiration data.

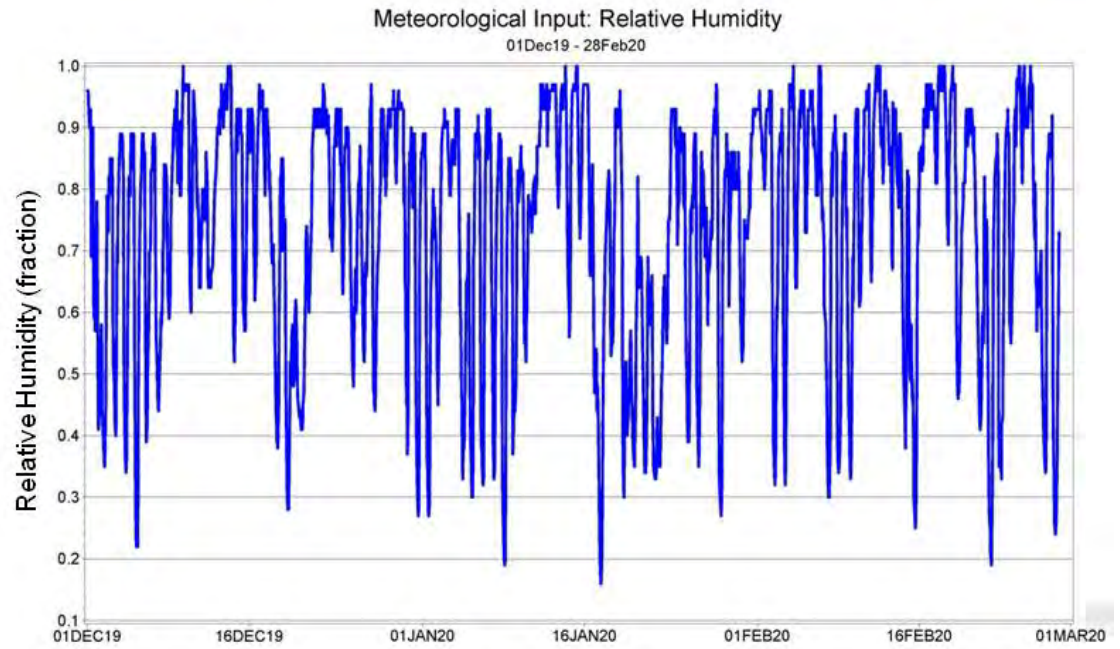

Figure 25. Hourly relative humidity from Tallahassee NWS site, December 1, 2019, to February 28, 2020.

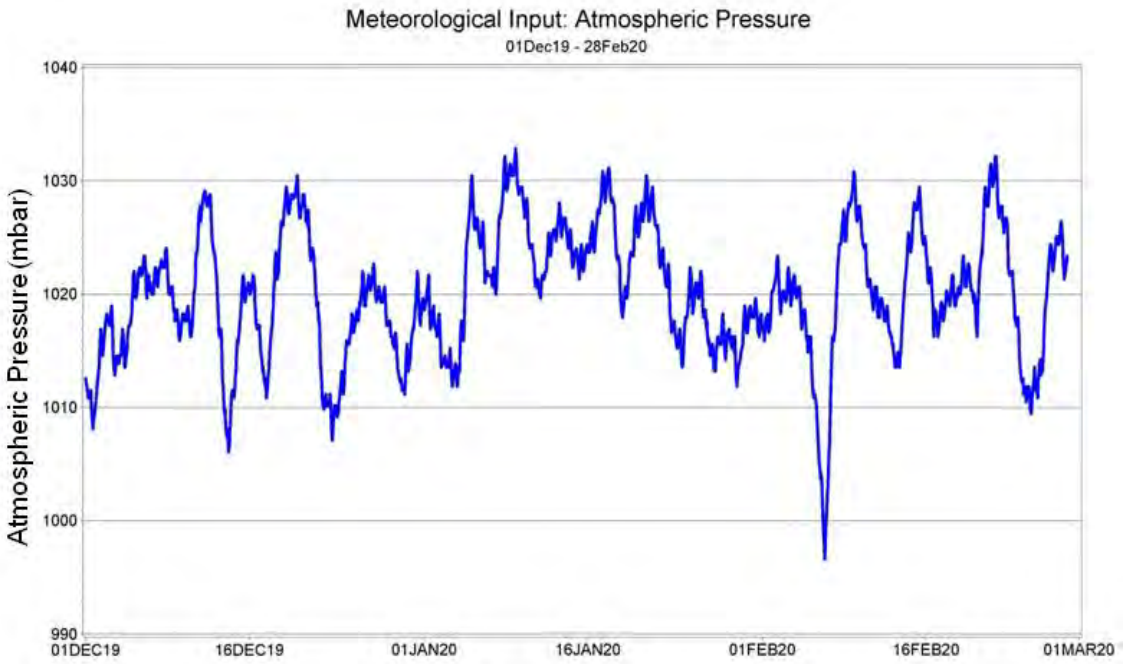

Figure 26. Hourly atmospheric pressure from Tallahassee NWS site, December 1, 2019, to February 28, 2020.

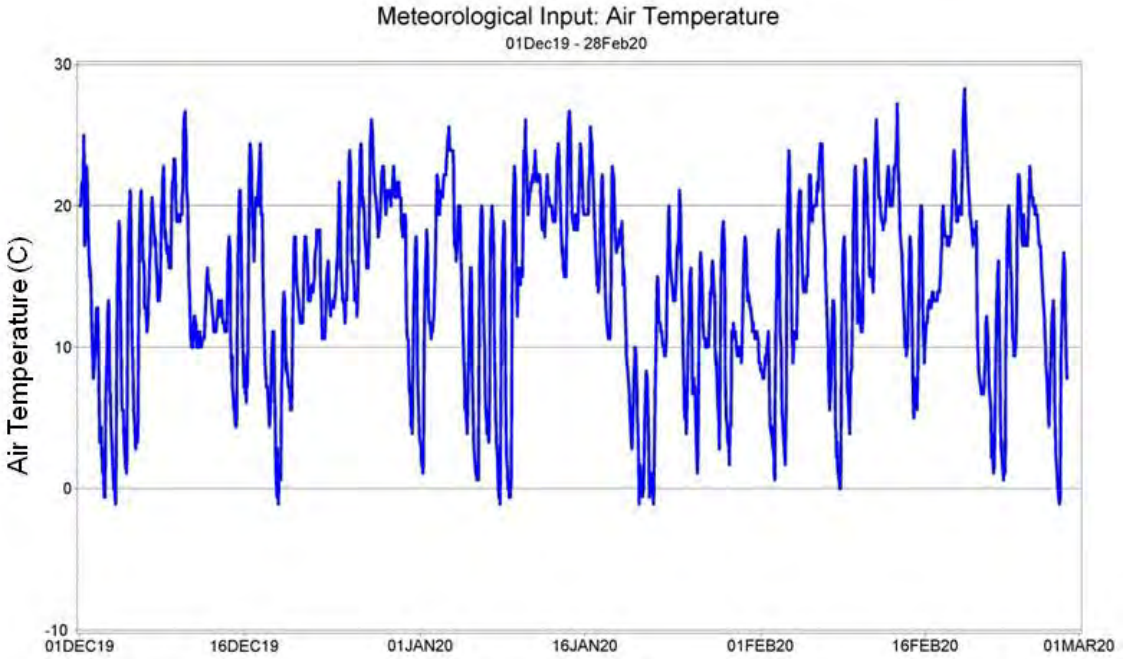

Figure 27. Hourly air temperature from Tallahassee NWS site, December 1, 2019, to February 28, 2020.

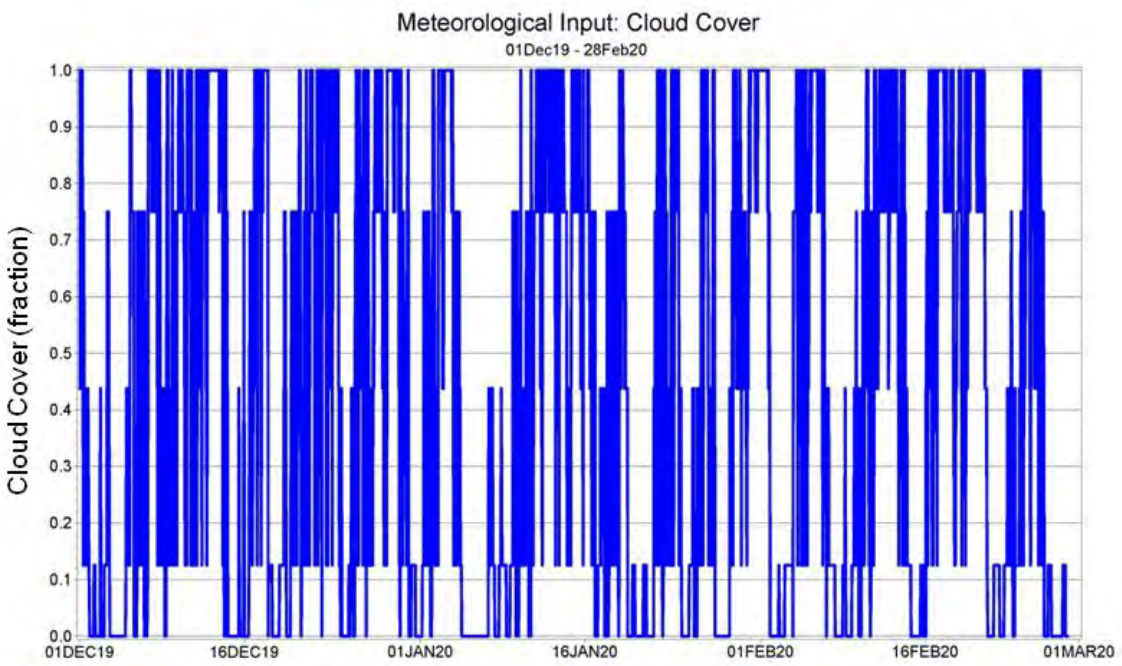

Figure 28. Hourly cloud cover from Tallahassee NWS site, December 1, 2019, to February 28, 2020.

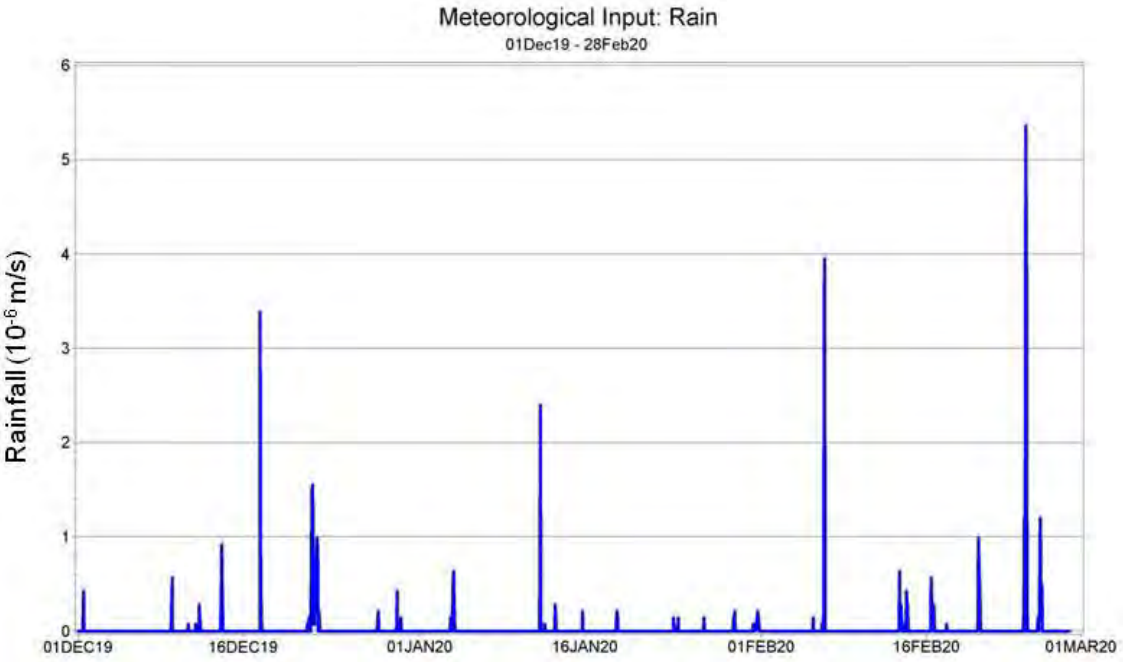

Figure 29. Hourly rainfall from Tallahassee NWS site, December 1, 2019, to February 28, 2020.

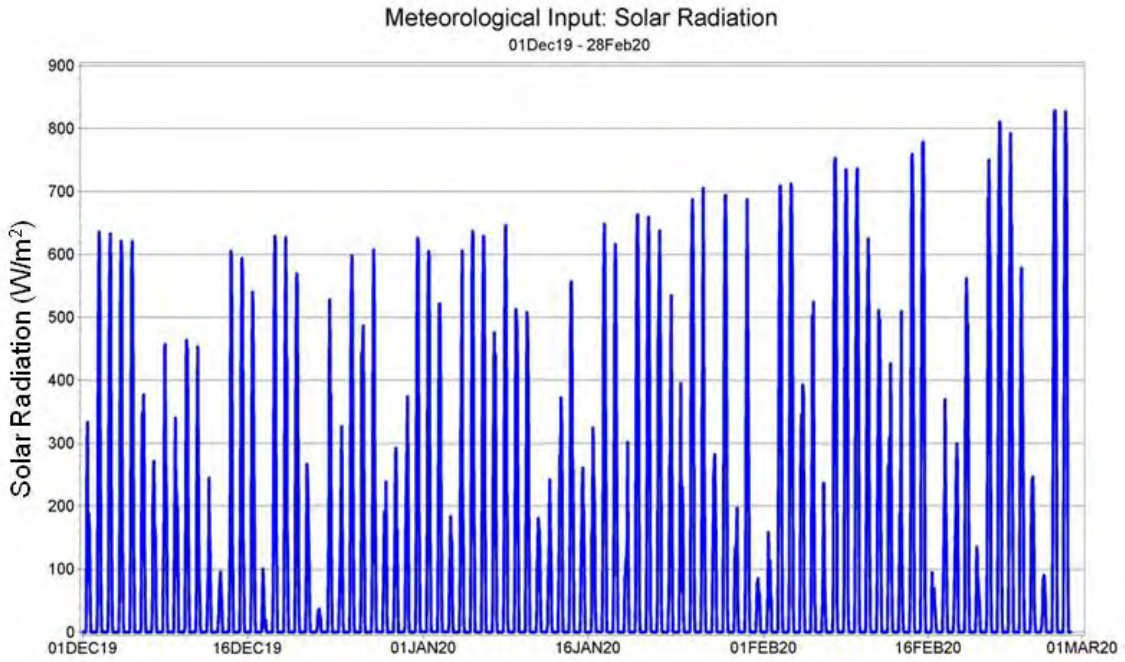

Figure 30. Hourly solar radiation from Monticello IFAS FAWN site, December 1, 2019, to February 28, 2020.

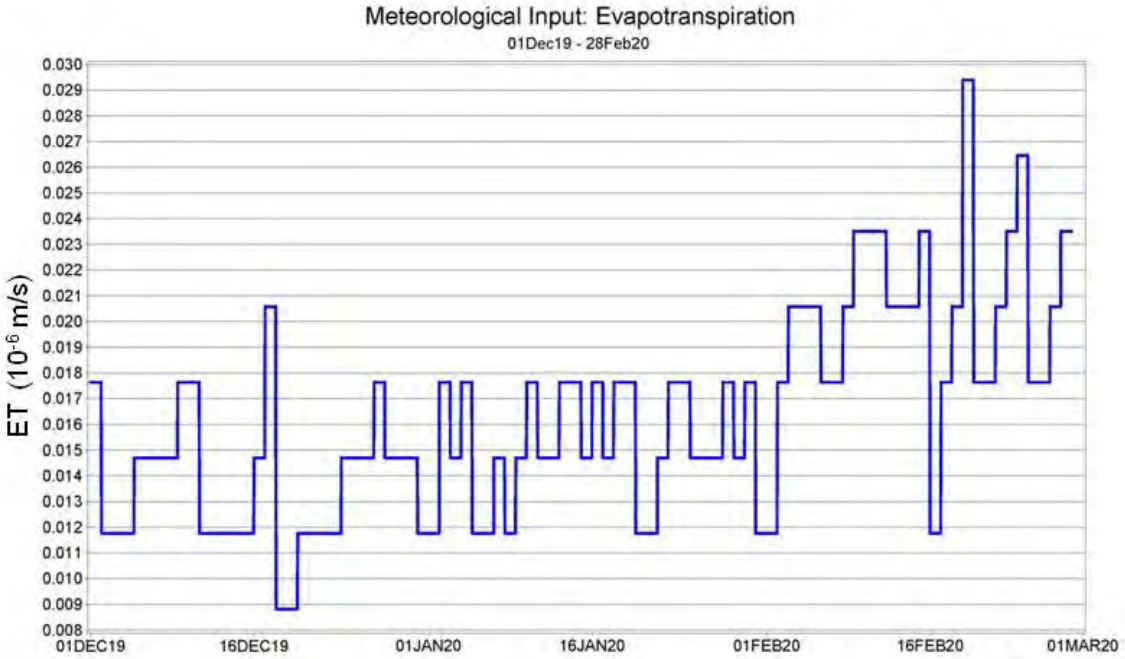

Figure 31. Daily evapotranspiration from Monticello IFAS FAWN site, December 1, 2019 to February 28, 2020.

Wind speed and wind direction data for the calibration period were obtained at 6-minute frequency from the USF COMPS Shell Point site on the Gulf Coast, with wind speed and direction provided in Figures 32 and 33, respectively, for the calibration period.

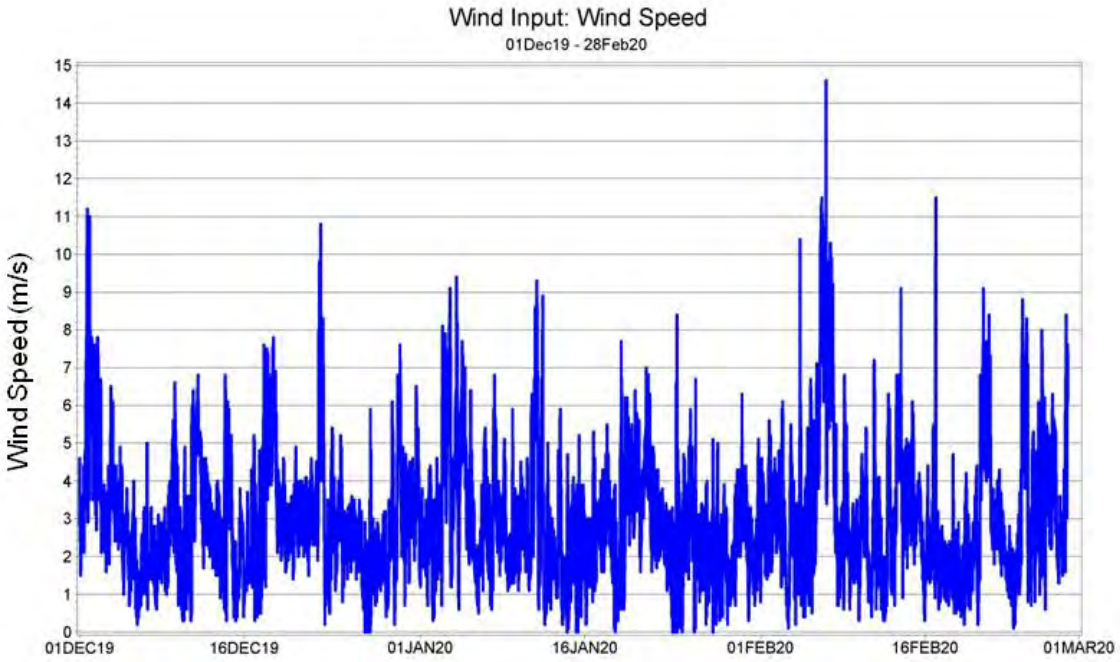

Figure 32. 6-minute frequency wind speed from Shell Point USF COMPS site, December 1, 2019, to February 28, 2020.

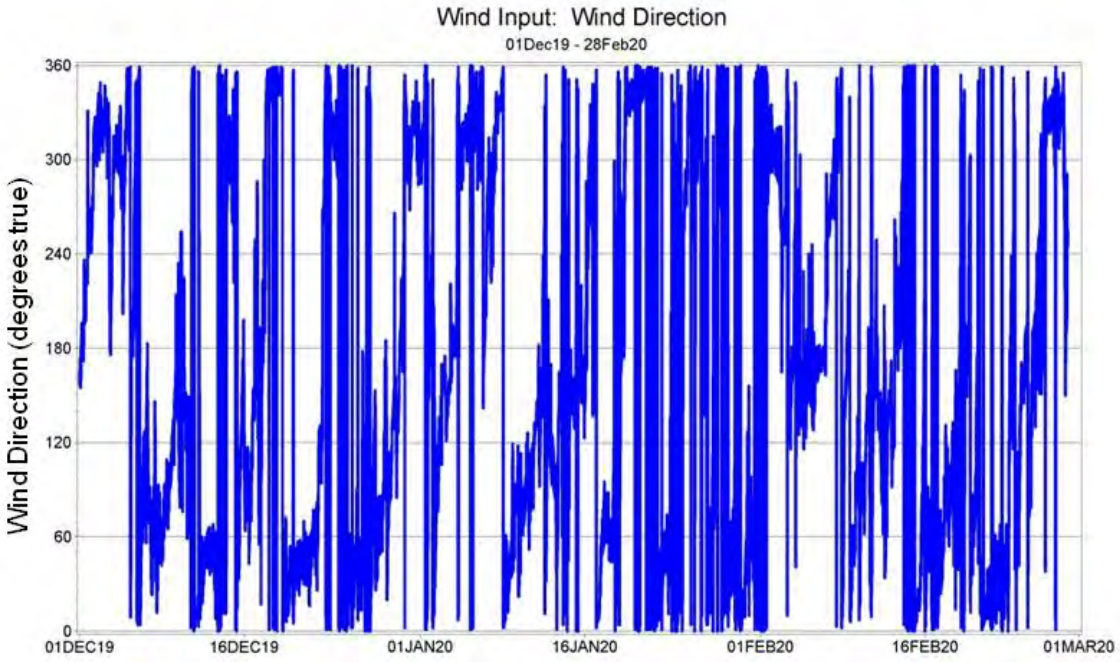

Figure 33. 6-minute frequency wind direction from Shell Point USF COMPS site, December 1, 2019, to February 28, 2020.

Initial conditions for water temperatures were set to 20.1 C for the entire model domain, similar to the temperatures observed on December 1, 2019 at the Boat Dock, the Main Bend, and the Boat Tram (Figure 20). The initial water surface elevations were set based on water surface elevations

measured at the Boat Dock and at the Boat Tram on December 1, 2019, with linear interpolation used to provide initial water surface elevations for the intervening cells.

The bathymetric data used for model development are described in the next section on grid development.

3.2 Model Grid Development

The model grid for the Wakulla Spring EFDC hydrodynamic model extends from the Wakulla Spring vent downstream to the continuous recording station located at the Boat Tram (Figure 3). Bathymetry transect measurements were taken by the District in February of 2016 (White, 2016), with additional depth measurements in the northern Sally Ward Spring run taken in 2019. More bathymetric data were collected in winter 2019-2020 during temperature profile data collection and incorporated into the updated bathymetry.

The spring pool is roughly circular in shape with a diameter of 315 ft and a maximum depth of 185 ft (cover page image, NWFWMD 2017). Discharge at Wakulla Spring flows from a large vent (50 ft x 82 ft) connected to an extensive submerged cave system (Loper et al. 2005). Water depths moving downstream from the spring vent become considerably shallower, particularly in the middle of the river where water depths can average less than 3 ft. On both the left and right edge of the water are deeper channels which were excavated in the early 1970s to allow for state park tour boat operation. These excavated areas have typical water depths ranging from three to nearly ten feet.

The shoreline of Wakulla Spring and the spring run was developed using the transect measurements and aerial photographs using ArcGIS software. The shoreline was imported into the WQMap gridding software package (Applied Science Associates 2003, 2004), which was used to create the model grid. Following model grid development, the transect bathymetry data were spatially joined with the grid system. Model grid cells with no bathymetry data were assigned depths using linear interpretation, with aerial photos and photographs of Wakulla Spring used in some places to determine the location of emergent vegetation and associated shallow water column. The bottom elevation assigned to each model grid cell represents the average bottom elevation within that cell. The model grid is shown below in Figure 34.

As seen in Figure 34, the larger islands along the north side of the spring run, separating the predominately Sally Ward water northern channel from the main run, are re-created in the model grid system, while smaller islands/shallows are incorporated within model grid cells, with the total volume of a specific cell approximating the total volume of water in the cell in the real world, by utilizing the mean cell depth as representative. The model grid contains 250 horizontal grid cells. Cell sizes in the cross-stream direction range from 19.3 ft to 118.0 ft and in the along-stream direction from 12.1 ft to 162.3 ft, with the smallest cells near the mouth of the Sally Ward Spring discharge and the largest cells just upstream of the downstream boundary at the Boat Tram location. The vertical dimension is divided into four layers, with each horizontal grid cell having

four equally-spaced layers. For example, if the cell is 4 ft deep, then each vertical layer is 1 ft deep. As water surface elevations change over time with increased or decreased flow, the cell water column depth, and thus the layers' vertical extents, vary according. The bottom elevations of the model grid cells, relative to NAVD88, range from 2.7 ft (above NAVD88) associated primarily with cells containing emergent vegetation to approximately -55.2 ft (below NAVD88) in the spring vent, and represent an average over the entire grid cell. The majority of the water depths were measured when Staff Gage A (at the Boat Tram) elevations ranged between 4.87 ft and 4.79 ft NAVD88. The initial water surface was therefore set to the average of these two values, 4.83 ft NAVD88, providing a reference system for establishment of bottom elevations with respect to NAVD88. The model time step is a constant 1 second.

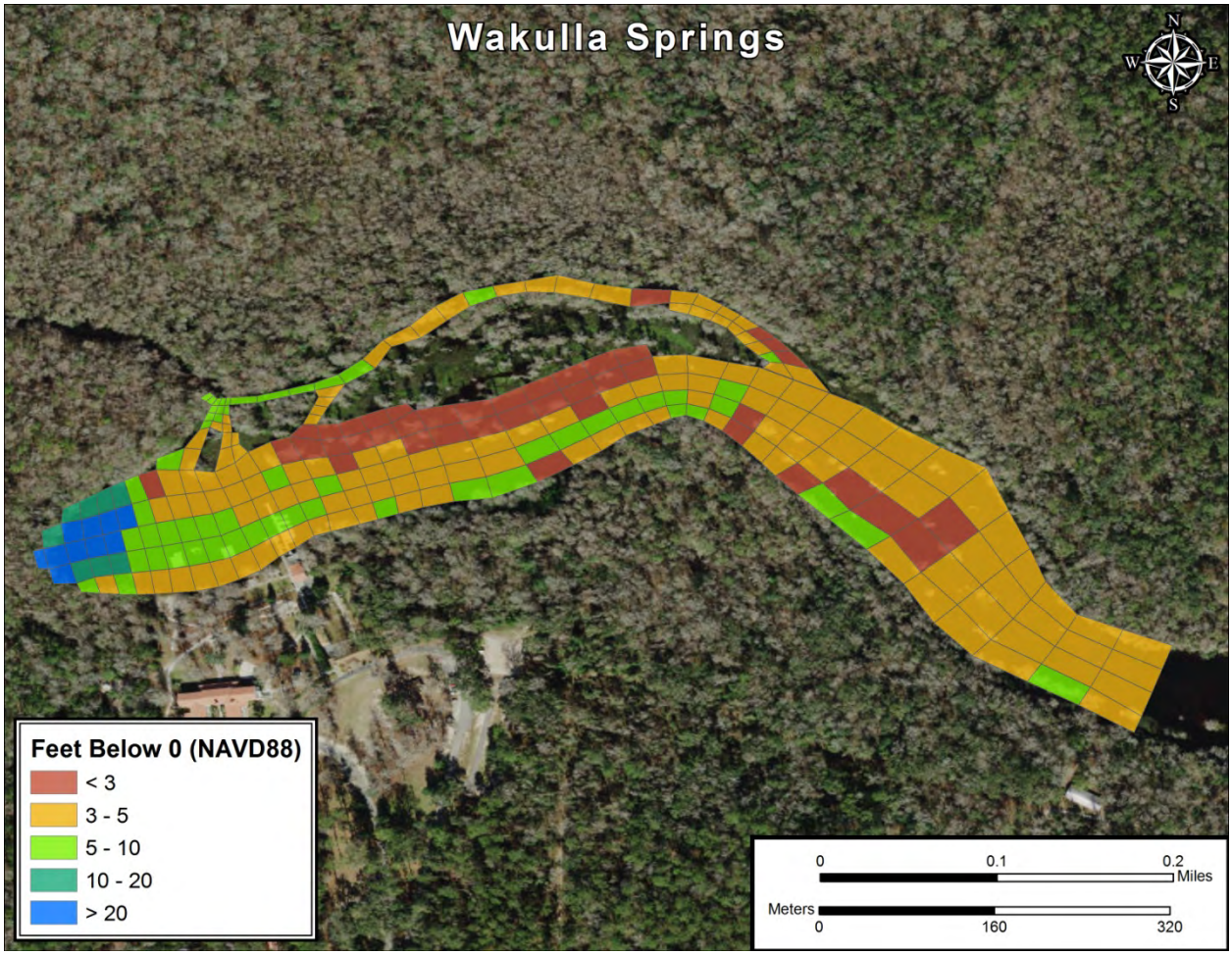

Figure 34. Wakulla Spring EFDC model grid and bathymetry.

3.3 Model Calibration

Model calibration was initially planned for the winter period 2017-2018. Prior to model calibration, additional transect profile data were collected during cold periods in January 2019. It was initially decided that data collected over both the winters of 2017-2018 and 2018-2019 would define the calibration period. However, during the course of the model calibration effort, it was

found that the frictional effects of the spring run system (drag caused by submerged vegetation, trees, bottom elevation changes) were considerably different during the two periods. Discussion with District staff indicated that the elevation-flow relationships downstream of the model domain were observably different before and after Hurricane Michael in October 2018, so that it was not surprising that the two model periods would require different frictional parameterizations in the model. Since the frictional parameterization does not allow for time variability, so that the model could not be calibrated to two different frictional conditions (pre- and post-Michael), the model was calibrated using the most recent cold period data available. By this time, the District had collected additional transect profile data in January and February 2020 (see Figure 16), and the data from this most recent period containing cold weather events is most representative of how the system would be expected to respond in the future.

The primary parameter adjusted to reach calibration was the bottom roughness height (model parameter z_{rough}), or bottom friction coefficient, associated with the physical grid system. This parameter can vary spatially, but for this model application was set to a spatially-constant value of $z_{rough} = 2.0$ to reach calibration for water surface elevations. For comparison, experience has found that for unvegetated straight channels with relatively smooth bottoms, values on the order of 0.01 for this parameter are often appropriate. Previously completed sensitivity analyses for the pre-Hurricane Michael period (Janicki Environmental, 2019a) found that a value of $z_{rough} = 2.5$ provided appropriate simulated water surface elevations at the boat dock location. In addition to the roughness height adjustment, the depths of the grid cells based on data collected prior to Hurricane Michael (Janicki Environmental, 2019b) were refined to reflect scouring and deposition which occurred as a results of the hurricane, based on additional bathymetric data collected by the District post-Michael. Overall, changes to the grid cell bathymetry were minor. It should be noted that the calibrated model cannot be used to back-cast historical conditions. However, the model can be used to simulate how water temperatures in the current river (geometry) are likely to change in response to changing spring flows with a given set of environmental conditions. Winter reference period simulations presented in Section 4 utilize climatic conditions (spring flows, air temperatures, water temperatures, etc.) observed pre-Hurricane Michael applied to current river geometry represented in the calibrated model. Direct simulations of winters pre-Hurricane Michael were not performed.

As described in Section 3.1, data used to compare to model output to determine model calibration over the December 1, 2019 - February 28, 2020 period were as follows:

- water surface elevation and water temperature data collected at the Boat Dock via continuous recorder (15-minute frequency);
- water temperature data collected at the Main Bend via continuous recorder (15-minute frequency); and
- transect profile data collected on January 22 and February 28, 2020 (Figure 16).

The calibration period included several days when the air temperature was near or below freezing for some portion of the day (Figure 27), as determined by both the profile data collection effort and the Tallahassee NWS data.

The vertical profile thermal data were collected by District staff using a calibrated YSI meter to record time of day, water temperature, specific conductance, depth of sample and total water column depth, pH, and dissolved oxygen, at a minimum of three points per location: near-surface (approximately 1.6 ft below the surface), mid-water column, and near-bottom (approximately 1.6 ft above bottom). In areas deeper than 6.5 ft, profile samples were taken approximately every 3.3 ft to the bottom or to a maximum depth of 13 ft, whichever was reached first. In areas less than 6.5 ft in depth, profile samples were taken approximately every 1.6 ft from the surface to the bottom. Samples were taken at five points approximately equidistant across each transect, as well as in the estimated thalweg location and the main channel if different from the thalweg. The latitude, longitude, and air temperature values were also recorded at each sample location. Equipment was calibrated prior to and after each sampling event. Measurements at all profile sample sites were completed between first light and 9:40 AM when air temperatures were lowest and safe boat operation was possible.

It should be noted that the continuous recorder temperature data collected at the Boat Dock are reported to the nearest 0.1°C, resulting in the time series provided in Figure 14. This has ramifications for comparison to simulated data as part of the calibration effort, as reported below, in that the simulated temperatures are not rounded to the nearest 0.1°C when output from the model.

Initial data exploration associated with early calibration attempts discovered a mismatch between reported water temperatures from the vent and those collected in the vent during profile measurements, of the order of 0.2 - 0.4 C, with the vent temperatures being lower, as shown in Figure 35. This discrepancy was determined to be unlikely since profile measurements were taken directly over the Wakulla Spring vent where discharge was flowing vertically and as a result had not yet come in contact with cooler air temperatures. In addition, profile measurements showed the water to be extremely well mixed with variations in water temperatures vertically and horizontally typically in the range of 0.05°C or less. Discussion with District staff found that the sensor in the vent has a calibration accuracy of 0.5°C. Model runs to test the effects of modifying the vent temperatures were completed with results compared not only to the profile data but to the continuous recorder temperature at the Boat Dock, and it was found that increasing the vent temperature record by 0.4°C allowed much more accurate simulation of the observed conditions. Therefore, the vent water temperature was increased by 0.4 C prior to model input, and all results presented in the following sections result from this input data revision. As the goal of the calibration effort is to develop a temperature model which simulates observed conditions appropriately based on measured input conditions, this adjustment to the vent input temperature is considered acceptable, given the calibration accuracy of the sensor.

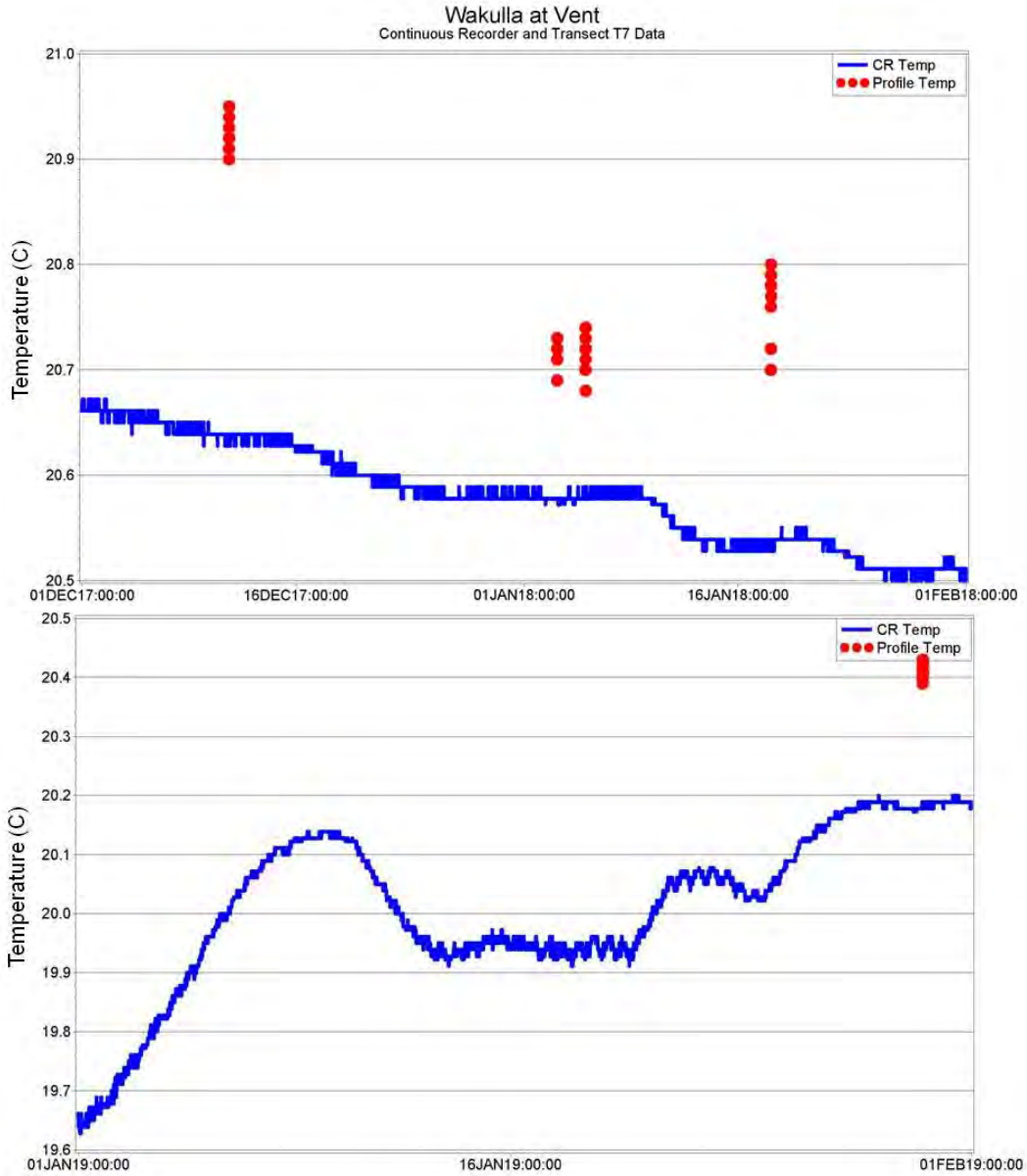

Figure 35. 15-minute water temperature (blue) from Wakulla vent, winter 2017-2018 (top panel) and 2019 (bottom panel), with profile data (red) collected at transect across the vent. The red dots are the measured profile temperatures at the vent at each data collection depth, at the time indicated on the x-axis.

For the model calibration process there are many ways to present data in order to allow for an assessment of the accuracy of the hydrodynamic model. Based on previous experience with model calibration, the list of primary methods for presenting and analyzing the data for calibration (water surface elevation and temperature) includes the following:

- Time series plot comparisons of measured data versus simulated data at scales to allow visual assessment
- The following quantitative calibration metrics:

Mean Error (ME)

$$\mathrm{ME} = \frac{1}{n}\sum_{i=1}^{n}(P_\mathrm{i} - O_\mathrm{i})$$

where P_i =predicted value
O_i =observed value
n = number of observations

Mean Absolute Error (MAE)

$$\mathrm{MAE} = \frac{1}{n}\sum_{i=1}^{n}|P_\mathrm{i} - O_\mathrm{i}|$$

where P_i =predicted value
O_i =observed value
n = number of observations

Root Mean Square Error

$$\mathrm{RMSE} = \sqrt{\frac{\sum_{i=1}^{n}(P_\mathrm{i} - O_\mathrm{i})^2}{n}}$$

where P_i =predicted value
O_i =observed value
n = number of observations

Coefficient of Determination (R^2)

$$R^2 = \left[\frac{\sum_{i=1}^{n} O_\mathrm{i}P_\mathrm{i} - \frac{(\sum_{i=1}^{n} O_\mathrm{i})(\sum_{i=1}^{n} P_\mathrm{i})}{n}}{\left[\sum_{i=1}^{n} (O_\mathrm{i})^2 - \frac{(\sum_{\mathrm{i}=1}^{\mathrm{n}} O_\mathrm{i})^2}{n}\right]\left[\sum_{i=1}^{n} (P_\mathrm{i})^2 - \frac{(\sum_{\mathrm{i}=1}^{\mathrm{n}} P_\mathrm{i})^2}{n}\right]}\right]^2$$

where P_i =predicted value
O_i =observed value
n = number of observations

The quantitative calibration metrics are provided for both temperature and water surface elevation. The metric values are intended to ensure that the model replicates responses to incoming flows and temperatures such that sufficient resolution exists to allow for informed management decision making regarding expected temperature envelope areas and volumes relative to the temperature criteria. The data from the model are extracted to match times and depths of available measured data for the calibration assessment. Plots comparing simulated and observed temperature and water surface elevation are provided. Calibration metrics and the associated calibration criteria values for these metrics are shown in Table 2 and provide assurance that the calibrated model is sufficient to resolve appropriate responses in temperature and water elevation conditions to changes in spring inflows. The criteria values were selected based on professional judgement and the need for resolving small differences in temperatures around the temperature criteria.

Table 2. Calibration criteria for water surface elevation and temperature.

Parameter	Mean Error	Mean Absolute Error	R^2	RMSE
Elevation (in)	+/-0.4	0.8	0.90	1.0
Water Temperature (ºC)	+/-0.2	0.5	0.90	1.0

The time series comparisons of model results to the data collected at the Boat Dock continuous recorder (USGS 02307000) are provided in Figure 36 (water surface elevation for December 1, 2019 - February 28, 2020) and Figure 37 (water temperature for December 1, 2019 - February 28, 2020). As mentioned previously, model parameter adjustment of the frictional coefficient to the post-Hurricane Michael system allowed for a much better fit than was originally found when attempting to parameterize the model to simulate both pre- and post-hurricane conditions. The comparison statistics for both elevation and temperature are provided in Table 3 for the Boat Dock continuous recorder, and for water temperature for the Main Bend continuous recorder. The time series comparison of model results to temperature data collected at the Main Bend continuous recorder is provided in Figure 38.

Table 3. Calibration assessment for water surface elevation and water temperature at the Boat Dock site, and for water temperature at the Main Bend site, December 1, 2019 - February 28, 2020.

Parameter	Mean Error	Mean Absolute Error	R^2	RMSE
Boat Dock Elevation (in)	-0.15	0.34	0.94	0.44
Boat Dock Water Temperature (ºC)	-0.10	0.10	0.44	0.11
Main Bend Water Temperature (ºC)	-0.01	0.03	0.88	0.03

Calibration assessment with respect to water surface elevation at the Boat Dock indicates that the model is very well calibrated with respect to elevation, with the metric values provided in Table 3 for elevation meeting the calibration criteria provided in Table 2. Visual comparison of the time series of the observed and simulated elevations at the Boat Dock, provided in Figure 36, shows the very close match between the two, with some slight under-prediction at lower elevations. When examining the metric values resulting from comparison of observed and simulated water temperature at the Boat Dock (Table 3), the coefficient of determination (R^2) value is less than the target metric value given in Table 2. As mentioned previously, the observed values are reported to the nearest 0.1°C, so the simulated values were rounded to the nearest 0.1°C prior to comparison, as depicted in Figure 37. As there is little variability in the observed Boat Dock water temperatures, and that variability is expressed in 0.1°C increments, the relatively low R^2 value of 0.44 results, as

this metric in a measure of the contribution of the dependent variable (modeled temperature) to the variability seen in the independent variable (observed temperature). The minimal variability in the observed temperature makes a high value for R^2 difficult to obtain without exactly matching the observed signal. However, the other calibration criteria (Table 2) are clearly met at the Boat Dock, and the time series graphic (Figure 37) shows the model is accurately simulating the observed water temperatures within 0.2°C or less at the Boat Dock. Similarly at the Main Bend (Figure 38), although the R^2 value is slightly less than the target value of 0.90, the other metric criteria are met, and the time series graphic shows that the model is accurately simulating the observed water temperatures here as well, within 0.1°C or less. Based on this assessment, the model is well calibrated with respect to both water surface elevation and temperature.

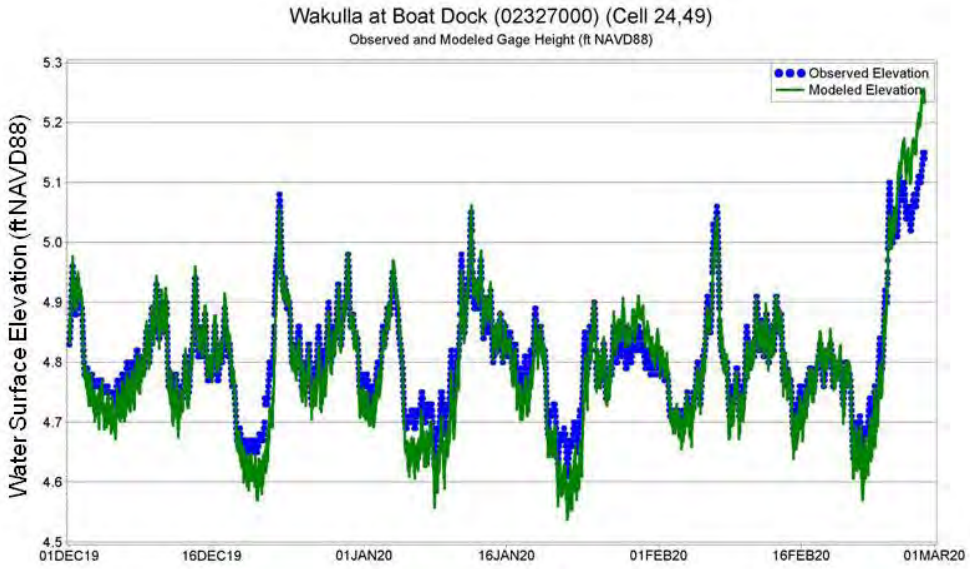

Figure 36. Time series comparison of modeled (green) and observed (blue) 15-minute water surface elevation at the Boat Dock Station (USGS 02327000) for December 1, 2019 - February 28, 2020.

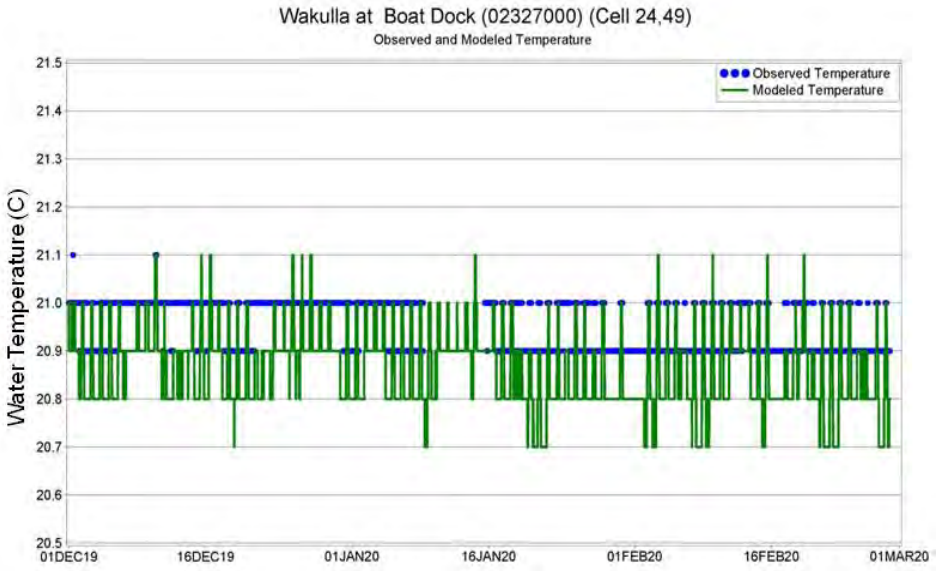

Figure 37. Time series comparison of modeled bottom temperature (green) and observed 15-minute temperature (blue) at the Boat Dock Station (USGS 02327000) for December 1, 2019 - February 28, 2020.

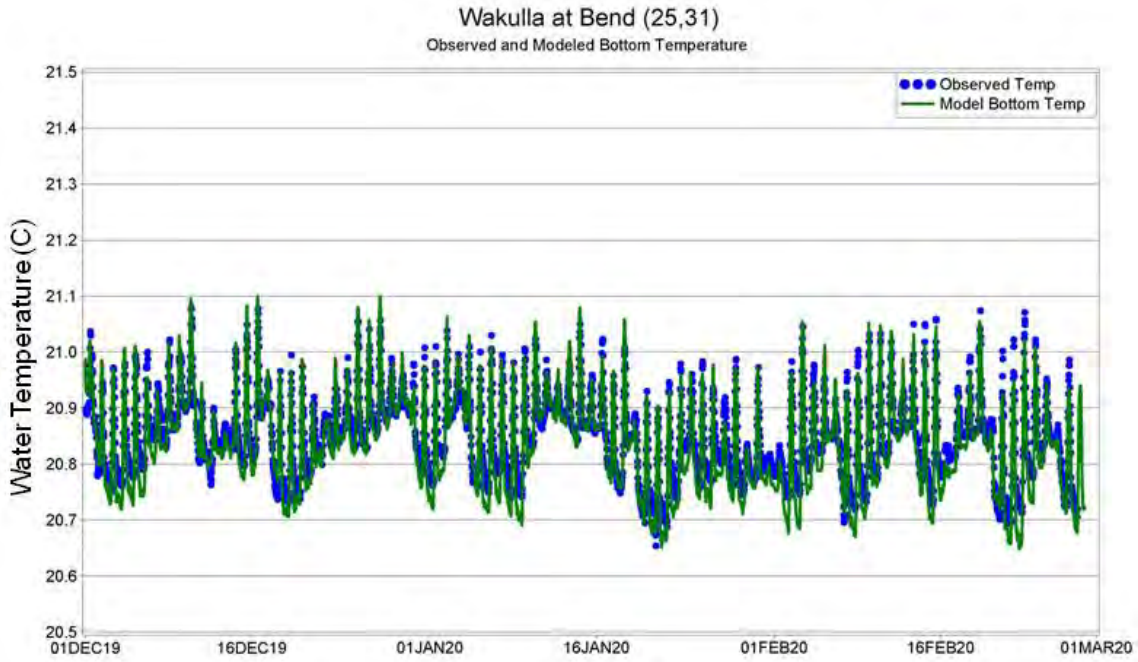

Figure 38. Time series comparison of modeled bottom temperature (green) and observed 15-minute temperature (blue) at the Main Bend Station for December 1, 2019 - February 28, 2020.

An additional visual method of comparing the observed and simulated temperatures at the Boat Dock is presented in Figure 39, which provides a scatter plot of the simulated vs. observed water temperature data.

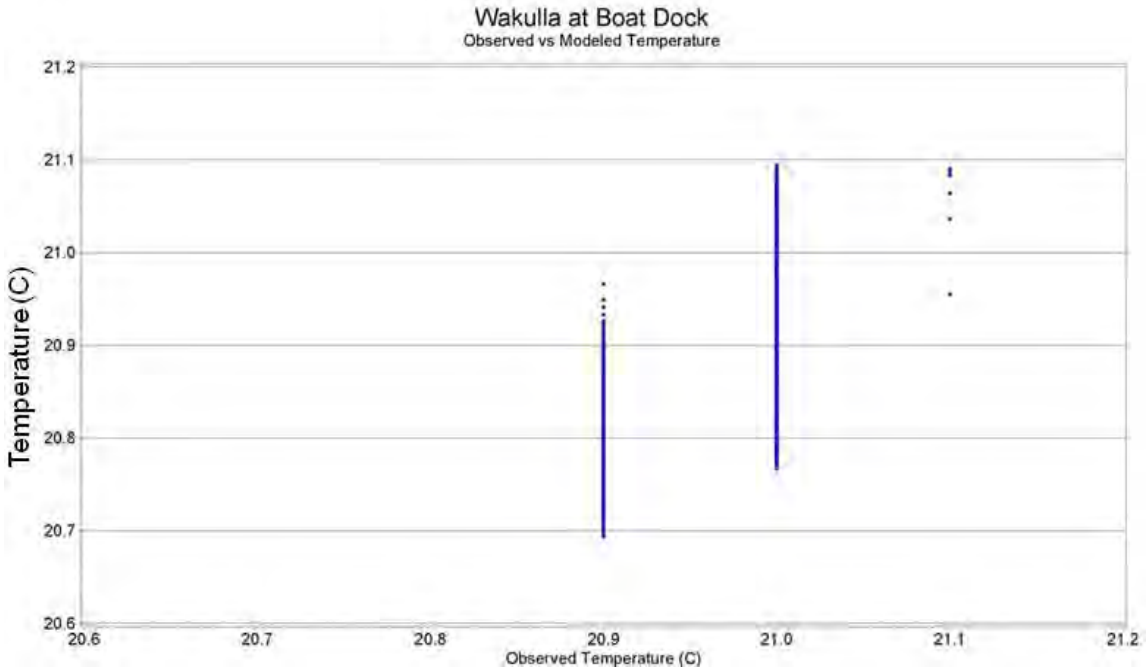

Figure 39. Scatter plot comparison of modeled bottom temperature (vertical axis) and observed 15-minute temperature (horizontal axis) at the Boat Dock Station (USGS 02327000) for December 1, 2019 - February 28, 2020.

For this graphical comparison, the simulated temperatures were not rounded to the nearest 0.1°C, so that the full distribution of simulated temperatures at the Boat Dock could be compared to the reported temperatures. As expected given that the observed temperatures were either 20.9°C, 21.0°C, or 21.1°C, the simulated temperatures are vertically aligned above each of these observed temperatures. This does show that for the Boat Dock, the simulated temperature ranges extend both below and above the reported temperatures of 20.9°C and 21.0°C, while the simulated temperatures when the reported temperature was 21.1°C were a bit below the reported level. The comparison of simulated values reported with three decimal place precision to observed values reported in 0.1°C increments is not ideal, but reflects the best available data and does provide some idea of the variability in model output as compared to reported values.

A similar comparison at the Main Bend is provided in Figure 40. This graphical comparison shows a slight under-prediction at the lower end of the observed range, with this under-prediction typically much less than 0.1°C. The relationship between simulated and observed water temperature here is as expected given the calibration statistics at this location provided in Table 3 above, with a Mean Error of -0.01°C and Mean Absolute Error of 0.03°C .

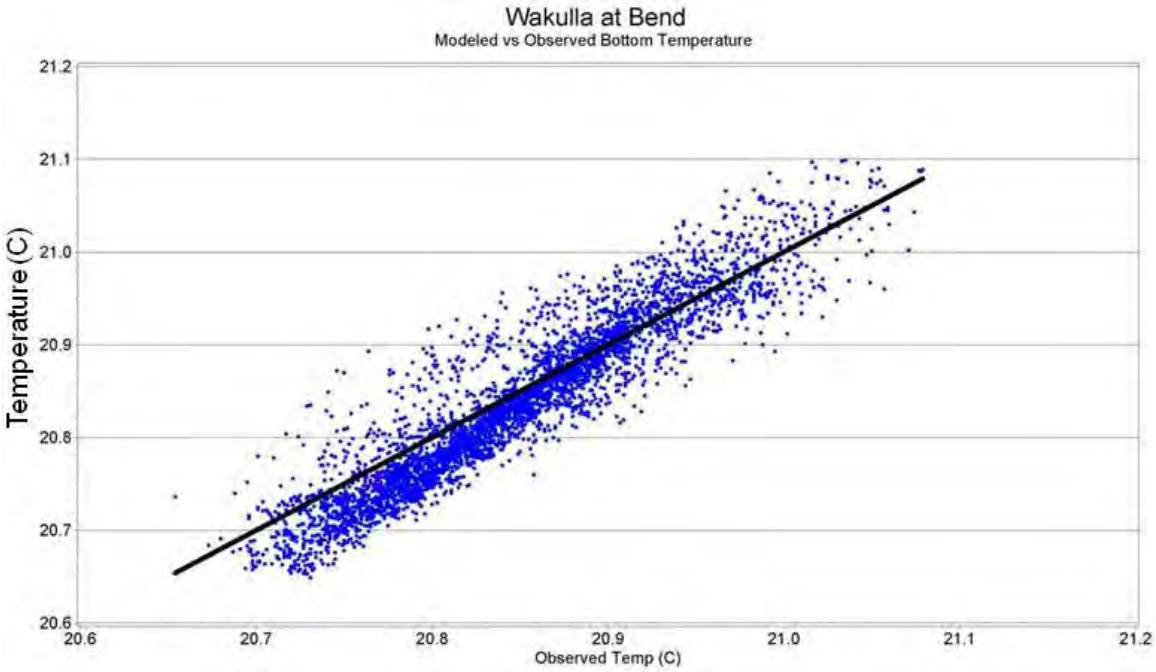

Figure 40. Scatter plot comparison of modeled bottom temperature (vertical axis) and observed 15-minute temperature (horizontal axis) at the Main Bend site for December 1, 2019 - February 28, 2020, with 1:1 black line.

The other dataset for comparison to model output is the profile data collected on January 22 and February 28, 2020. A plot of modeled (vertical axis) vs. observed (horizontal axis) water temperatures for these dates is provided in Figure 41, with a one-to-one line provided for orientation. As shown here, the model accurately simulated the majority of the observations, although did miss simulating five values by greater than 0.5 C. Table 4 provides the statistical

comparison between modeled and observed temperature from the profile data. For these comparisons, both the modeled and observed data were first calculated as water column means over an entire grid cell, as most measurements and model simulations showed very little vertical gradient in temperature, typically less than 0.1°C.

Table 4. Calibration assessment for water temperature from January 22 and February 28, 2020 profile data collection.

	Mean Error (C)	Mean Absolute Error (C)	R^2	RMSE (C)
2 Events	-0.01	0.18	0.51	0.29

The model is sufficiently accurate in simulation of elevations, with very accurate simulation (<0.34 inch mean absolute error, Table 3) during the December 1, 2019 - February 28, 2020 period. For water temperature, the model under-predicts by <0.1 C at the Boat Dock (mean error) and much less than that (0.01 C) at the Main Bend (Table 3). The temperature simulation results in a model that will provide very accurate estimates of iso-temperature areas and volumes available at given vent flows (Figure 21), spring water temperatures (Figure 11), and air temperature (Figure 27) conditions, so that it is appropriate for use in evaluating potential flow reduction scenarios and the resultant effect on water temperature areas and volumes available.

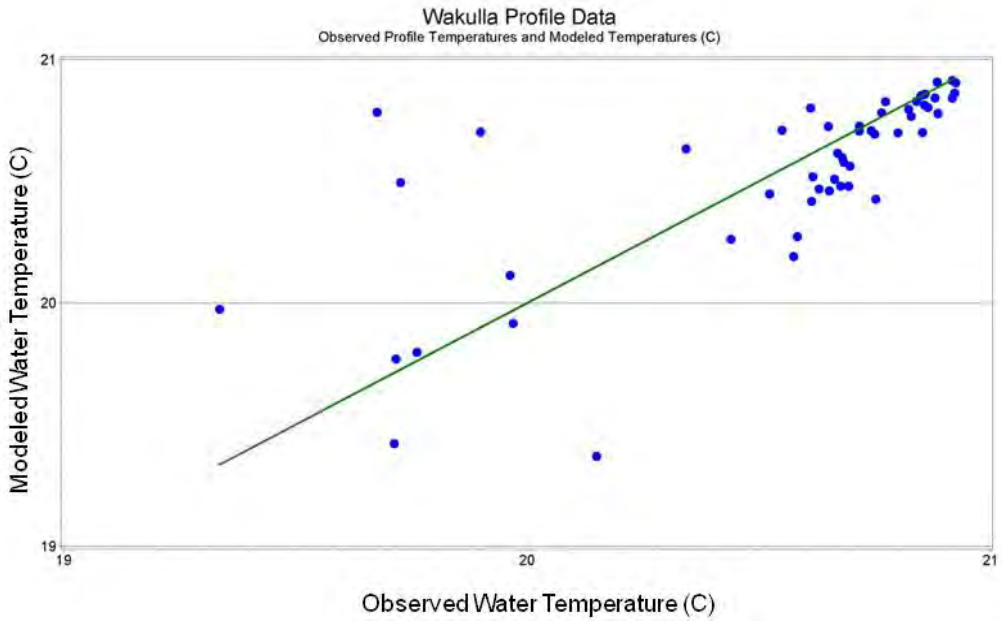

Figure 41. Comparison of modeled and observed temperature profile data, January 22 and February 28, 2020.

4 Winter Reference Periods

Several factors were considered in selection of the Winter Reference Periods for use in evaluation of flow reduction scenarios on the available manatee warm water refuge habitat near the vent and for 1 km downstream to the Boat Tram location. First, the available period of record for vent discharges and associated water temperatures was limited to the winter period during which manatees have utilized the spring as a warm water refuge, which began in the winter of 2007-2008

(see Figure 1). Due to changes in the Wakulla Spring flow, Wakulla River channel dimensions, etc., during the past 20 years, the period when manatees have been documented as utilizing the spring as a warm water refuge was selected to avoid modeling conditions which are outside of the range of calibration values and which may have prevented manatee use of the spring. Second, the selected winter periods should have a wide range of vent discharges. Third, it was necessary to have concurrent vent discharges and vent water temperatures during the selected periods. Lastly, only those winter periods with events of relatively cold vent water temperatures (less than or near 20 °C) were considered for analysis. While the periods listed below were observed prior to the river geometry and grid cell conditions used in the model (post-Michael), they were selected as examples of the environmental conditions observed around Wakulla Spring during typical winters when manatees were known to utilize Wakulla Spring as a warm water refuge.

The winter period (November-March) vent discharges and water temperatures were examined for each winter beginning in 2007-2008. Four winter periods were selected, based on the availability of concurrent vent discharge and vent water temperature data:

- February 9 - March 31, 2013;
- November 14, 2014 - March 31, 2015;
- November 6, 2017 - March 31, 2018; and
- November 1, 2018 - March 31, 2019.

Time series plots of the vent discharge and vent water temperatures for each of these periods, along with the air temperature at the Tallahassee NWS site, are provided below, in Figures 42-44 for winter 2012-2013, Figures 45-47 for winter 2014-2015, Figures 48-50 for winter 2018-2018, and Figures 51-53 for winter 2018-2019. Discharge and water temperature data plotted are those concurrently available for each winter period.

As seen during the February-March 2013 winter period (Figures 42 and 43), the high flow event of late February-early March resulted in a decline in vent water temperatures to less than 20°C, followed by a rebound in temperatures above this level when flows declined. Similar occurrences were observed in winter 2014-2015 (Figures 45 and 46) and winter 2018-2019 (Figures 51 and 52). During those higher flow periods when water temperatures emerging from Wakulla Spring are depressed below 20°C, the water temperatures declined following a flow increase and increased during the following flow decrease.

Given the temperature responses during the winter periods to changes in flows, it is likely that the effects on available warm water refuge are dependent on the environmental and spring conditions at any given time. For example, flow reductions during a period of time when vent temperatures are greater than 20°C may result in reduced levels of warm water refuge above this temperature, while flow reductions during a period when vent temperatures are below 20°C may result in increased levels of warm water refuge above this temperature, as less colder water enters the system. The evaluation of flow reduction scenarios for the four winter reference periods will provide the likely impacts on warm water refuge habitat over the range of environmental conditions represented during the four periods.

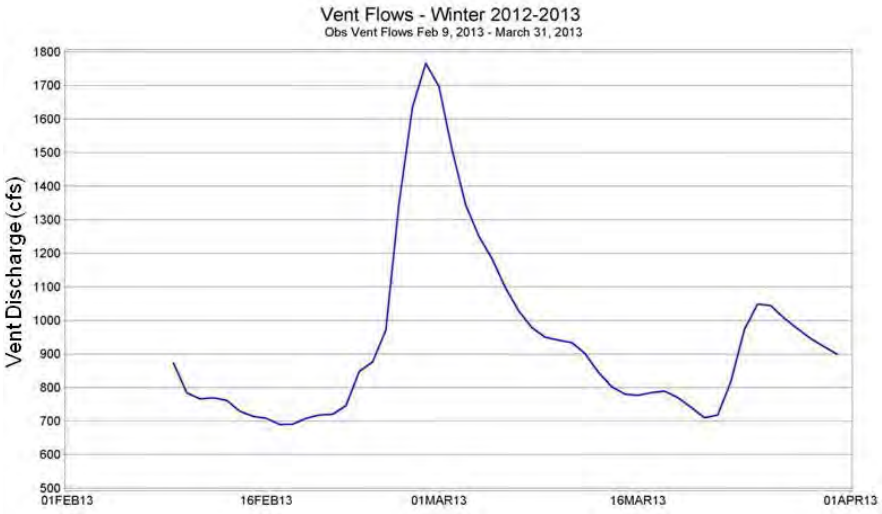

Figure 42. Vent discharges during winter 2012-2013, for February 9 - March 31, 2013.

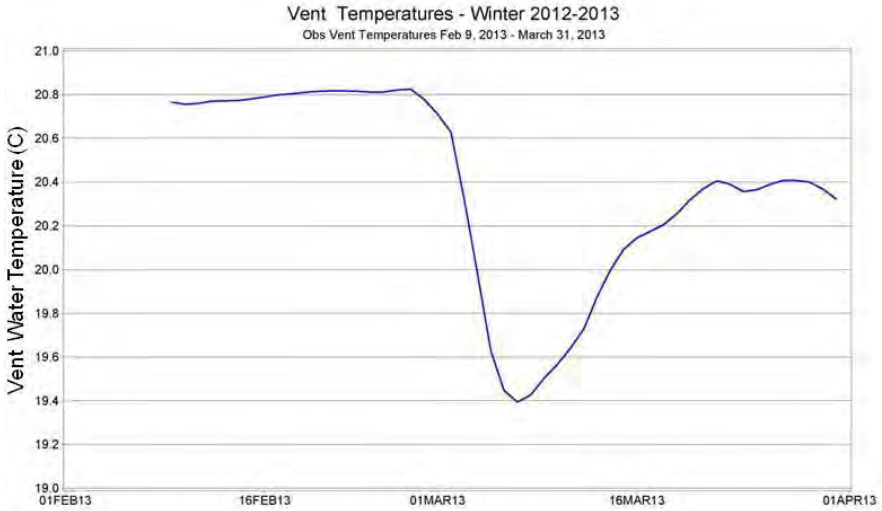

Figure 43. Vent water temperatures during winter 2012-2013, for February 9 - March 31, 2013.

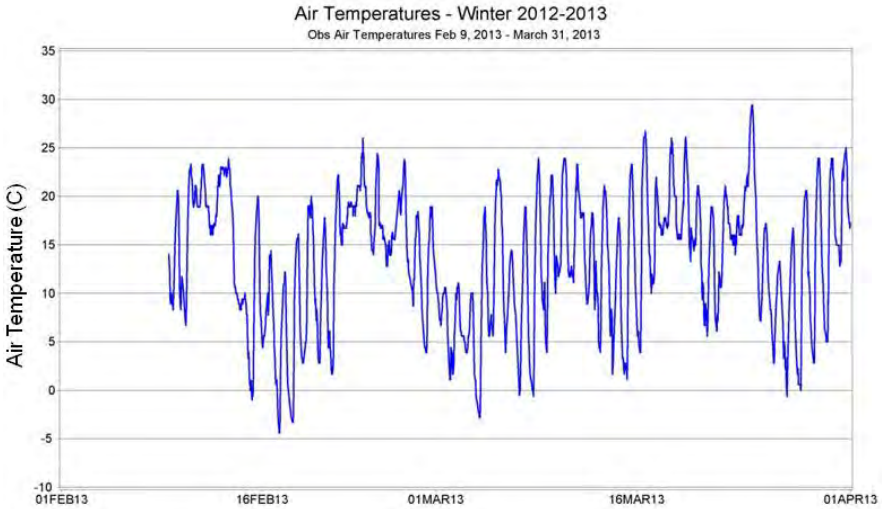

Figure 44. Air temperatures from Tallahassee NWS site for February 9 - March 31, 2013.

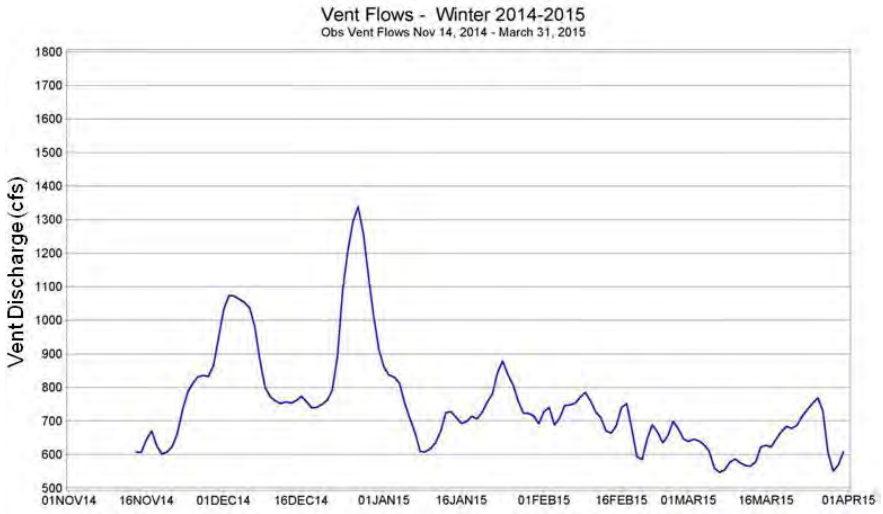

Figure 45. Vent discharges during winter 2014-2015, for November 14, 2014 - March 31, 2013.

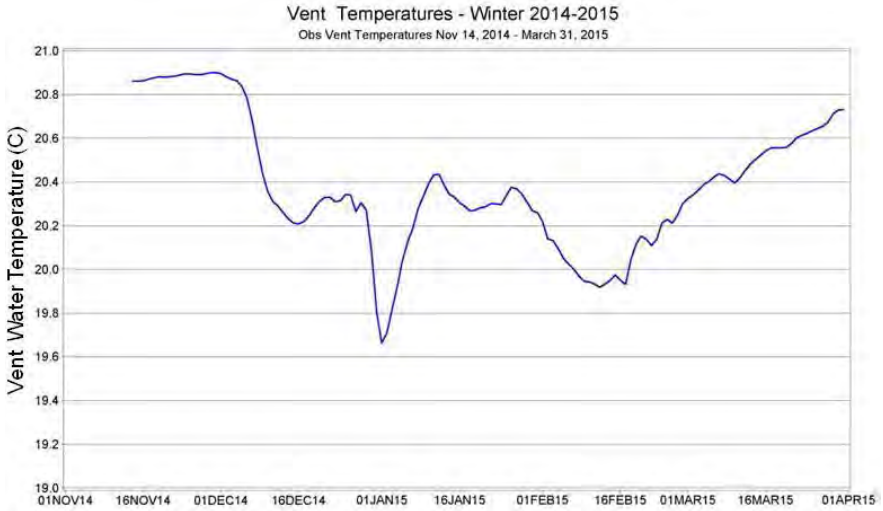

Figure 46. Vent water temperatures during winter 2014-2015, for November 14, 2014 - March 31, 2013.

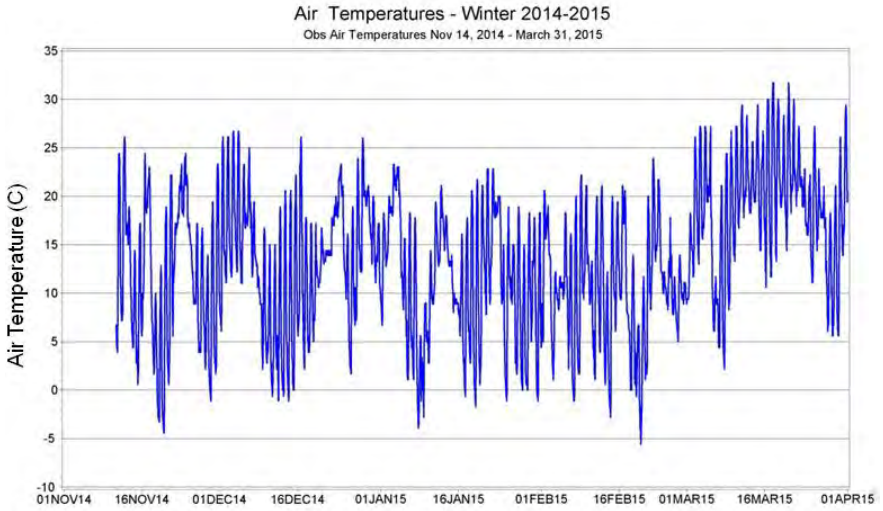

Figure 47. Air temperatures from Tallahassee NWS site for November 14, 2014 - March 31, 2015.

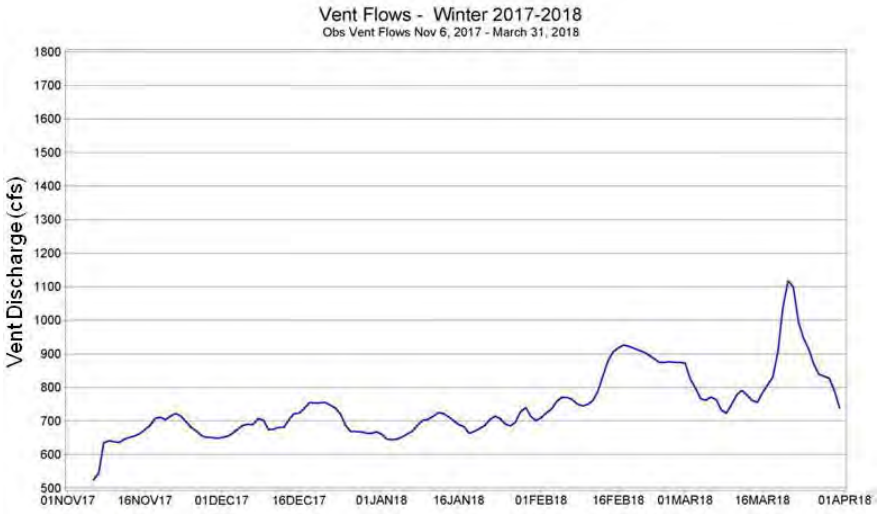

Figure 48. Vent discharges during winter 2017-2018, for November 6, 2017 - March 31, 2018.

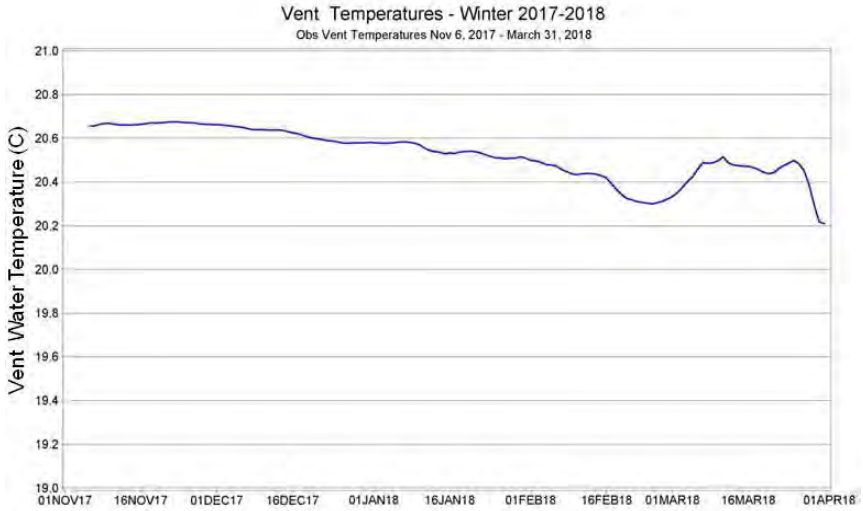

Figure 49. Vent water temperatures during winter 2017-2018, for November 6, 2017 - March 31, 2018.

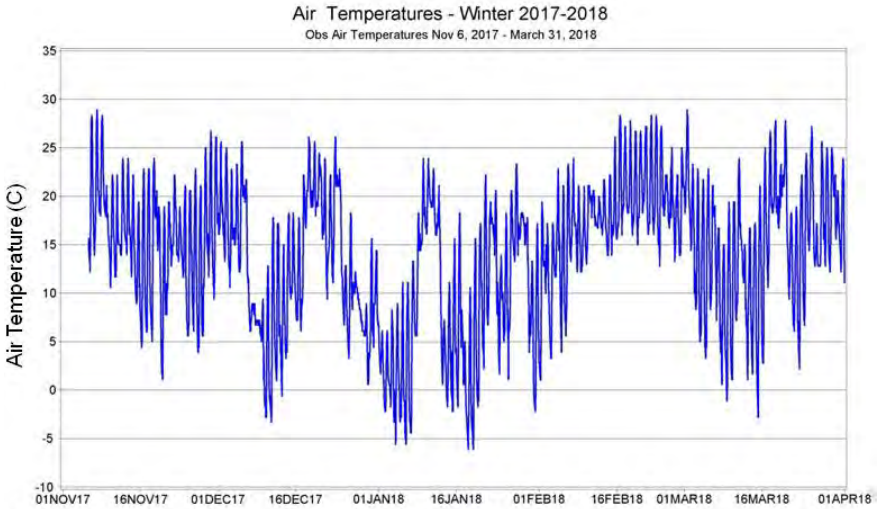

Figure 50. Air temperatures from Tallahassee NWS site for November 6, 2017 - March 31, 2018.

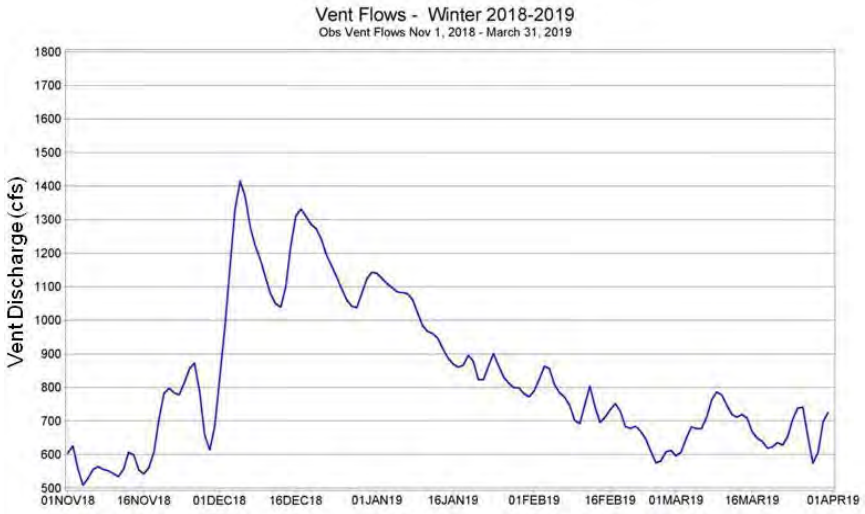

Figure 51. Vent discharges during winter 2018-2019, for November 1, 2018 - March 31, 2019.

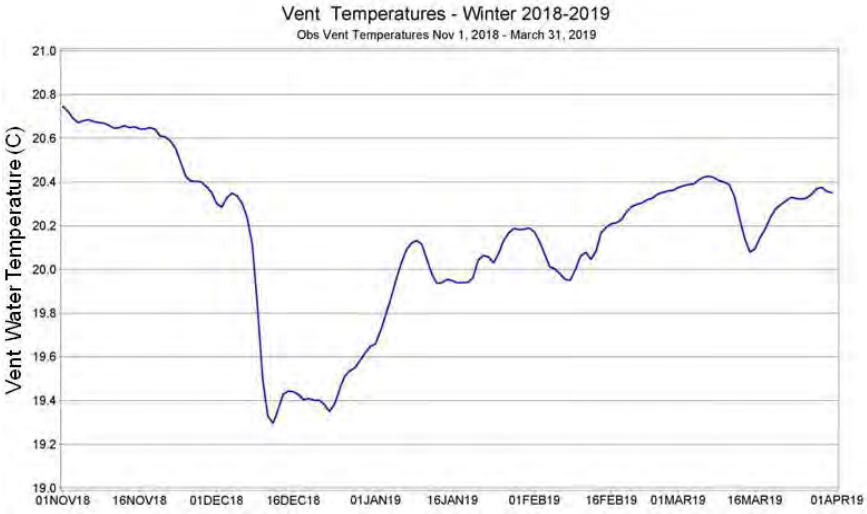

Figure 52. Vent water temperatures during winter 2018-2019, for November 1, 2018 - March 31, 2019.

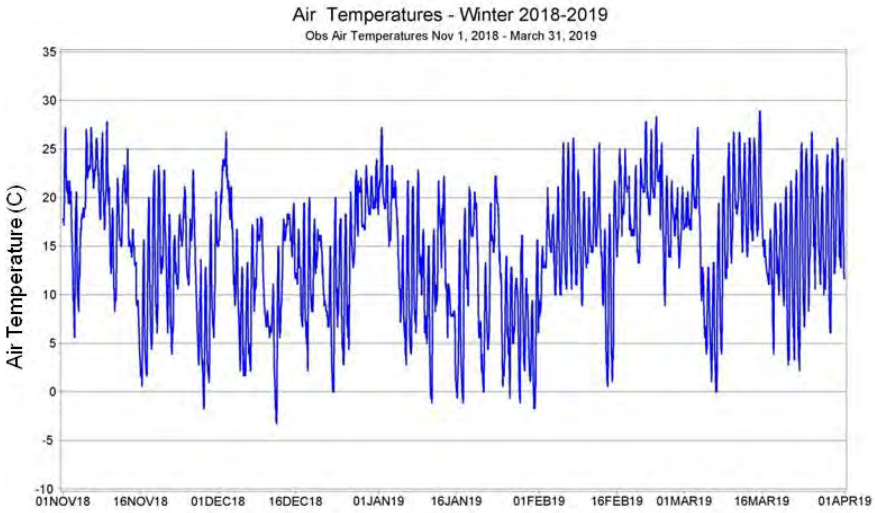

Figure 53. Air temperatures from Tallahassee NWS site for November 1, 2018 - March 31, 2019.

The four winter reference periods include one during which the vent water temperatures did not reach below 20°C, winter 2017-2018, but the associated air temperatures were well below 0°C for several days during this period (Figure 50).

The relationships between vent flow and vent temperatures for the four winter reference periods are provided in Figures 54-57. Comparing flows and water temperatures during Winter 2012-2013 (Figures 42 and 43) indicates that there is a response in water temperature at the vent to increased flows during the winter period. The increased discharge during late February - early March 2013 (Figure 42) preceded by a few days a drop in vent water temperatures (Figure 43). This is seen in Figure 54 below as well, where the highest discharges are not directly associated with minimum water temperatures during the period due to the slight lag in temperature response seen when comparing Figures 42 and 43.

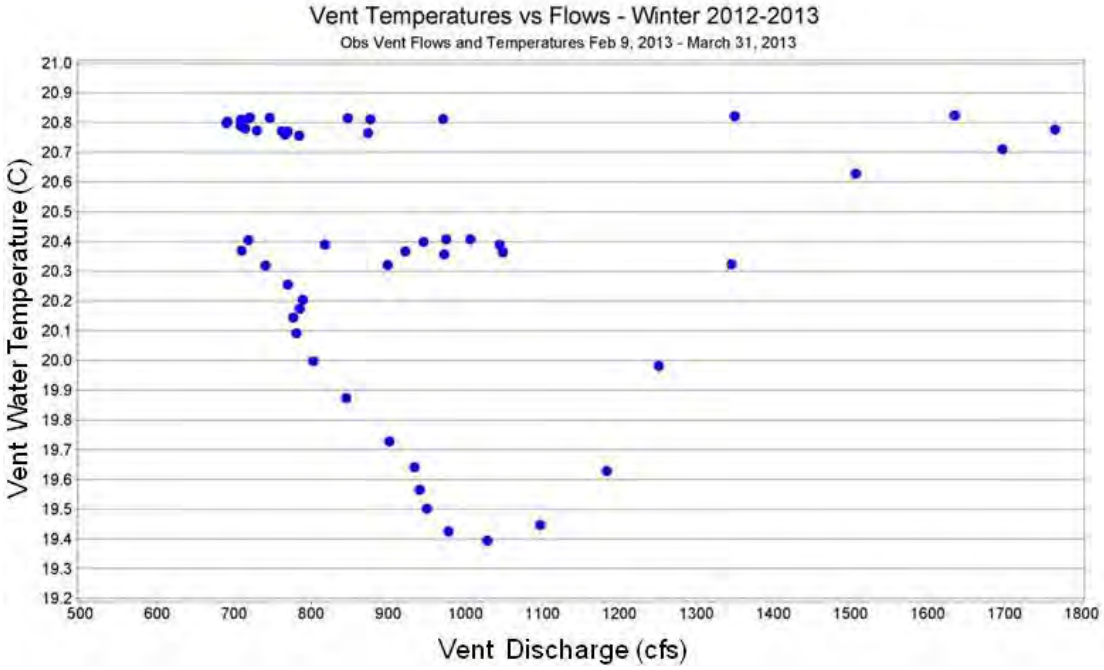

Figure 54. Daily average vent water temperatures vs. daily vent discharge for February 9 - March 31, 2013.

Similar responses in vent water temperatures to increased vent flows were seen during winter 2014-2015 (Figures 45 and 46) and winter 2018-2019 (Figures 51 and 52). Periods of increased flows preceded periods of reduced water temperature, so that the water temperature minima did not coincide directly with the flow increases, as seen in Figures 55 and 57. The winter 2017-2018 period did not have large changes in flows or vent temperatures during cold periods, so that no decline in vent temperatures below 20°C were seen (Figure 56).

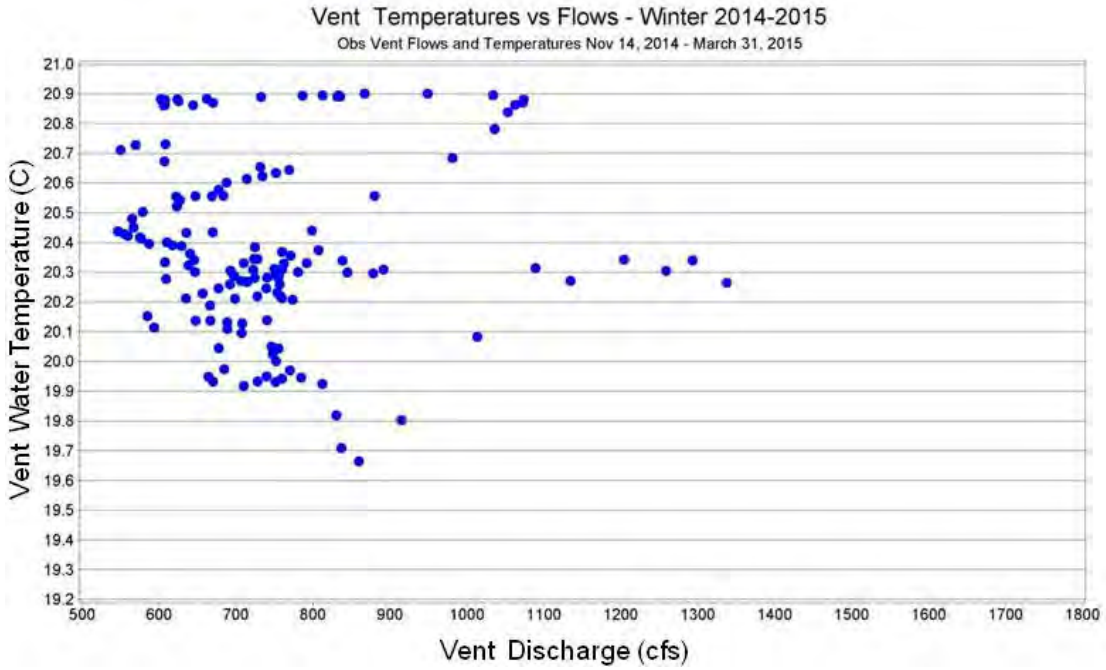

Figure 55. Vent water temperatures vs. vent discharge for November 14, 2014 - March 31, 2015.

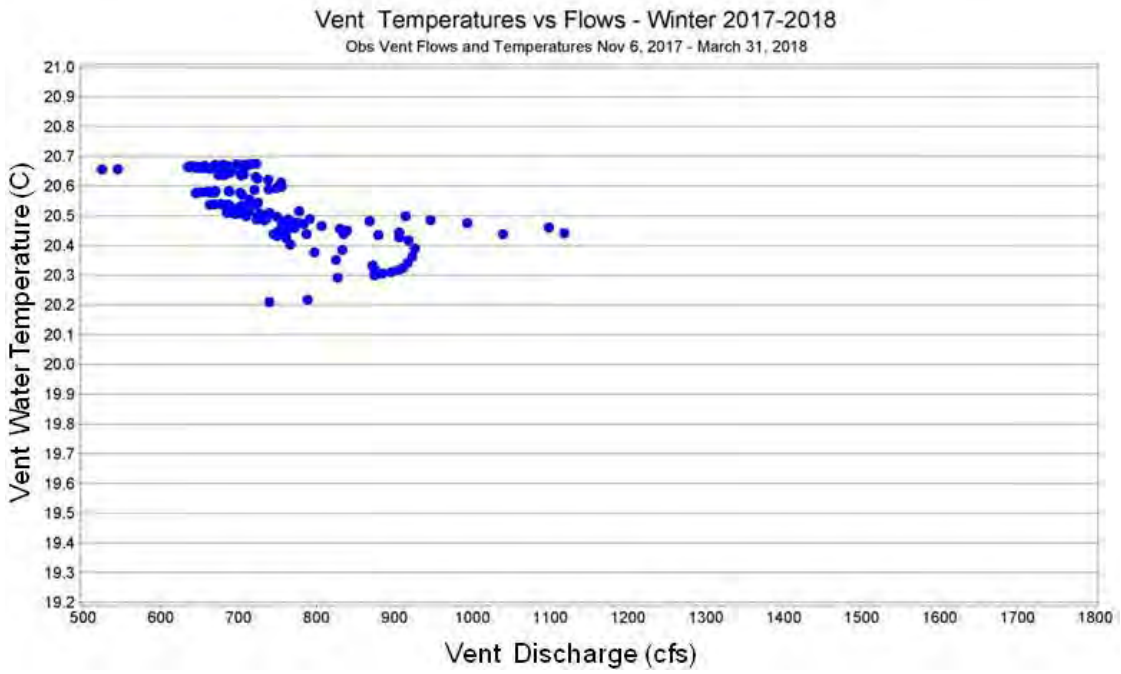

Figure 56. Vent water temperatures vs. vent discharge for November 6, 2017 - March 31, 2018.

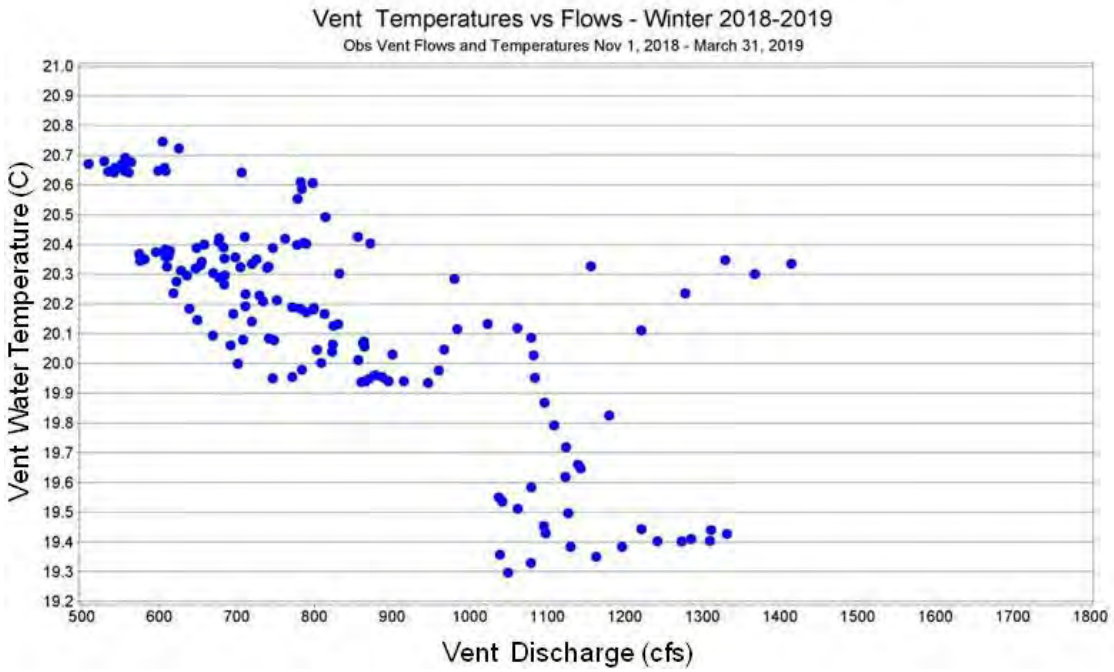

Figure 57. Vent water temperatures vs. vent discharge for November 1, 2018 - March 31, 2019.

The winter reference period scenario vent discharge and vent temperature records were prepared for simulation by concatenating the records from the four winter reference periods selected. Thus, the February 9 - March 31, 2013 period is represented as model days 0-50, the November 13, 2014 - March 31, 2015 period is represented as model days 51-188, the November 6, 2017 - March 31, 2018 period is represented as model days 189-334, and the November 1, 2018 - March 31, 2019 period is represented as model days 335-485.

Additional input data are required to complete the analysis involving the four winter reference periods. These input data include the following:

- discharge and water temperature for Sally Ward spring;
- downstream water surface elevation and water temperature for the Boat Tram; and
- meteorological (relative humidity, atmospheric pressure, air temperature, cloud cover, rainfall, solar radiation, evapotranspiration) and wind data (wind speed and direction).

Sally Ward Discharge and Temperature

For Sally Ward discharge and water temperature, the period of record was evaluated for the winter months to determine when concurrent discharge and water temperature data were available. Four winter periods were available for examination, for winter 2016-2017, winter 2017-2018, winter 2018-2019, and winter 2019-2020. Of these, winter 2016-2017 had the most complete record of concurrent discharge and water temperatures for Sally Ward, for the period December 1, 2016 - March 31, 2017, displayed in Figures 58 and 59, respectively.

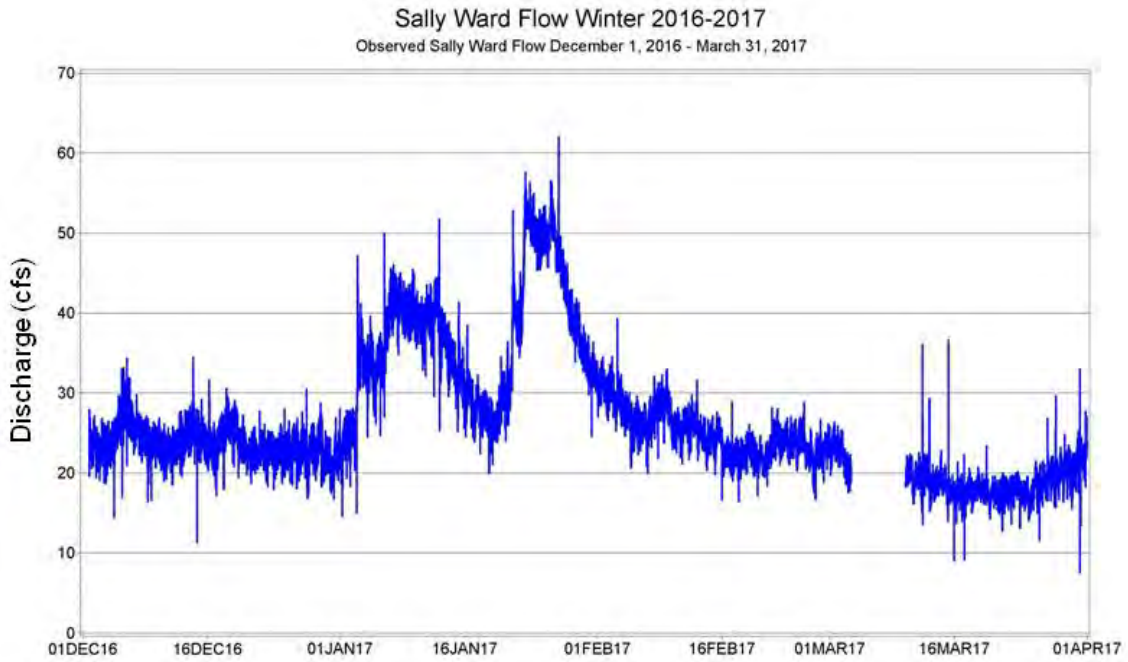

Figure 58. Sally Ward discharge for December 1, 2016 - March 31, 2017.

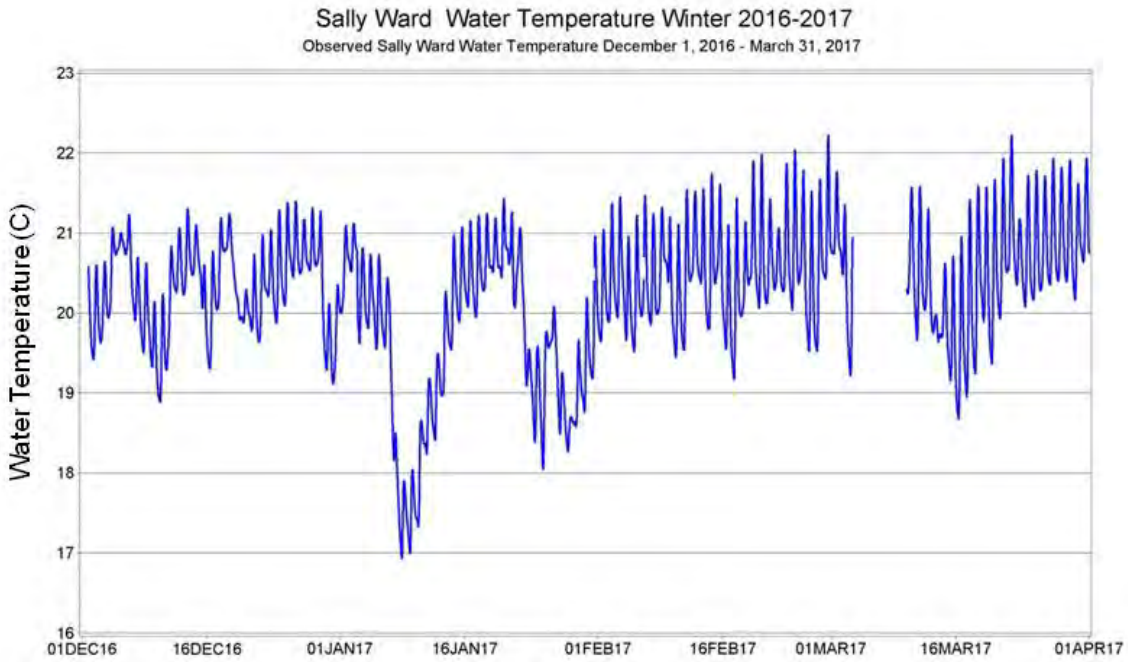

Figure59. Sally Ward water temperatures for December 1, 2016 - March 31, 2017.

The development of the November flow and temperature records for Sally Ward is based on comparison of the available data for the months of November and December of 2016-2019. Figures 60-63 and 64-67 provide the November-December Sally Ward discharges and water temperatures, respectively, for the four years. The greater variability in discharge measurements during November and December 2017 compared to that in December 2016 was due to a shortened instrument averaging period for continuous measurements in 2017, resulting in greater variability in the 2017 measurements.

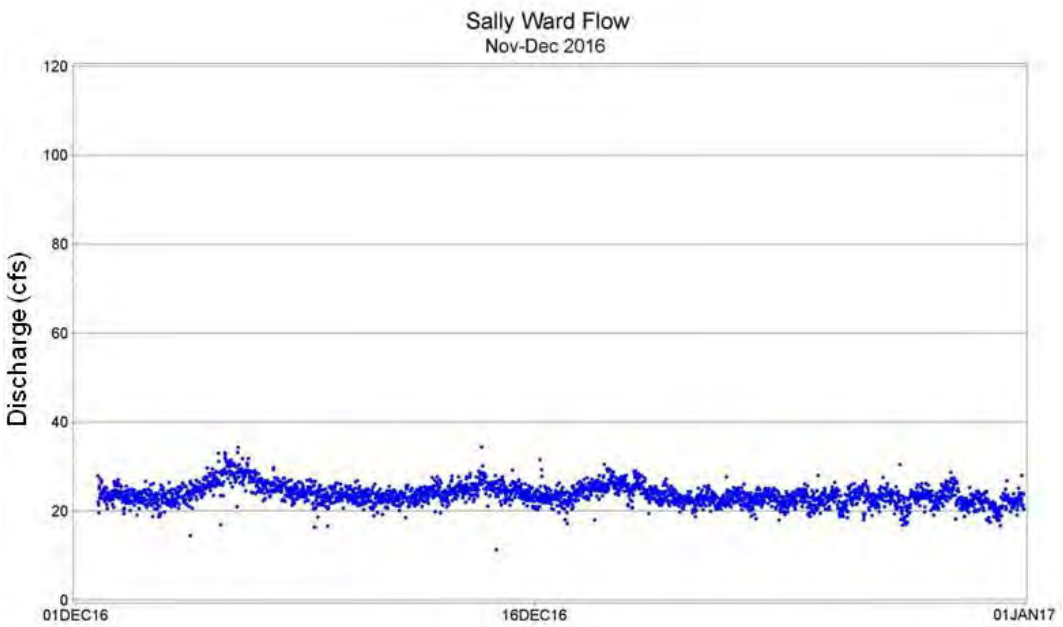

Figure 60. Sally Ward discharge for months of December, 2016. There were no discharge data for November 2016.

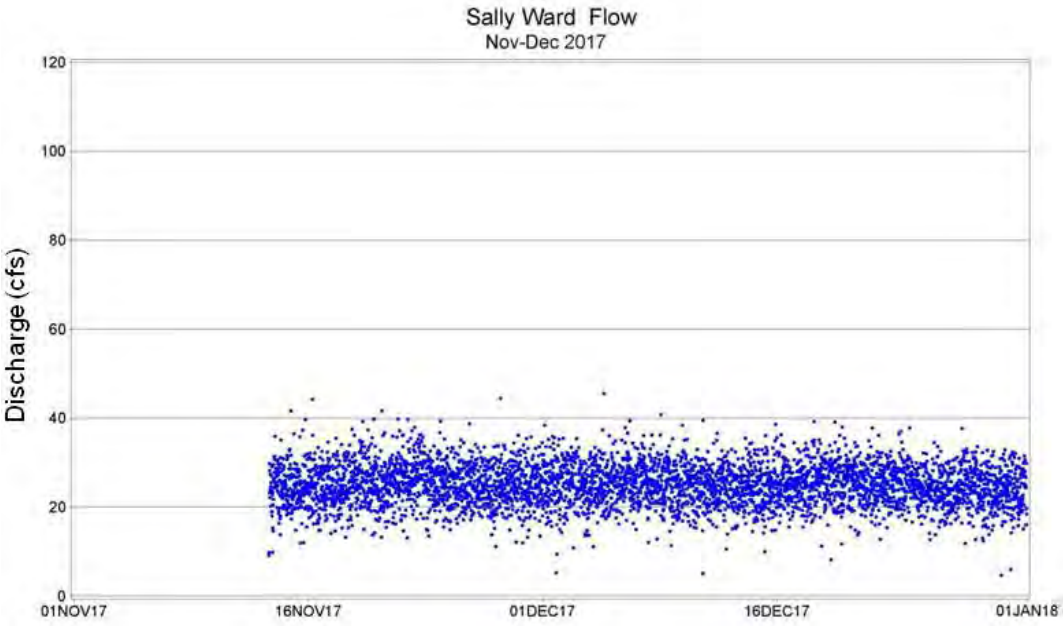

Figure 61. Sally Ward discharge for months of November and December, 2017.

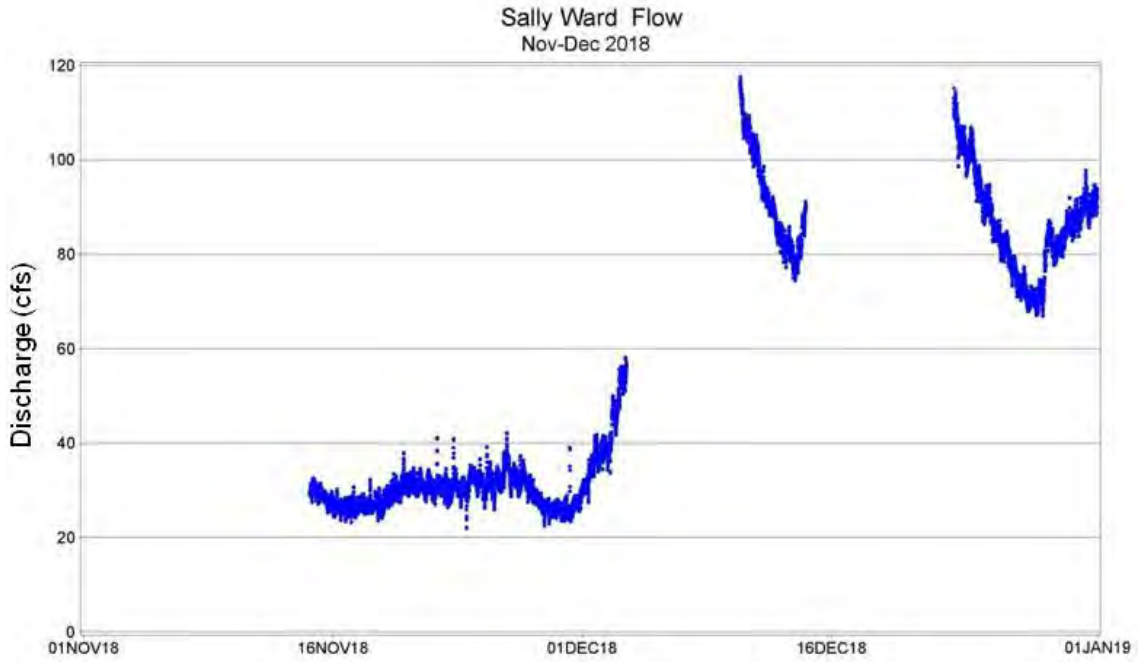

Figure 62. Sally Ward discharge for months of November and December, 2018.

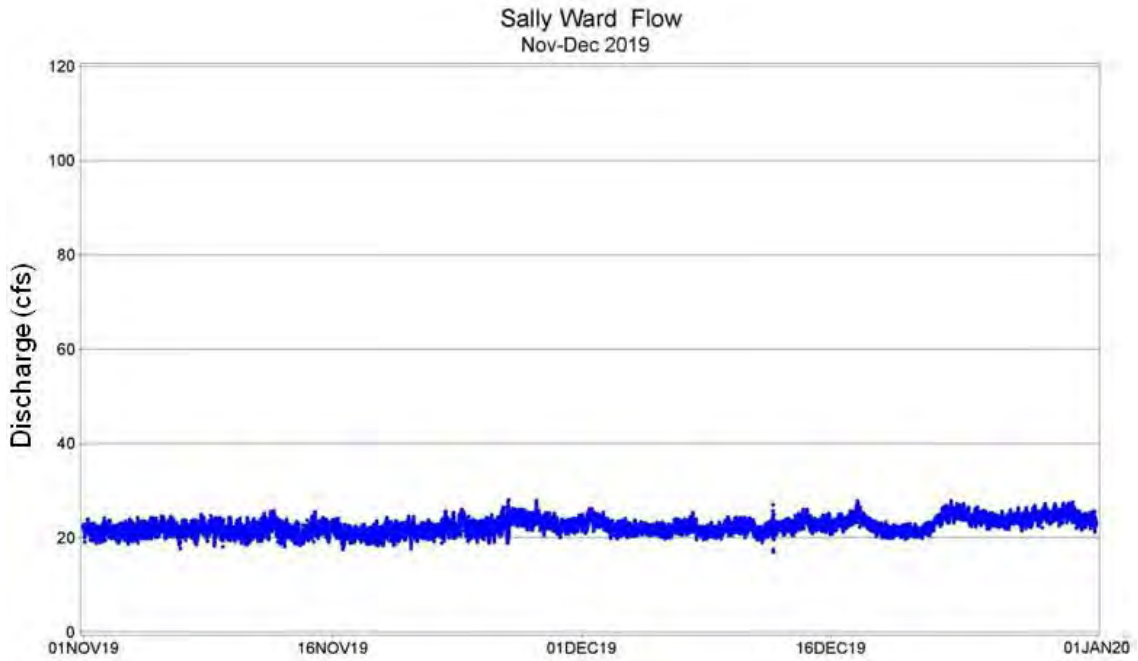

Figure 63. Sally Ward discharge for months of November and December, 2019.

For two of the three November-December periods with data in both months, discharge from Sally Ward was relatively constant (2017 and 2019). During 2018, the available flow data show a large increase in flows during December, in keeping with the increase seen from the Wakulla Spring vent (Figure 51), with the Sally Ward flow (Figure 62) approximately 10% of the Wakulla Spring vent

flow. However, the November flow data during 2018 are similar to those in November-December 2017 and 2019, and to those in December 2016, fluctuating between 20 cfs and 40 cfs.

In the same manner, the Sally Ward water temperatures for November-December of 2016-2019 (Figures 64-67) indicate that the November and December temperatures are very similar, with the exception of the 2018 period.

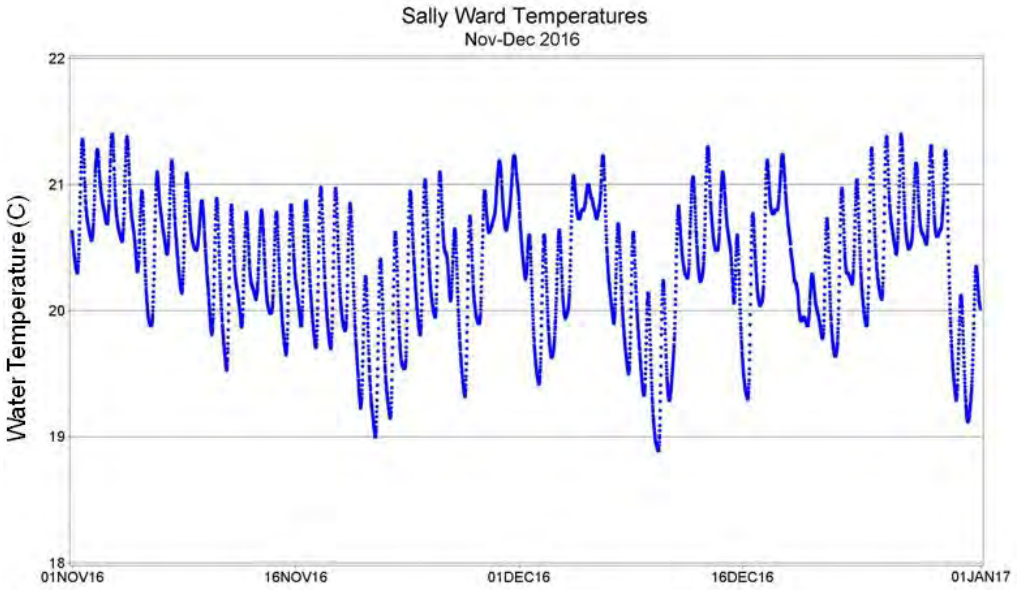

Figure 64. Sally Ward temperature for months of November and December, 2016.

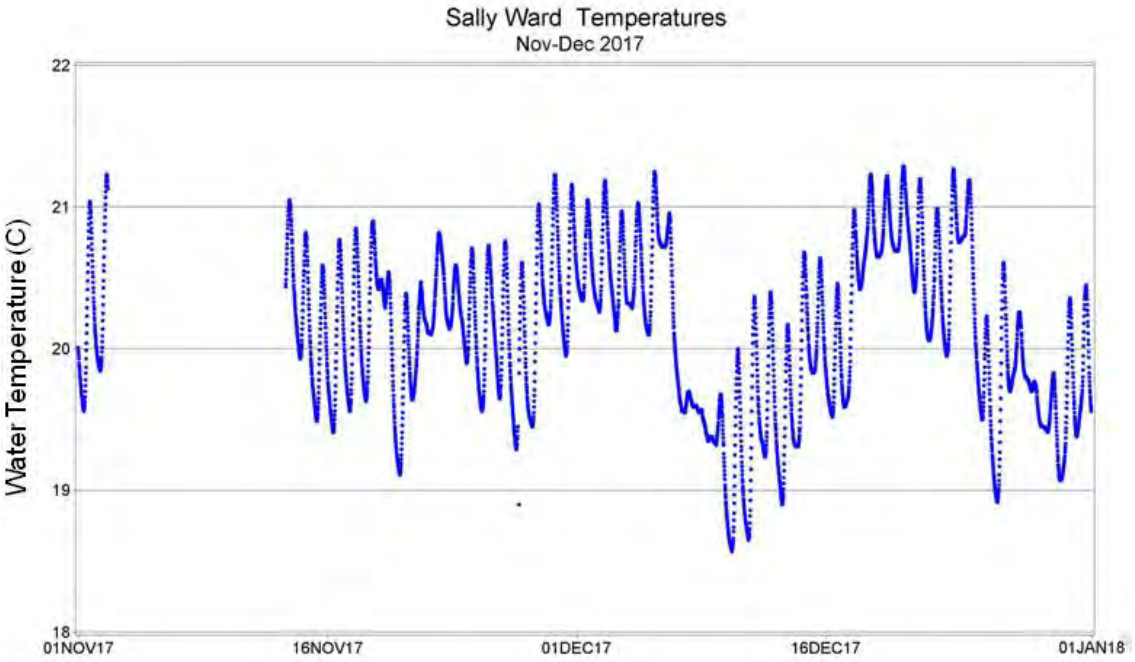

Figure 65. Sally Ward temperature for months of November and December, 2017.

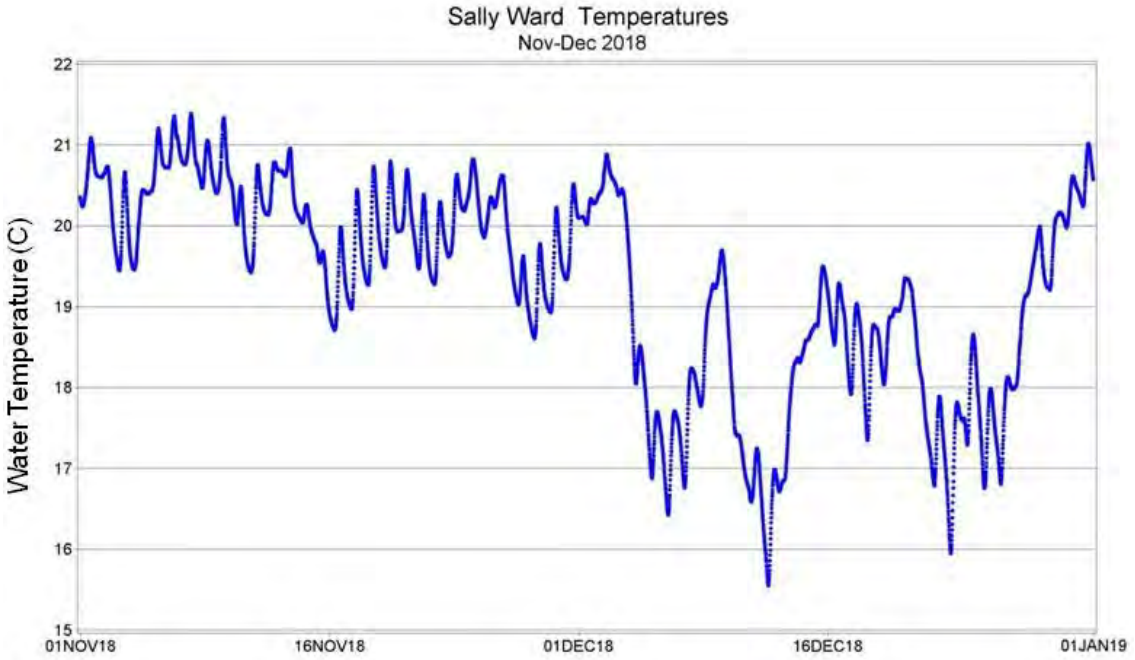

Figure 66. Sally Ward temperature for months of November and December, 2018.

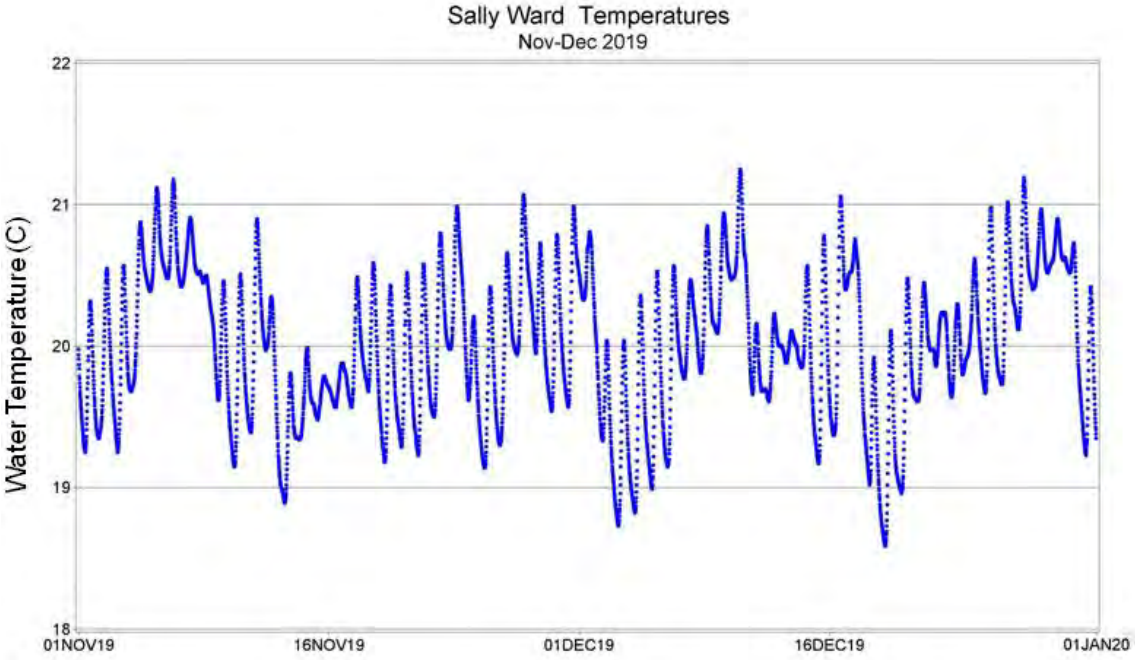

Figure 67. Sally Ward temperature for months of November and December, 2019.

Complete records for flow and temperature were developed for the full November 1, 2016 - March 31, 2017 period by setting the November 1-30, 2016 data equal to those for December 1-30, 2016, as there were no flow data for November 2016. This provided a full November 1 - March 31 data record to be utilized for the four winter reference periods, with the records for the same calendar

days from the November 2016 - March 2017 assigned to each of the four winter reference periods. The resultant November 1 - March 31 Sally Ward discharge and water temperature time series are provided in Figures 68 and 69, respectively.

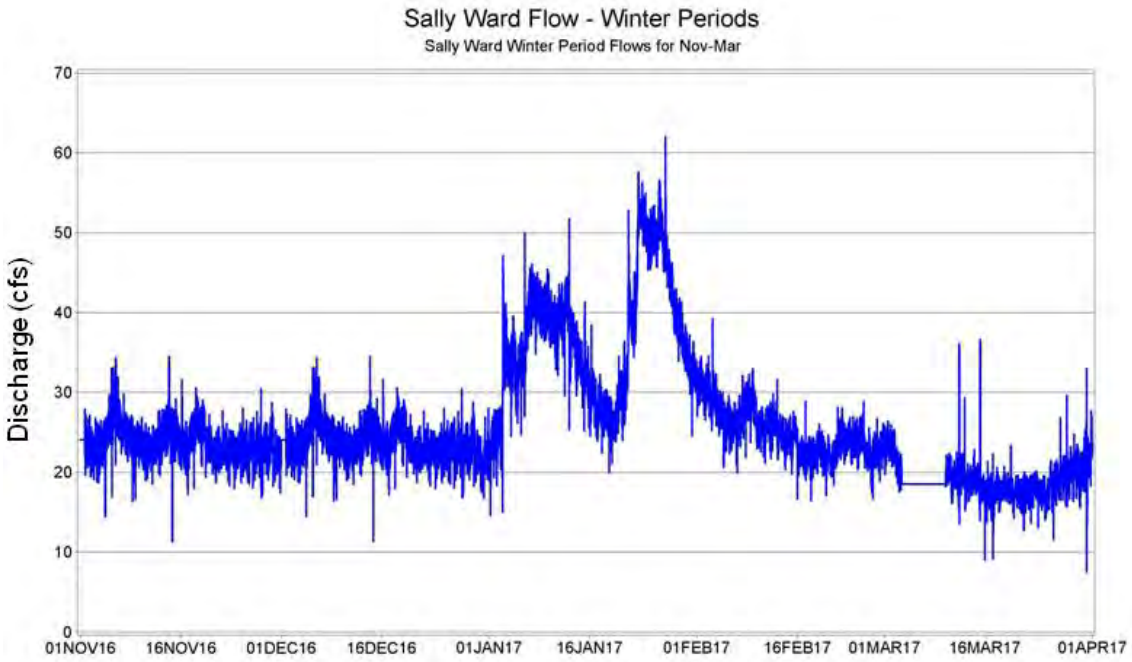

Figure 68. Sally Ward discharge used for each of the four winter periods evaluated.

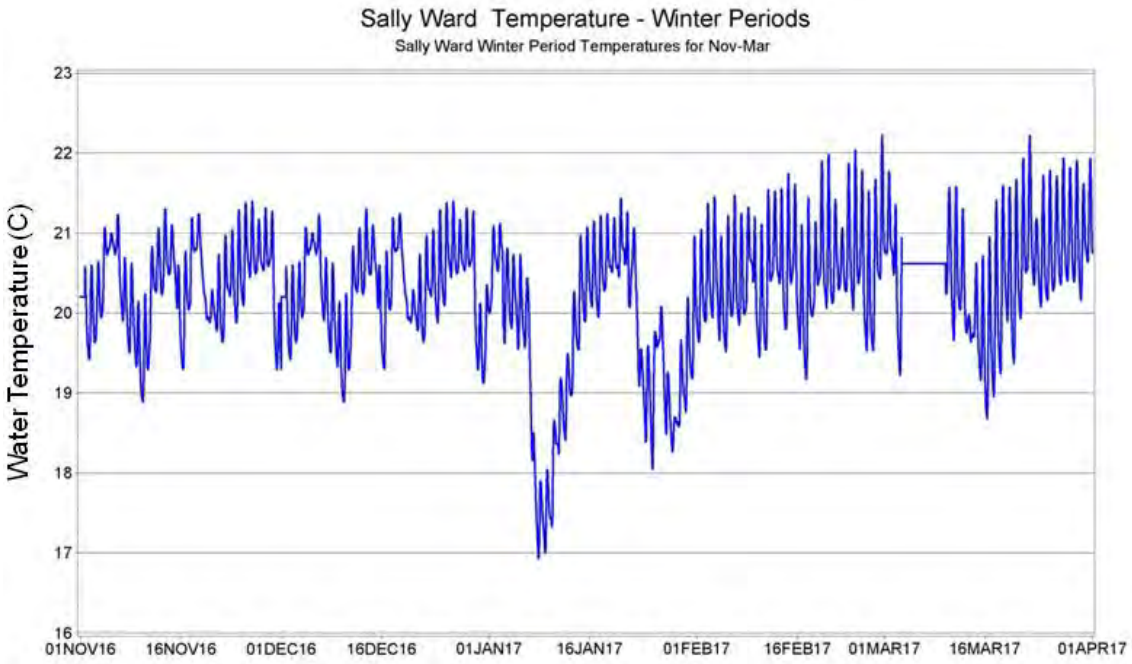

Figure 69. Sally Ward water temperatures used for each of the four winter periods evaluated.

Boat Tram Temperature and Water Surface Elevation

The downstream boundary conditions at the Boat Tram require both water temperature and water surface elevation to evaluate each of the four winter reference periods. However, no water temperature data were available at the Boat Tram for these periods. A comparison of Sally Ward water temperatures to those at the Boat Tram for the winter periods when data were available for both sites indicated that the Sally Ward water temperatures would provide an acceptable estimate for the Boat Tram water temperatures (Figures 70-73). Setting the Boat Tram downstream boundary condition to that from the Sally Ward water temperature for the winter period provides a conservative estimate here, as the Sally Ward water temperatures are typically less than those from the vent discharge during cold weather events. Water temperatures measured near the downstream end of the Sally Ward spring run are impacted longer by atmospheric temperatures than are those measured at the Wakulla Boat Tram. During cold periods the Sally Ward water is colder due to the extended period of contact with cold air temperatures as compared to the Wakulla Spring water measured at the Boat Tram. Using the Sally Ward water temperature as a surrogate for the Boat Tram water temperature results in the downstream water temperature boundary condition applied likely being colder during cold weather events than the actual water temperatures at this location, such that, if any upstream movement of boundary water occurs, the model does not move warmer water into the model domain than likely existed in the real world.

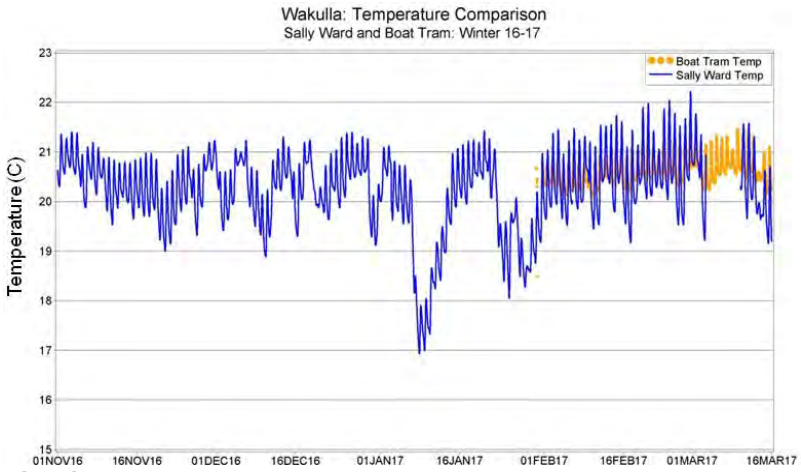

Figure 70. Sally Ward and Boat Tram water temperatures, Winter 2016-2017.

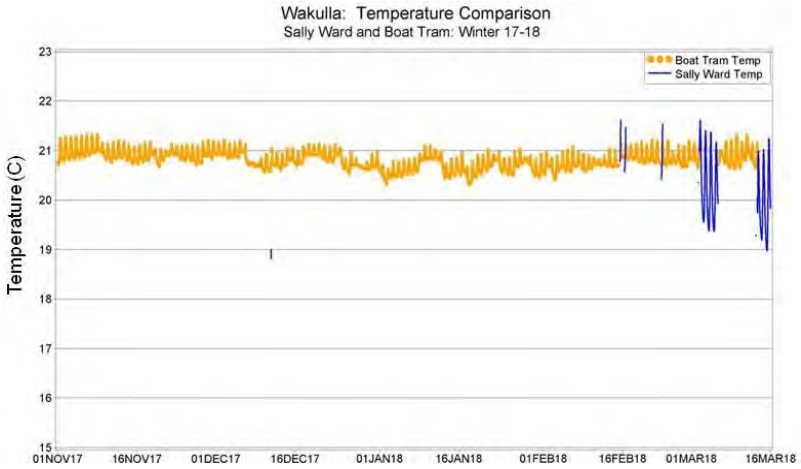

Figure 71. Sally Ward and Boat Tram water temperatures, Winter 2017-2018.

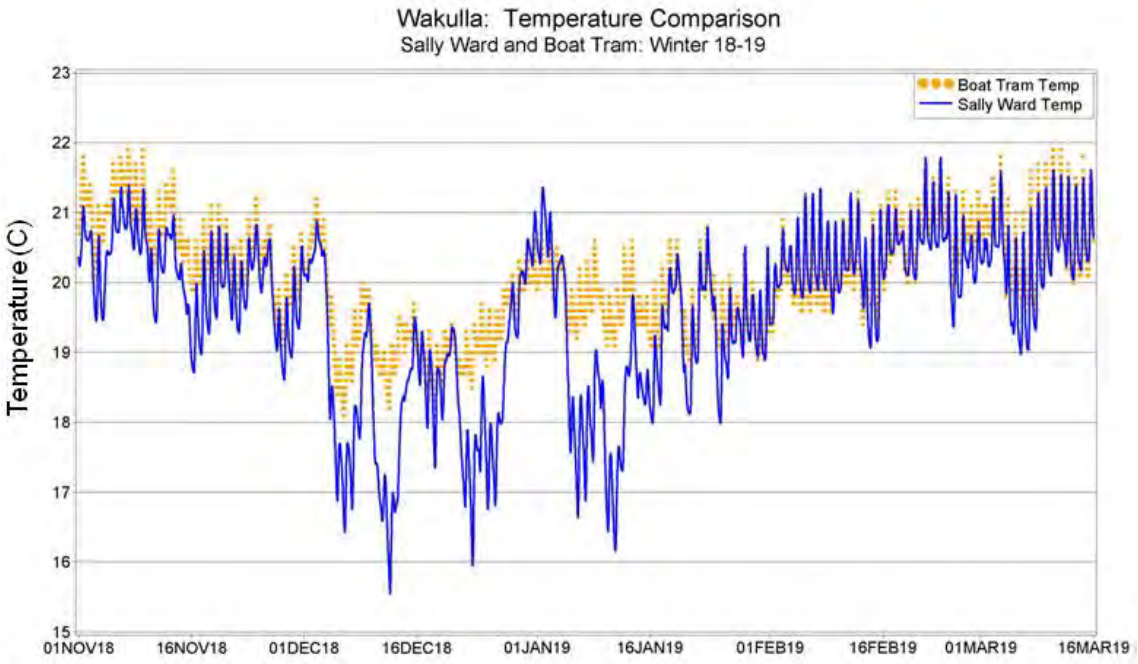

Figure 72. Sally Ward and Boat Tram water temperatures, Winter 2018-2019.

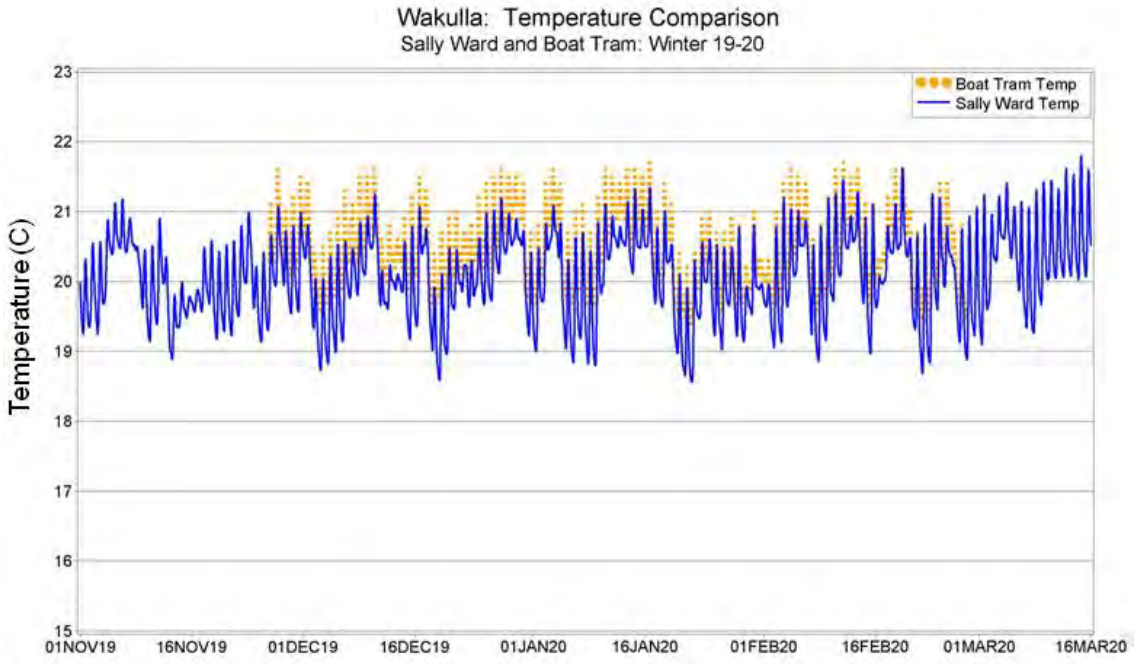

Figure 73. Sally Ward and Boat Tram water temperatures, Winter 2019-2020.

Water surface elevation data were available for the Boat Tram location during each of the four winter reference periods, so that these data were used for the downstream water surface elevation boundary condition (Figures 74-77).

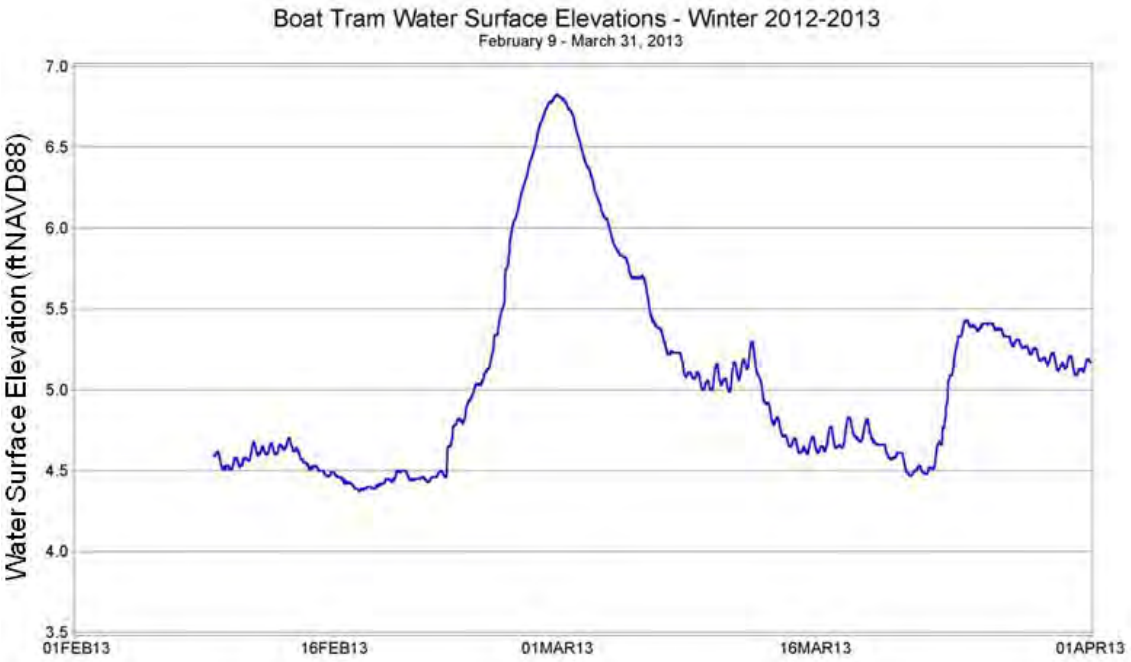

Figure 74. Boat Tram water surface elevations for downstream boundary condition for period February 9 - March 31, 2013.

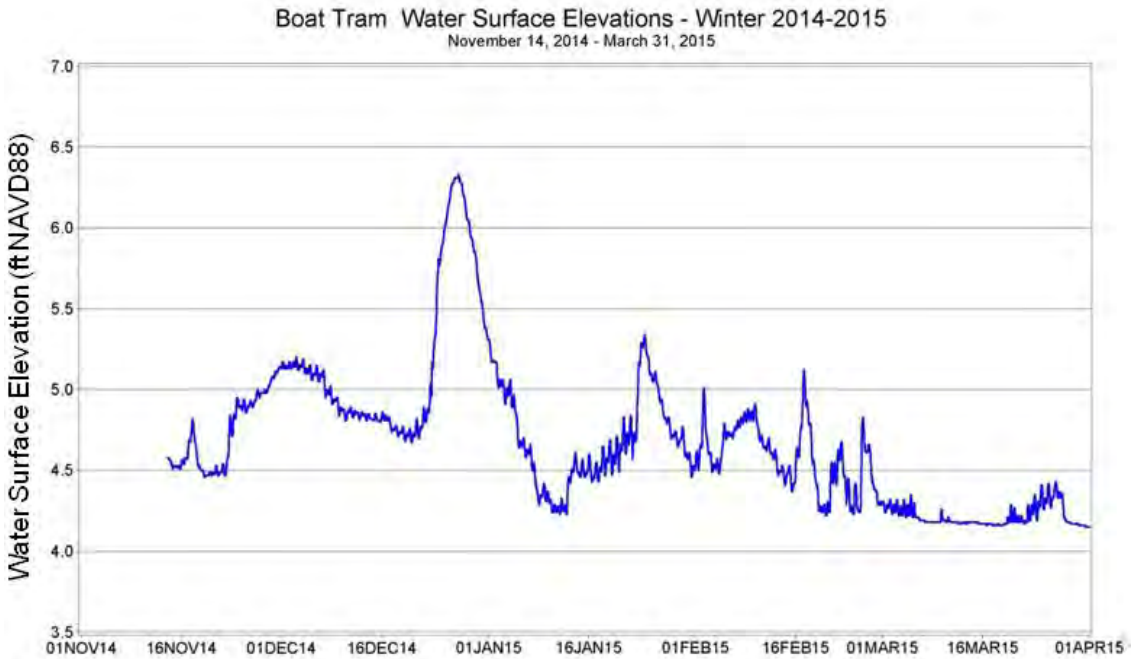

Figure 75. Boat Tram water surface elevations for downstream boundary condition for period November 14, 2014 - March 31, 2015.

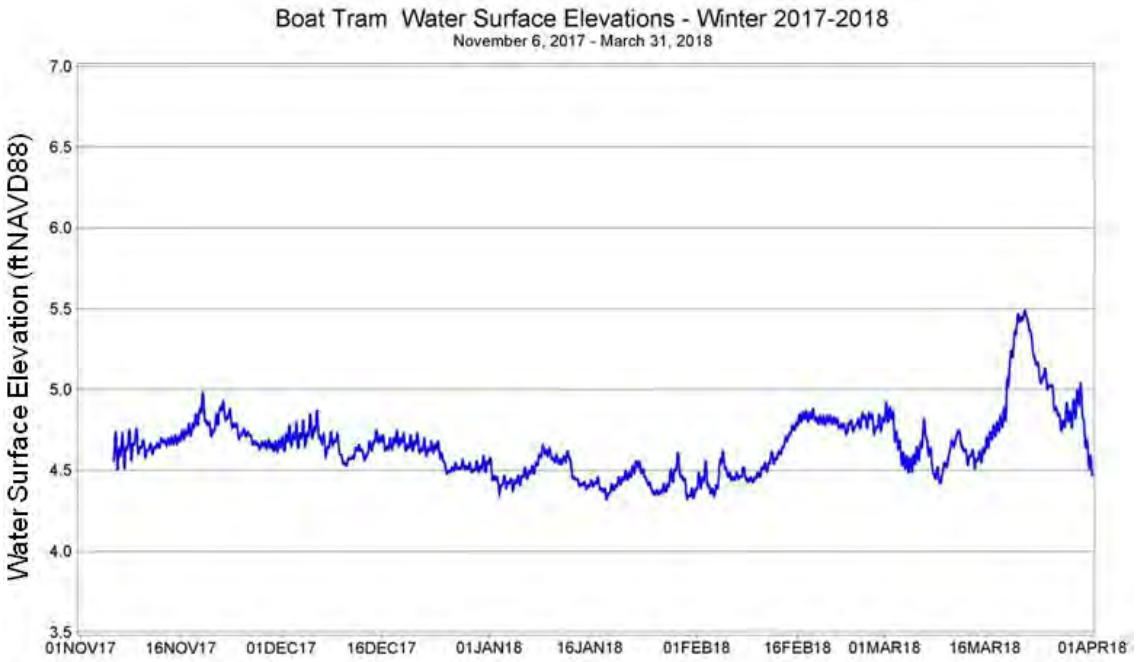

Figure 76. Boat Tram water surface elevations for downstream boundary condition for period November 6, 2017 - March 31, 2018.

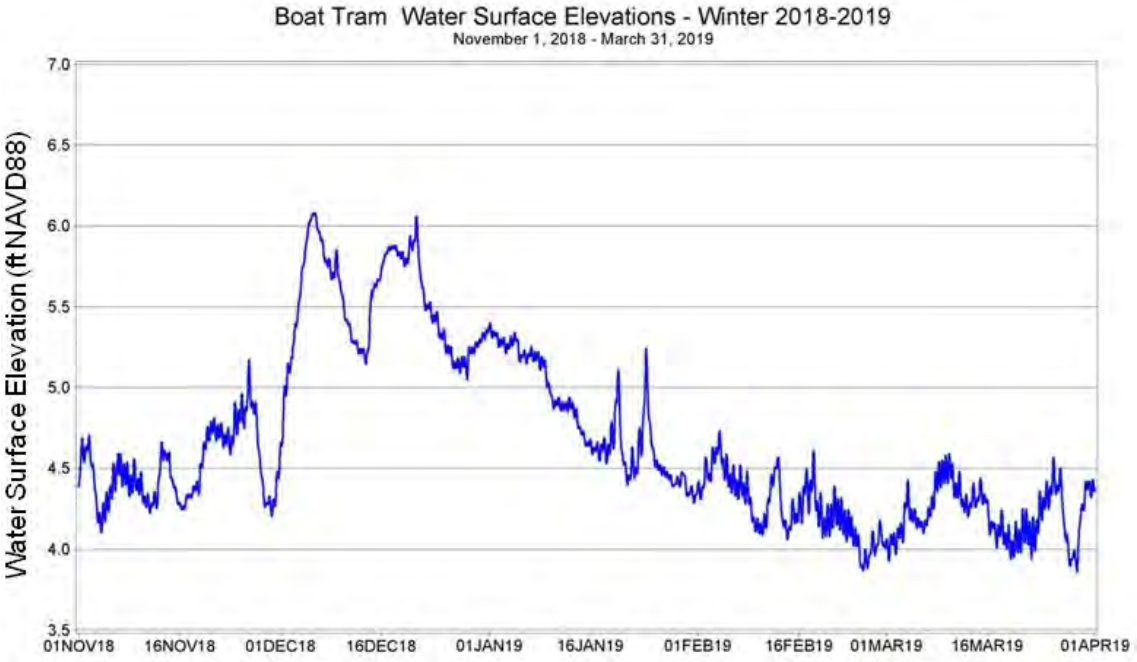

Figure 77. Boat Tram water surface elevations for downstream boundary condition for period November 1, 2018 - March 31, 2019.

Meteorological and Wind Data

Meteorological data for the four winter periods were obtained from the Tallahassee NWS site, including relative humidity, atmospheric pressure, air temperature, cloud cover, rainfall, and the Monticello IFAS FAWN site, including solar radiation and evapotranspiration. Wind speed and

direction data for the four winter periods were obtained for the Shell Point USF COMPS site. Time series plots of these inputs are provided in Appendix 1 for the four winter reference periods.

5 Comparison of Winter Reference Periods Under Flow Reduction Scenario

Given that the volume of water discharged from the Wakulla Spring vent is in excess of 500 cfs during the four winter reference periods, with water temperatures from the vent seldom dropping below 20°C (see Figures 2 and 4), the winter warm water refuge available for manatees is typically vastly greater than that needed for the relatively few manatees (maximum of 46 in winter 2012-2013, see Figure 1) that utilize the spring during cold weather events. As noted previously, the 1.1 acre spring pool primarily utilized by manatees during cold events could provide enough surface area to provide warm water refuge for more than 1,600 manatees, and this does not consider the depth of the spring pool (up to 185 ft), or the length of the Wakulla Spring run downstream from the Boat Tram, with water temperatures >20°C frequently extending downstream of this location during freezing air temperature events. This information lead to developing an initial spring flow reduction scenario of 30% as a test to determine if this magnitude of flow reduction would result in winter warm water refuge habitat reduction likely to be of consideration for MFL establishment.

Comparisons of the measured Wakulla Spring discharges and the discharges for the 30% Flow Reduction Scenario for the four winter reference periods are provided in Figures 78-81. The reduction in Wakulla Spring vent discharges is the only difference in input conditions between the four winter reference periods evaluated and the 30% Flow Reduction Scenario applied to these periods.

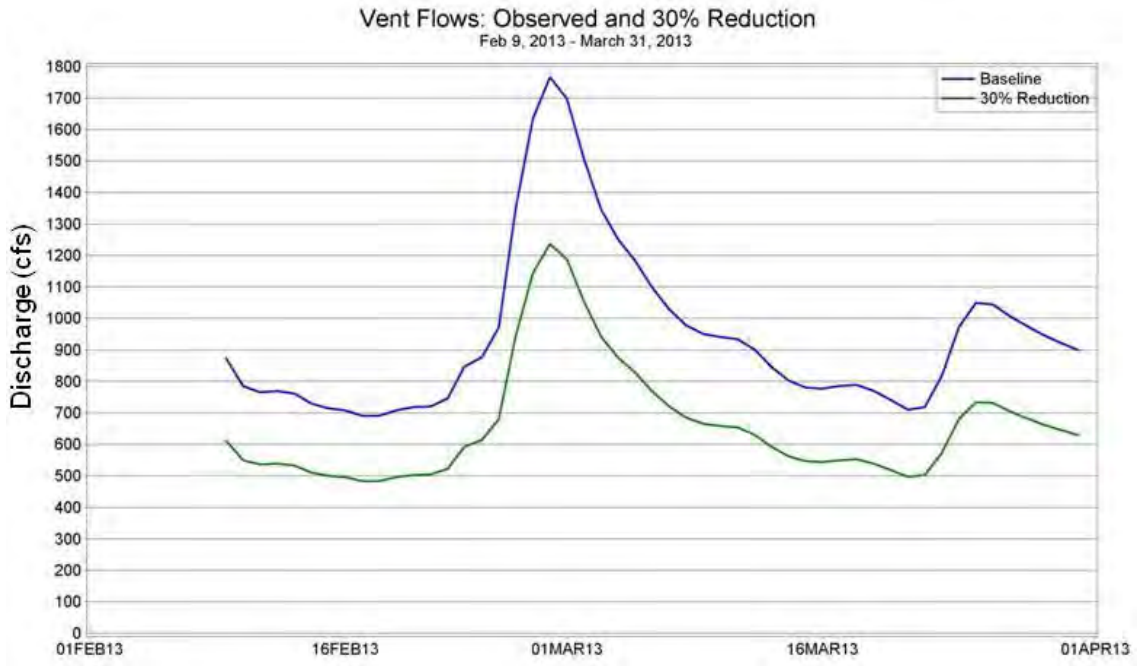

Figure 78. Measured Wakulla Spring flows and 30% Flow Reduction Scenario for period February 9 - March 31, 2013.

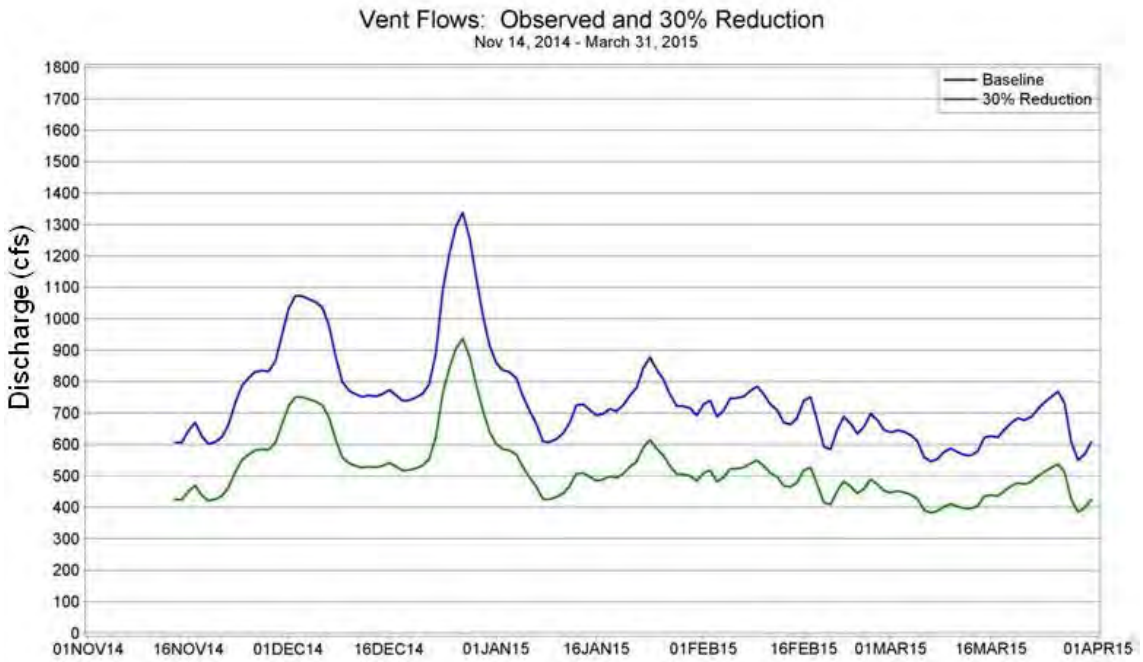

Figure 79. Measured Wakulla Spring flows and 30% Flow Reduction Scenario for period November 14, 2014 - March 31, 2015.

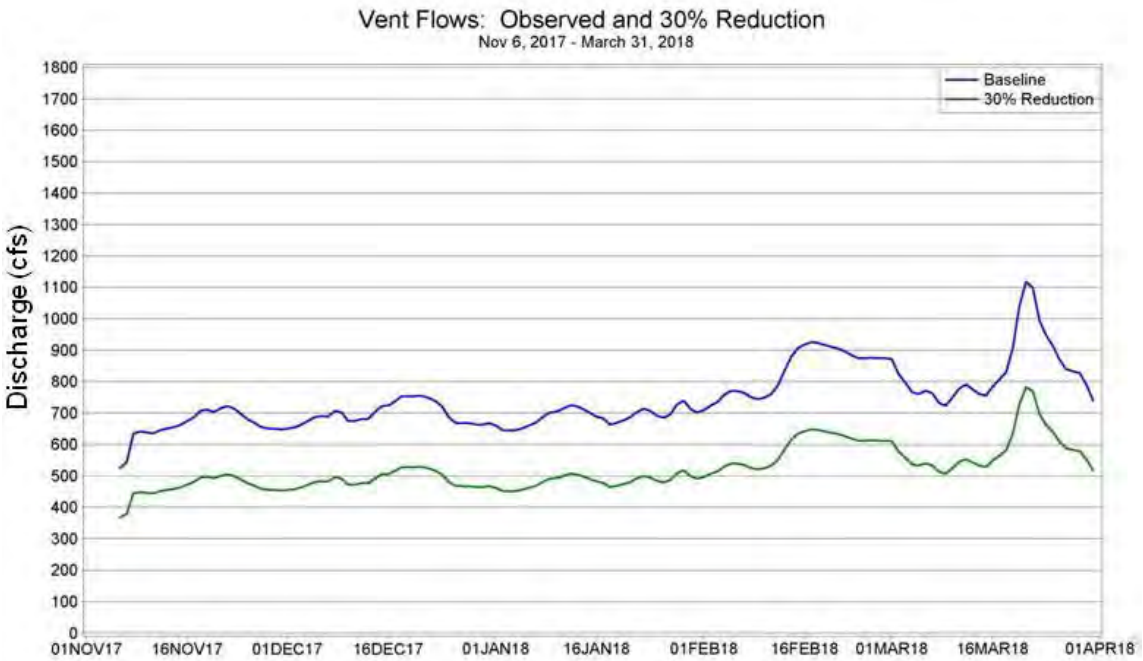

Figure 80. Measured Wakulla Spring flows and 30% Flow Reduction Scenario for period November 6, 2017 - March 31, 2018.

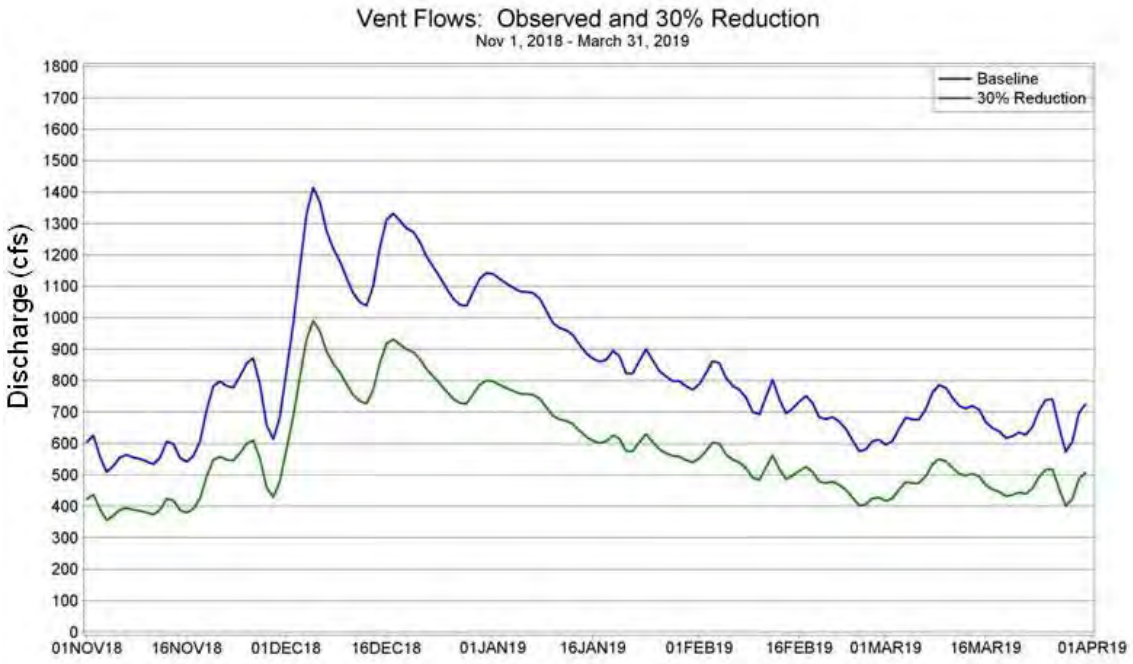

Figure 81. Measured Wakulla Spring flows and 30% Flow Reduction Scenario for period November 1, 2018 - March 31, 2019.

The effects of a 30% Wakulla Spring flow reduction on the available warm water refuge availability also took into account only those model grid cells in the vent area and downstream to the boat tram, excluding those cells along the northern Sally Ward discharge path that enters the main run just downstream of the Main Bend location. This portion of the river was excluded since this portion consists primarily of water flowing from the Sally Ward Spring run where water temperatures are frequently below 20°C during freeze events. The evaluation also made the conservative assumption that manatee usage of the available habitat was limited to the depth of only one manatee equivalent, or the upper 3.8 ft (1.16 m) of the water column. This limited the evaluation to only those model grid cells where the total water column depth was at least 3.8 ft deep. In addition, suitable warm water refuge also exists downstream of the model domain (i.e. downstream of the boat tram station) during many times. As a result, the analysis provided below is a conservative estimate and likely represents an underestimation of the amount of available warm water refuge.

The evaluation was completed with respect to the chronic criterion for manatee thermal refuge, that water temperatures must not fall below 20°C for more than three consecutive days (Rouhani et al. 2007). The acute criterion, that water temperatures not fall below 15°C for more than four consecutive hours, never occurred in either the observed conditions or flow reduction scenario within the evaluation region. The minimum water temperature during the observed flow scenario or the flow reduction scenario was a simulated value of 17.2°C.

The first step in the model output processing for the concatenated four winter reference periods was to first remove the initial seven days of each period to account for model "spinup" due to the new

period's input conditions. This addressed the concern that the first few days of a given winter period may have potentially been impacted by input conditions from the preceding period. Given the large flows through the system it is highly unlikely that any effects of inputs from a week in the past are seen within the model domain. In support of this assumption, the daily minimum flow through the system from the combined Wakulla Spring and Sally Ward discharges observed during the selected winter periods was 1.3 million m^3/day (533 cfs). The maximum daily volume of the model domain grid cells is approximately 39,664 m^3 during the winter periods. At this minimum flow rate and this maximum system volume (to get the maximum replacement time), the volume of the model domain would be replaced approximately 33 times/day, so the removal of the first week of each winter period to account for model "spinup" is justified.

Results of a comparison of the daily average surface areas with sufficient depth for manatees and temperatures of 20°C or greater are shown for each of the four evaluation periods for the observed flow condition and the 30% Flow Reduction Scenario in Figures 82-85. Evaluation of the comparison found that during 41 days of the 458-day record, the 30% Flow Reduction Scenario resulted in greater surface area of ≥20°C than was simulated to occur under measured Wakulla Spring flows. In other words, the amount of warm water refuge increased under the 30% Flow Reduction Scenario. This resulted from the combination of increasing vent flows and associated declining vent water temperatures. The first example of this is in February-March 2013 (Figure 82), with the flows and vent temperatures provided in Figures 42 and 43, respectively. A similar occurrence during the end of December 2018 - early January 2019 (Figure 85) resulted from similar increases in vent discharge and declines in vent temperatures (Figures 51 and 52, respectively). The reduction in flows during a period of vent temperatures <20°C results in less cold water flowing from Wakulla Spring, so that the area of water >20°C is larger during the flow reduction scenario as water temperatures can increase due to longer period of contact with warmer atmospheric temperatures. Notably, these results of greater surface area available under the flow reduction condition were only found when surface areas of >20°C due to observed flow conditions were minimal (Figures 82 and 85).

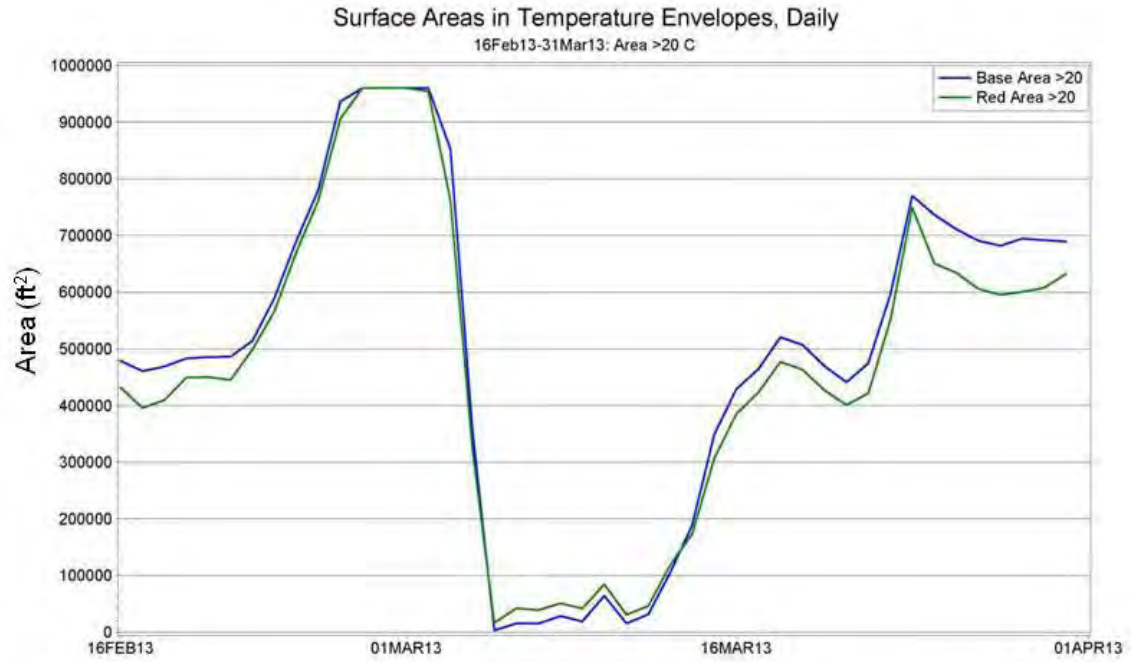

Figure 82. Surface areas available for manatee habitat with waters of 20°C or greater for measured Wakulla Spring flows and 30% Flow Reduction Scenario for period February 16 - March 31, 2013.

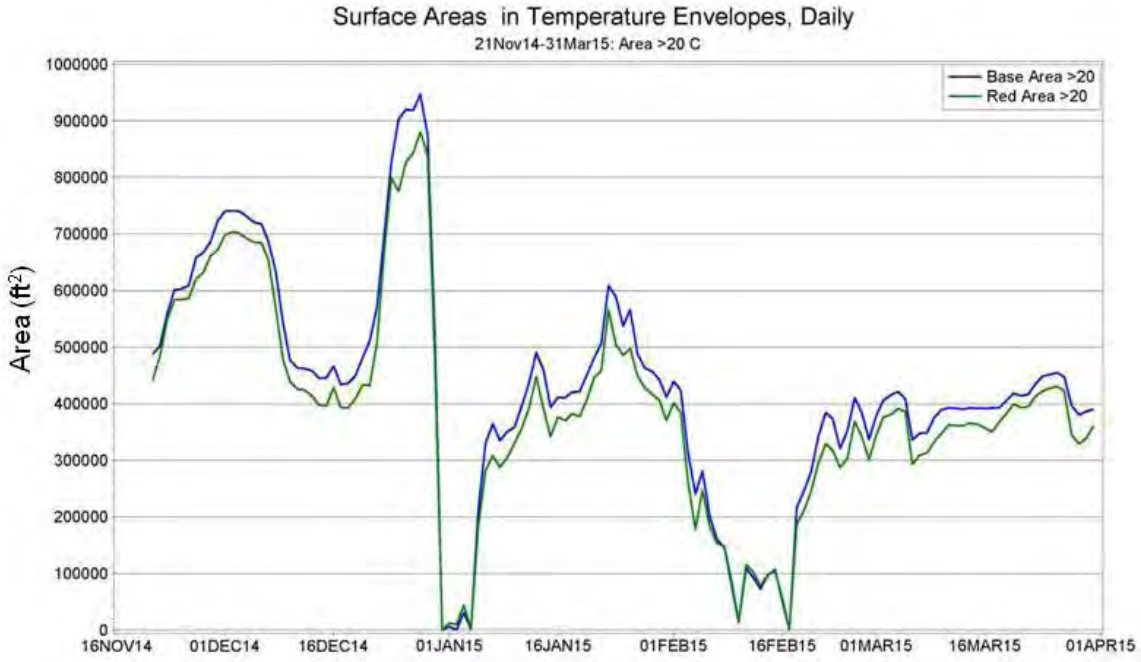

Figure 83. Surface areas available for manatee habitat with waters of 20°C or greater for measured Wakulla Spring flows and 30% Flow Reduction Scenario for period November 21, 2014 - March 31, 2015.

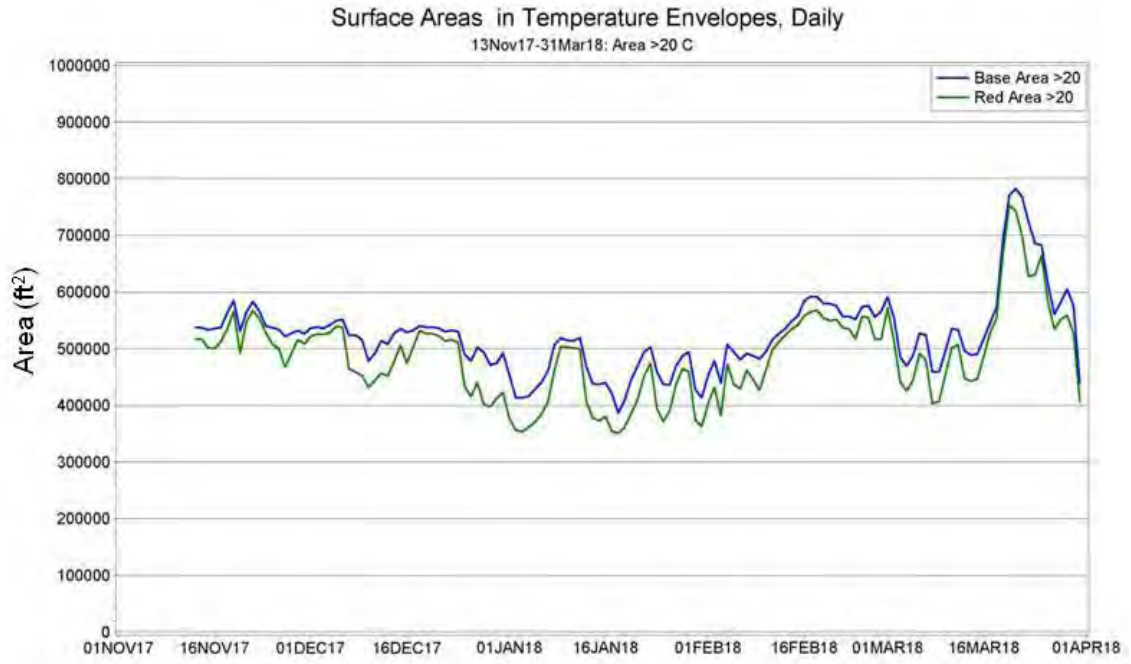

Figure 84. Surface areas available for manatee habitat with waters of 20°C or greater for measured Wakulla Spring flow and 30% Flow Reduction Scenario for period November 13, 2017 - March 31, 2018.

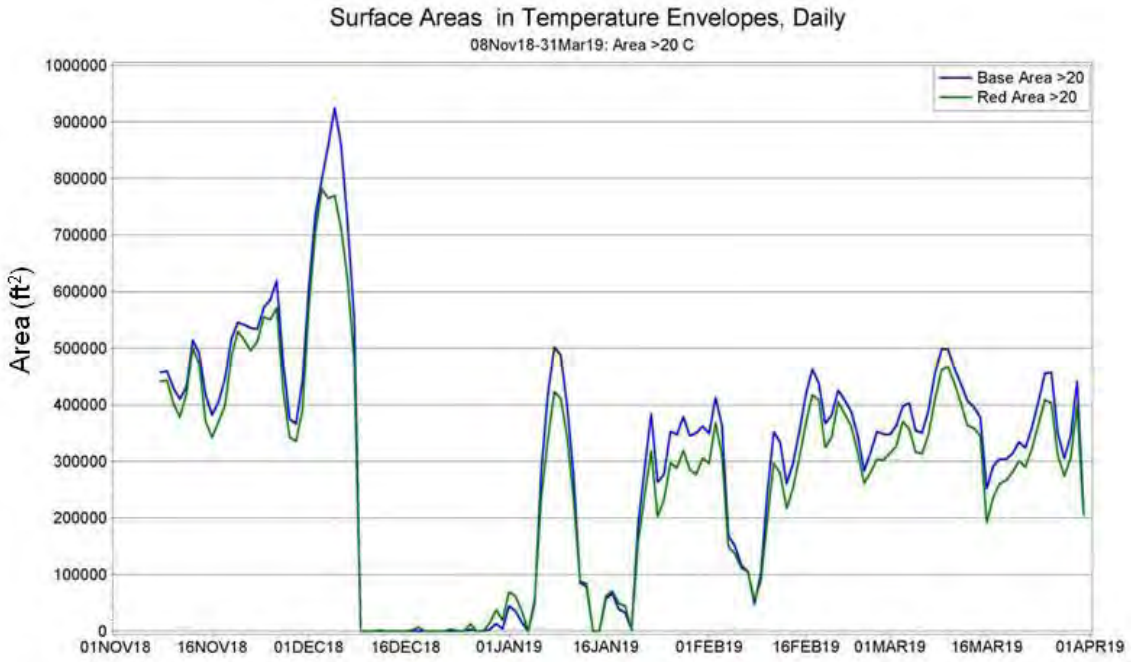

Figure 85. Surface areas available for manatee habitat with waters of 20°C or greater for measured Wakulla Spring flow and 30% Flow Reduction Scenario for period November 08, 2018 - March 31, 2019.

The finding of potential increase in warm water refuge of ≥20°C due to the 30% Flow Reduction Scenario was further evaluated by selecting a period when this system response occurred and mapping the extent of the habitat for both flow conditions. This provides insight, based on this modeling effort, of how the system functions during such an event. December 30, 2018, was

selected as representative of this condition. Figure 86 provides the locations of the areas where the observed conditions flows resulted in available warm water refuge on December 30, 2018 (top panel), the locations where the 30% Flow Reduction Scenario resulted in available warm water refuge (middle panel), and a comparison of the two (bottom panel). Both flow conditions resulted in available warm water refuge primarily along the shore on both the north and south sides of the river upstream of the boat tram and downstream of the Main Bend, as well as across the river near the downstream boundary (green in upper and middle panels). The additional warm water refuge available in the 30% Flow Reduction Scenario (light blue in bottom panel) is downstream of the Main Bend along both the north and south shores, and across the river near the downstream boundary.

Since the available warm water refuge under both flow conditions, and the increase in available warm water refuge under the 30% Flow Reduction Scenario, were found primarily downstream of the Main Bend, the downstream temperature boundary condition was examined to determine what role if any this may have played on the availability of the ≥20°C regions, in case this boundary condition was translating upstream into the model domain. This was found to not be the case, however, as the downstream temperature boundary was less than 20°C for all but a 3.5-hour period on that date, and did not contribute to the changes in ≥20°C water found within the model domain.

The air temperature input to the model on this date reached above 20°C from 11AM to 8PM. The vent water temperatures input to the model on this date were less than 20°C over the entire day. This information and the location of the available warm water refuge under both flow conditions, and the location of the increase in available warm water refuge under the 30% Flow Reduction Scenario, combine to indicate that the exposure of the vent water to the warmer air results in the water warming as it moves downstream, reaching temperatures in excess of 20°C downstream of the Main Bend. The reduced flows of the 30% Flow Reduction Scenario result in slower movement of the water out of the model domain, so that it has longer exposure to the warmer air while still upstream of the Boat Tram, resulting in water above 20°C further upstream from the Boat Tram.

It is important to note that this evaluation was only for one day of the periods selected for evaluation, and may not be applicable to other times in the selected periods when air temperature and/or vent water temperatures could be different. It is indicative, however, of how reduced spring flows may not always result in reduced areas of ≥20°C water within the spring vent area and that immediately downstream.

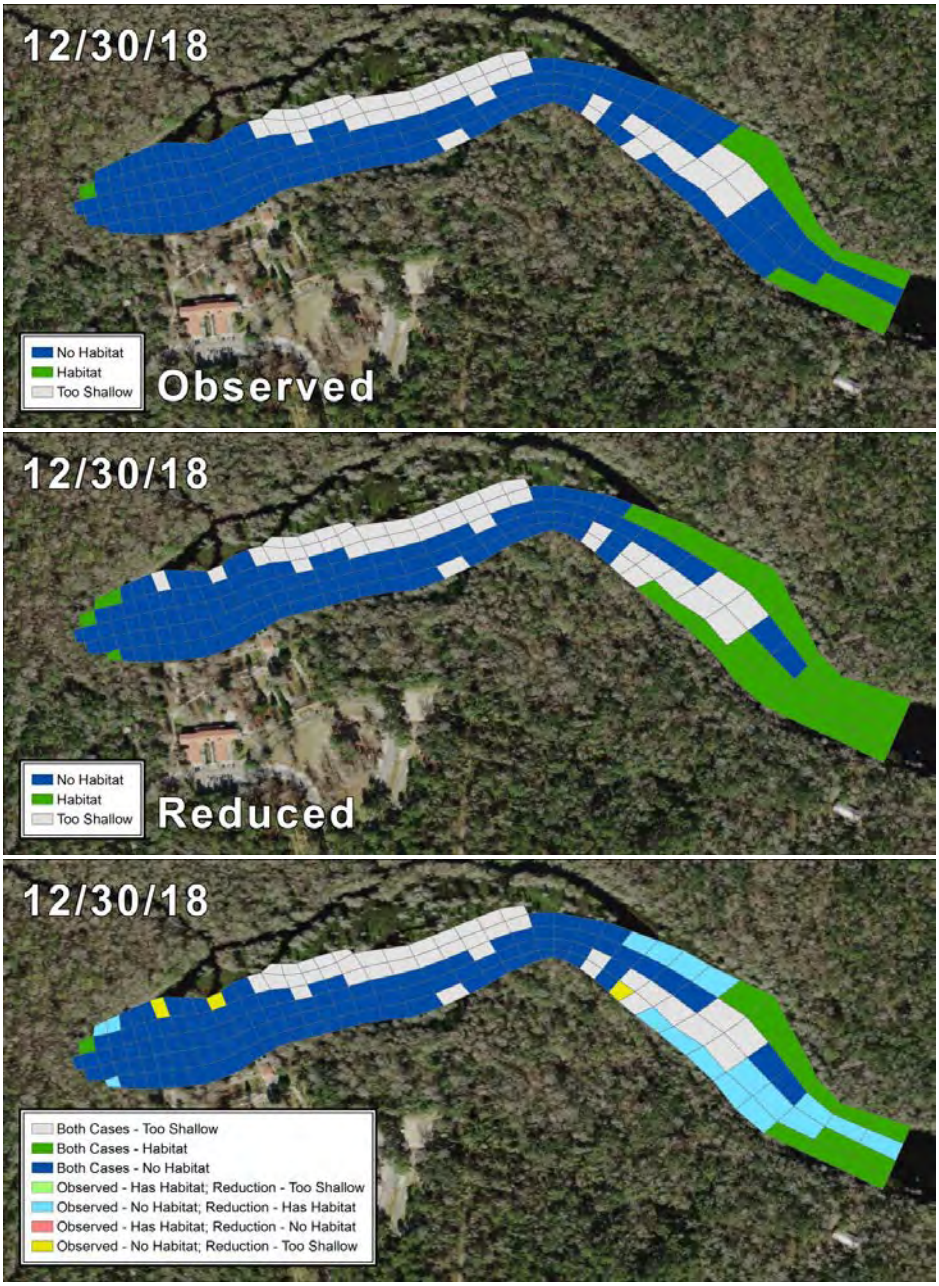

Figure 86. Location of available warm water refuge habitat ≥20°C under observed flows (top panel), 30% Flow Reduction Scenario flows (middle panel), and comparison (bottom panel), for December 30, 2018. Most of the area available in the 30% Flow Reduction Scenario is downstream of the Main Bend (middle panel, green), with the additional warm water refuge available in comparison to the observed condition shown (bottom panel, light blue) along both shores and across the river in the downstream portion of the model domain.

Model results from the concatenated winter reference periods timeseries and the 30% Wakulla Spring flow reduction for these periods were aggregated into daily averages for analysis. To facilitate a conservative analysis of only those days with reductions in the surface areas of ≥20°C warm water refuge, changes for all days when there was an increase in surface area of ≥20°C due

to the 30% Flow Reduction Scenario were set to zero. In addition, reductions for all days with no surface area of ≥20°C in both cases were also set to zero. In total, 58 days of the 458 days evaluated either had zero surface area of ≥20°C under measured spring flows or increases in the surface area of ≥20°C resulting from the 30% Flow Reduction Scenario. For this analysis, the time series plots of percentage differences provided below show the differences for these 58 days as zero.

Time series plots of the percentage differences for each of the four periods evaluated are provided in Figures 87-90. Of the 458 days evaluated, a ≥15% reduction in the surface area of ≥20°C habitat for a given day was found on 35 days. Of these days, only two dates, February 17, 2015 and December 9, 2018 provided suitable warm water refuge for less than 6,240 manatees under the 30% Flow Reduction Scenario. However, on both these dates, the amount of warm water refuge was already severely limited as the average daily water temperature flowing from the Wakulla Vent was below 20°C (19.9°C and 19.8°C, respectively).

When these data were evaluated for the chronic thermal stress criterion that states that water temperatures of suitable depth for manatees must not fall below 20°C for more than three consecutive days, it was found that during the most limiting period (February 15, 2015 through February 17, 2015) warm water refuge existed to support more than 1,900 manatees in the 30% Reduced Flow Scenario. The next most limiting period (February 16, 2015 through February 18, 2015) could still support more than 2,800 manatees under a 30% spring flow reduction. All remaining periods could support more than 4,460 manatees under reduced spring flow conditions.

Given the large amount of suitable chronic warm water refuge available under the 30% Reduced Flow Scenario and comparing this with the maximum number of manatees observed at Wakulla Spring on record (n=46), it is apparent that even with a flow reduction of this magnitude, Wakulla Spring would continue to provide more than sufficient warm water refuge habitat for manatees.

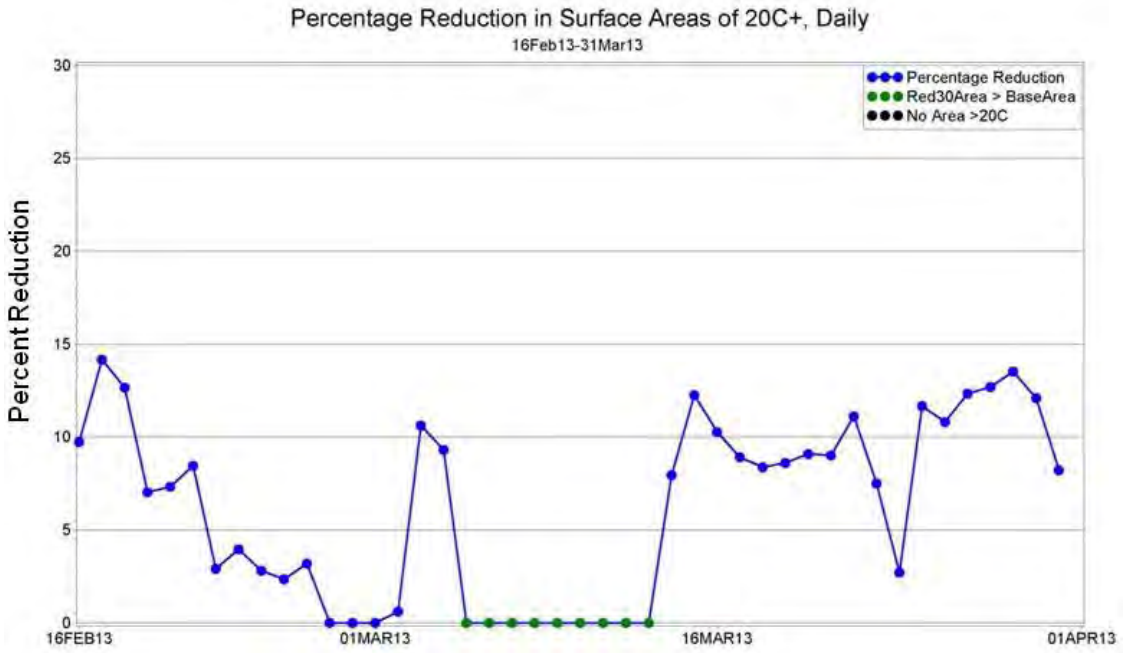

Figure 87. Percentage reduction in surface area available for manatee warm water refuge with waters of 20°C or more due to the 30% Flow Reduction Scenario for period February 16 - March 31, 2013. Dates when manatee warm water refuge of 20°C or more was greater in the Flow Reduction Scenario (green dots): March 5-13, 2013.

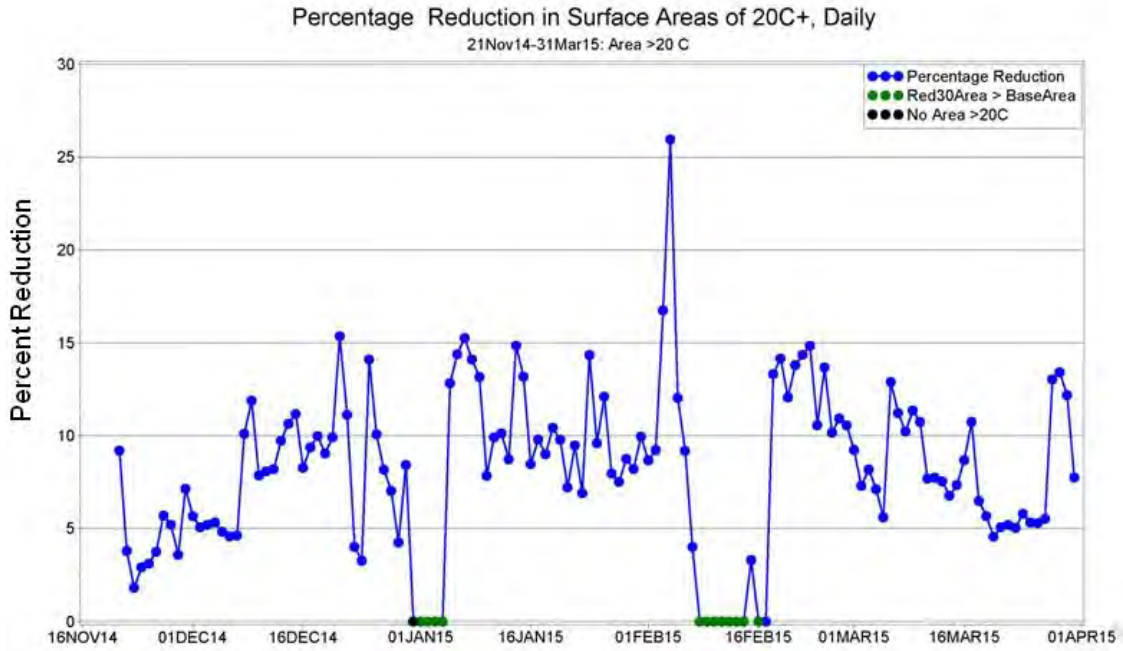

Figure 88. Percentage reduction in surface area available for manatee warm water refuge with waters of 20°C or more due to the 30% Flow Reduction Scenario for period November 21, 2014 - March 31, 2015. Dates when manatee warm water refuge of 20°C or more was greater in the 30% Flow Reduction Scenario (green dots): January 1-4, 2015, February 8-14 and 16, 2015. On Feb 17, 2015, the 667 ft^2 of available warm water refuge under the observed flows was completely lost: this 100% reduction was set to 0 to maintain vertical scale here. On December 31, 2014, there was no manatee warm water refuge of 20°C or more in either scenario (black dot).

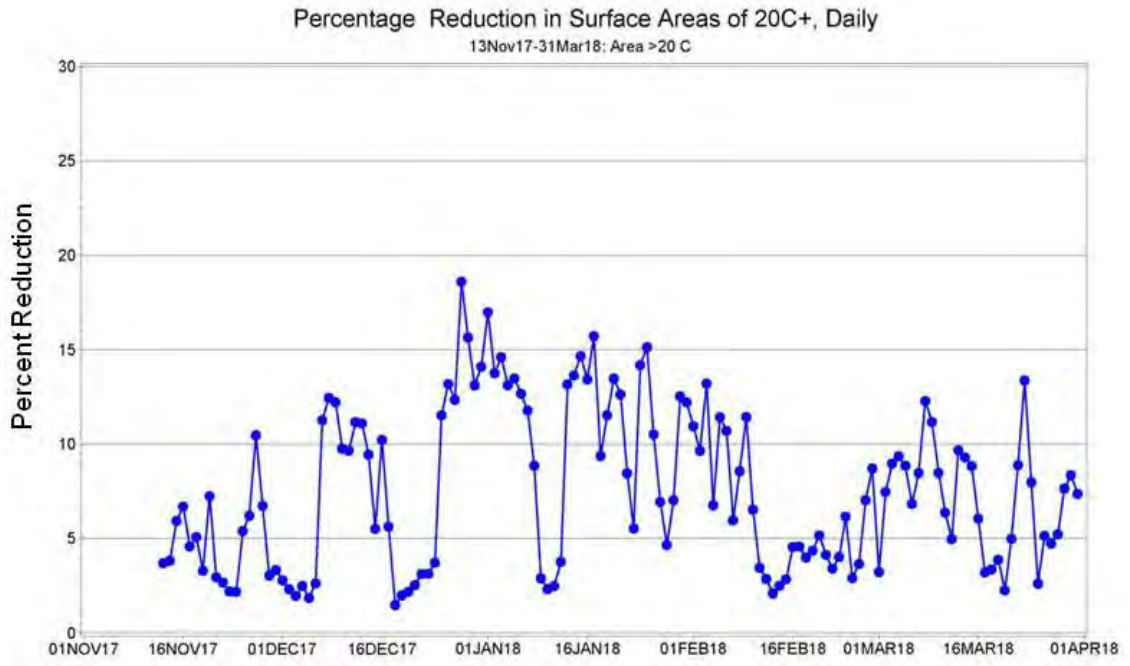

Figure 89. Percentage reduction in surface area available for manatee warm water refuge with waters of 20°C or more due to the 30% Flow Reduction Scenario for period November 13, 2017 - March 31, 2018.

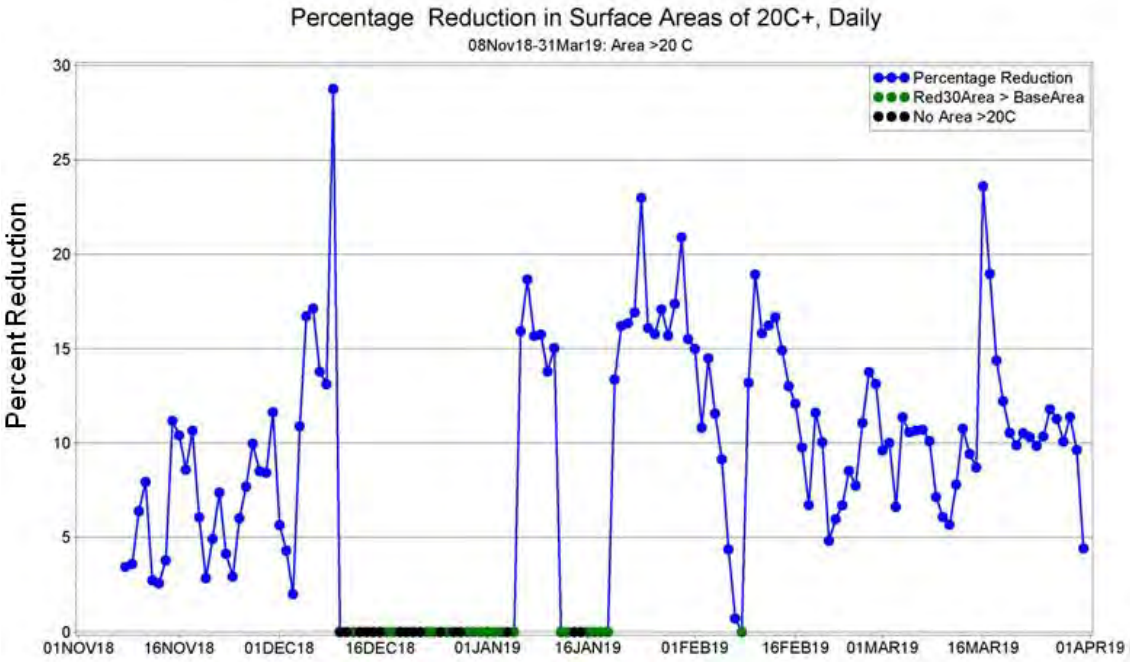

Figure 90. Percentage reduction in surface area available for manatee warm water refuge with waters of 20°C or more due to the 30% Flow Reduction Scenario for period November 8, 2018 - March 31, 2019. Dates when manatee warm water refuge area of 20°C or more was greater in the Flow Reduction Scenario (green dots): December 12, 17, 18, 23, 24, 26, 29-31, 2018; January 1-3, 5, 12, 13, 16-19, and February 8, 2019. There was no manatee warm water refuge of 20°C or more in either scenario (black dots) on December 10, 11, 13-16, 19-22, 25, 27, and 28, 2018; January 4, 14, 15.

6 References

Applied Science Associates. 2003. WQMAP Technical Manual.

Applied Science Associates. 2004. WQMAP User Manual.

Florida Geological Survey. 2012. Demonstrating Interconnection Between a Wastewater Application Facility and a First Magnitude Spring in a Karst Watershed: Tracer Study of the Southeast Farm Wastewater Reuse Facility, Tallahassee, Florida. Florida Geological Survey Report of Investigations No. 111. 202 pages.

Janicki Environmental, Inc. 2018. Hydrodynamic Model Development and Calibration in Support of St. Marks River Rise MFL Evaluation. Appendix D in Northwest Florida Water Management District, 2018. Minimum Flows for the St. Marks River Rise Leon County, Florida Prepared for Northwest Florida Management District, Havana, FL.

Janicki Environmental, 2019a. Wakulla Spring Hydrodynamic Model Sensitivity Analysis for Thermal Refuge Evaluation. Prepared for Northwest Florida Water Management District, Havana, FL.

Janicki Environmental, 2019b. Wakulla Spring Hydrodynamic Model Calibration for Thermal Refuge Evaluation. Prepared for Northwest Florida Water Management District, Havana, FL.

Loper, D.E., C.L. Werner, E. Chicken, G. Davies, and T. Kincaid. 2005. Coastal carbonate aquifer sensitivity to tides. EOS, Transactions, American Geophysical Union. 86 (39): 353-357.

Northwest Florida Water Management District. 2017. St. Marks River and Apalachee Bay Watershed Surface Water Improvement and Management Plan, September 12, 2017. Program Development Series 17-03. https://www.nwfwater.com/Water-Resources/Surface-Water-Improvement-and-Management.

Northwest Florida Water Management District. 2021. Recommended Minimum Flows for Wakulla and Sally Ward Springs, Wakulla County, Florida.

Rouhani, S., P. Sucsy, G. Hall, W. Osburn, and M. Wild. 2007. Analysis of Blue Spring Discharge Data to Determine a Minimum Flow Regime. St. Johns River Water Management District Special Publication SJ2007-SP17.

Suwannee River Water Management District (SRWMD). 2013. Minimum Flows and Levels for the Lower Santa Fe and Ichetucknee Rivers and Priority Springs.
http://fl-suwanneeriver.civicplus.com/DocumentCenter/View/9023.

Southwest Florida Water Management District (SWFWMD). 2004. The Determination of Minimum Flows for Sulphur Springs, Tampa, Florida. Technical Report of the Southwest Florida Water Management District, Brooksville, FL.

Southwest Florida Water Management District (SWFWMD). 2008. Weeki Wachee River System Recommended Minimum Flows and Levels. Technical Report of the Southwest Florida Water Management District, Brooksville, FL.

Southwest Florida Water Management District (SWFWMD). 2012a. Recommended Minimum Flows for the Homosassa River System. Technical Report of the Southwest Florida Water Management District, Brooksville, FL.

Southwest Florida Water Management District (SWFWMD). 2012b. Recommended Minimum Flows for the Chassahowitzka River System. Technical Report of the Southwest Florida Water Management District, Brooksville, FL.

Southwest Florida Water Management District (SWFWMD). 2017. Recommended Minimum Flow for the Crystal River/Kings Bay System, Revised Final Report. Technical Report of the Southwest Florida Water Management District, Brooksville, FL.

White, C. 2016. Wakulla Bathymetry Profile. Northwest Florida Water Management District.